Issues in DS-CDMA Integrated Wireless Access Networks

by

A. Annamalai Jr.
Bachelor of Electrical Engineering,
Universiti Sains Malaysia, 1993

A Thesis Submitted in Partial Fulfillment of the
Requirements for the Degree of

MASTER OF APPLIED SCIENCE

in the Department of
Electrical and Computer Engineering

We accept this thesis as conforming
to the required standard

Dr. V. K. Bhargava, Dept. of Electrical & Computer Engineering

Dr. K. F. Li, Dept. of Electrical and Computer Engineering

Dr. C. Konzelman, Dept. of Mechanical Engineering

Dr. D. Olesky, External Examiner

Supervisor: Prof. Vijay K. Bhargava

ABSTRACT

A consequence of the exploding demand for wireless multimedia services is the need to provide a large number of heterogeneous users with various quality requirements, despite the scarcity in the radio spectrum. In light of these considerations, this dissertation addresses three issues pertaining to integrated wireless access networks which use code division multiple access with direct-sequence modulation.

We first assess the performance of a flexible multi-chip rate multi-processing gain DS-CDMA system architecture which supports teletraffic of different information rates via different spreading bandwidths. This evaluation is particularly important due to the anticipated evolution path of the IWAN architecture from currently proposed 1.25 MHz to wider spreading bandwidths. In addition, we provide a method to efficiently integrate multimedia traffic while ensuring downward compatibility.

Subsequently, we develop an analytical framework to evaluate the performance of different pre-detection diversity techniques in various mobile radio environments. As an example, antenna diversity reception of spread-spectrum signals is illustrated. It is shown that diversity reception is effective for combatting the deep fades experienced on wireless channels. Besides, in an interference hampered network, mitigation of channel fading through the use of diversity can translate into improved interference tolerance. This in turns means greater ability to support additional users, and therefore higher system capacity.

Finally, we devise a simple packet combining mechanism that will enhance the system throughput and delay characteristics of slotted DS-CDMA packet radio networks. Emphasis is placed on improving the system performance without incurring a substantial penalty in terms of implementation complexity or cost. Moreover, the proposed S+I selection scheme is well suited for high data rate transmissions because accurate measurements of the signal-to-noise ratio becomes difficult or expensive.

Examiners:

[redacted]

Dr. Vijay K. Bhargava (Dept. of Electrical and Computer Engineering)

[redacted]

Dr. Kin F. Li (Dept. of Electrical and Computer Engineering)

[redacted]

Dr. Charles Konzelman (Dept. of Mechanical Engineering)

[redacted]

Dr. Dale Olesky (Dept. of Computer Science)

Table of Contents

List of Figures

List of Tables

Acknowledgments

I don't think that it is truly possible to express in words alone my gratitude and appreciation to the many individuals that have helped and supported me both throughout my career and throughout my life. I consider myself very fortunate to have had Professor Vijay K. Bhargava as my thesis advisor. Since the day I began my education at this institution, he has always been available to offer advice and encouragement. I would like to take this opportunity to express my deepest appreciation to Professor Vijay for giving me an invaluable opportunity to pursue my graduate studies under his supervision, a generous financial assistance, and all the resources and support necessary to proceed with this research in a timely manner.

My sincere thanks are also extended to all my colleagues at the Communications Research Laboratory for their friendship and assistance in various ways. In particular, I wish to express my gratitude towards Mr. Mao Zeng, Professor Taakaki Hasegawa, Mr. Joe Mueller, Drs. Ron Kerr, Roman Pichna and Jialin Zou, and Mr. Lorenz Freiberg, for having helped inspire this topic of research and also for having provided numerous useful comments and criticisms at several points throughout the last twenty months. It is not possible to mention all the people that have in some way influenced this work, and I apologize to those individuals whose names are omitted.

I am indebted to Professors P. A. Venkatachalam and B. C. Gargash for their guidance and encouragement during my years as an undergraduate at Universiti Sains Malaysia, and for inspiring me to pursue my graduate studies. I would also like to acknowledge and thank Professors Kin F. Li, C. Konzelman and Dale Olesky for serving on my dissertation defense committee.

Last but not the least, I thank my family for their love and devoted support throughout my life. My parents have always been there for me and supported me in every way possible. My brothers have always given me their encouragement and support. As I have mentioned previously, I don't think it is possible to express my gratitude and appreciation in words alone. I can only hope that the friendship, encouragement, and support that I offer in return is received with equal gratitude and appreciation.

To
My Beloved Parents

List of Acronyms

ACK	Positive acknowledgment (ARQ feedback message)
ALOHA	Random multiple access protocol
ARQ	Automatic repeat request
ATM	Asynchronous transfer mode
AWGN	Additive white Gaussian noise
BCH	Bose-Chaudhuri-Hocquenghem code
BER	Bit error rate
BPSK	Binary phase shift keying
CDF	Cumulative distribution function
DS-CDMA	Direct-sequence code division multiple access
ECC	Error control code (or coding)
EEP	Equal error probability
ESS	Equal signal strength
FCC	Federal Commission on Communications
FDM	Frequency division multiplex
FDMA	Frequency division multiple access
FEC	Forward error correction
GA	Standard Gaussian approximation
IGA	Improved Gaussian approximation
IID	Independent and identical distributed random variable
ISM	Instrumentation, Scientific and Medical
IWAN	Integrated wireless access network

LOS	Line of sight (with respect to transmission path)
MAI	Multiple access interference
MAN	Metropolitan area network
MIP	Multipath intensity profile
MLD	Maximum likelihood decoding
MRC	Maximal ratio combining
NACK	Negative acknowledgment (ARQ feedback message)
PCS	Personal communications systems (or service)
PDF	Probability density function
PSK	Phase shift keying
QoS	Quality of service
QPSK	Quadrature phase shift keying
QR	Quality requirement
RAKE	Multipath (spread-spectrum) diversity reception
R&D	Research and development
SC	Selection diversity combining
SNIR	Signal to noise plus interference ratio
SNR	Signal to noise ratio
SSMA	Spread-spectrum multiple access
S+I	Signal plus interference and noise
UMTS	Universal mobile and telecommunication services

Chapter 1

Introduction

In the information era, communication links are backbones of all large information systems. The final frontier in communications is personal wireless communications by which multi-media can take place between any persons, anywhere and anytime via a pocket size terminal. As we attempt to make wireless technology available for a broader range of applications, we are faced with challenges of spectrum overcrowding, privacy considerations, fading mobile channel as well as complexities of the propagation environment inside buildings, safety concerns (e.g., health hazards), to name a few. Many of these issues have been tackled for military applications where complex and costly solutions have often been considered acceptable, if the desired performance was achieved. Spread spectrum communications has been one of the most intriguing and exciting technologies to emerge from these efforts.

Recently, the FCC has allocated 160 MHz spectrum in 1850 to 2200 MHz range to the personal communications services due to the congested nature of the frequency spectrum in the U.S. This frequency band is currently occupied by microwave users of various groups, and spectrum sharing was the only viable option to satisfy the spectrum needs of PCS. Most would agree that until the band is completely cleared and exclusively used for PCS, interference between the new service users with the primary users, is the primary concern. Consequently, code-division multiple access (CDMA) technology becomes very attractive because of its potential for operation at low-power density, which permits overlay communications and therefore is feasible to co-exist with the narrowband microwave traffic. The desirable properties of CDMA include jamming protection, multipath mitigation, privacy, soft handover, operation at low power spectral density, reduced network synchronization (uncoordinated cellular approaches), increased capacity by exploiting voice activity (speech pattern), overlay communications and flexi-

bility in accommodating multi-media traffic. The concept of spectrum sharing and suitability of CDMA technology for such a scenario are backed up by several years of both defence and commercial R&D which validate these properties. In 1985, the FCC issued Part 15.247 which allows for the unlicensed use of spread-spectrum radios with up to one watt of output power in three shared frequency bands [49] (Instrumentation, Scientific and Medical bands), as depicted in Table 1.1. This ruling has stimulated a wide range of commercial applications for spread-spectrum radios.

Carrier Frequency	Bandwidth
902 - 928 MHz	26.0 MHz
2.4 - 2.4835 GHz	83.5 MHz
5.725 - 5.850 GHz	125.0 MHz

Table 1.1. FCC Part 15, ISM Frequency Bands

Future third-generation systems are expected to support several distinct traffic types with different source characteristics (information rates, activity factor, burstiness), various grades of service and latency requirements through the same bandwidth simultaneously. Thus, issues in system architecture and bandwidth management, and methods for efficient integration of wireless multi-media traffic are important research topics. Moreover, the severe deep fades experienced on wireless channels deteriorate the system performance significantly, and therefore reduce the system capacity. This thesis discusses and analyzes some important issues in this subject, by focusing into the key techniques that can be used to facilitate transmission of voice, video and data in offering untethered personal communication services (PCS) which will become reality in the near future. These include the performance evaluation of a multi-chip rate multi-processing gain direct-sequence CDMA network, micro-diversity reception techniques to mitigate multipath fading, and finally adaptive retransmission diversity with packet combining for data networks that demand stringent bit-error rate requirements but are relatively insensitive to delay.

1.1 Significance of Research

It is known that error tolerance is media-dependent. Given an allocated frequency band for a cellular network, spreading all types of media (voice, data, video services) traffic over the entire available bandwidth can be wasteful since the highest-quality require-

ments have to be satisfied even for the lowest-quality demanding services. Therefore, we investigate the performance of a multi-chip rate DS-CDMA system which supports tele-traffic of different information rates via different bandwidths. The basic idea of this approach is somewhat similar to the radio interface proposed for the third generation universal mobile and personal communication (UMTS) [1]. However, there is no clear evidence thus far that this subject has been treated analytically except for in [7] where the authors studied the performance of a single processing gain system. We extend this work in the following manner: (a) by deriving an expression for the more general case of a multi-chip rate multi-processing gain network; (b) by investigating the effect of different user distributions in various sub-bands on system capacity, and subsequently proposing two admission policies that maximize the system capacity or alternatively improve the service quality; and (c) by evaluating the maximum achievable capacity with optimum power allocation to various classes of traffic.

In the proposed system, the traffic of the highest rate occupies the entire system bandwidth, while each of other lower-rate traffics uses only a portion of the bandwidth. The performance of this hybrid FDM/DS-CDMA network architecture is then compared with the conventional single chip-rate system. It is observed that the new system offers higher capacity than the latter, and is capable of facilitating different quality of service (QoS) contracts for heterogeneous traffic in a multi-media scenario. Alternatively, power requirements, e.g., for data services, can be reduced with respect to the CDMA system with a single type of media-transparent channel. Various admission policy strategies have been examined, which were found to have a strong influence on the system capacity. Further capacity enhancement with optimum power control criteria is also presented.

Next, we have developed a theoretical framework to evaluate the performance of different pre-detection diversity techniques in various mobile radio environments. The average bit-error rate analysis applies to phase coded spread-spectrum systems, over a Nakagami multipath fading channel. A simple and practical selection combining rule has been proposed, in which the amplitude of the received composite signal is used in the selection diversity process. The scheme lends itself to a low-complexity receiver structure, and is particularly attractive for high signalling rates. It is also shown that the new scheme outperforms the traditional selection diversity model. Further, numerical results indicate that this simple scheme exhibits comparable performance with respect to that of an optimum linear diversity combiner when the channel does not experience severe fading (e.g., Rician channels), and for small diversity orders. In brief, the proposed S+I-

selection scheme improves the system performance significantly while ensuring a low-complexity receiver structure.

Finally, we have studied the performance of a slotted DS-CDMA ALOHA system with packet combining. In particular, we have derived the expressions that will enable us to compute the upper bounds for the average number of retransmissions required before a packet is received successfully, and the corresponding lower bounds on the system throughput. In this new scheme, the receiver retains and processes all the retransmissions of a single data block (packet) using post-demodulation diversity combining, instead of discarding those which are detected in error. Simply discarding the noisy packet seems to be wasteful in particular when one realizes that a portion of that packet may have been received correctly. Therefore, we propose to improve the throughput performance, delay characteristics and reliability of the system by using a simple packet combining mechanism. To do so, selection diversity is employed at the bit level to form a more reliable block by using the erroneous copies of that packet, which were retained at the receiver. While using each copy alone might not enable the receiver to recover the transmitted packet, combining these copies enhances the probability of this recovery.

Two forms of selection diversity have been investigated. To facilitate the analysis, we have derived simple and computationally efficient formulas for evaluating the bit-error rate of a practical S+I-selection scheme and the computation of the average number of transmissions for the packet combining scenario. It is shown that in an interference limited environment, the proposed S+I selection scheme outperforms the conventional SNIR-selection model. This is particularly interesting in that the proposed packet combining scheme (which focuses on selecting the bit with the largest amplitude of the received composite signal) lends itself to a low-cost and reduced complexity receiver structure. This scheme is also well suited for high data-rate transmissions because accurate measurements of the signal-to-noise ratio becomes difficult or expensive. Our numerical results show that the proposed adaptive retransmission scheme with a simple packet combining method enhances the system performance significantly, and ensures a more stable network. Also, it was observed that packet combining is more effective when the retransmission rate is high (poor channel conditions), and the application of FEC is crucial to achieve a reasonable system performance in a CDMA network. Moreover, this scheme can be readily applied to CDMA wireless data networks with a little added complexity.

1.2 Organization of Thesis

This dissertation consists of five chapters. In Chapter 2, we assess the performance of a direct-sequence CDMA with multiple chip rates for an integrated network. This evaluation is particularly important due to the anticipated evolution path of the Integrated Wireless Access Network (IWAN) architecture from currently proposed 1.25 MHz to wider spreading bandwidths. Such a network topology may also exist in the ISM bands with different applications supported via different bandwidths in overlapping bands. Two admission policies and an optimum power allocation criterion that maximizes the system capacity are provided.

Whereas in Chapter 3, we employ diversity reception techniques to mitigate multipath fading experienced in wireless mobile environments. In this chapter, we first analyze the performance of two different selection schemes in a Nakagami multipath fading channel. Nakagami's m-distribution is a versatile statistical model, which can accurately fit experimental data for many physical propagation channels. Accurate and time-efficient formulas are derived to evaluate the average bit error probability of a phase-coded spread-spectrum receiver with antenna diversity reception. In addition to the SNIR and S+I-selection methods, performance of an optimum linear diversity combiner is also evaluated for comparison.

Subsequently, throughput analysis of a slotted DS-CDMA ALOHA with packet combining is presented in Chapter 4. Here we restrict our analysis to multipath Rayleigh fading channels. Since the time-varying nature of the multi-user interference (i.e., the number of interfering users may be different during the transmission of each of the combined packets) impose considerable analytical and computational difficulties, we resort to bounding techniques to investigate the system performance. Finally, in Chapter 5, conclusions and suggestions for future work are furnished.

Chapter 2

Evaluation of DS/CDMA Communications with Multiple Chip Rates in an Integrated Network

A gradual evolution of the IWAN (Integrated Wireless Access Network) architecture from the currently proposed 1.23 MHz and 2.5 MHz systems to 5 MHz bandwidths (that may be introduced around 1997) and subsequently 15 MHz systems (to follow some three years later) near the spectrum space of 2 GHz is expected [6]. An implication of this evolutionary picture is that systems with different bandwidths will co-exist and it appears desirable that systems be sufficiently flexible so as to allow both terminal and base station interfaces to operate at multiple chip rates and processing gain values. We offer an open and flexible radio interface to efficiently integrate the heterogeneous traffic and fully utilize the available resources, while ensuring downward compatibility. The basic idea of this approach is somewhat similar to the radio interface proposed for the third generation universal mobile and personal communication (UMTS) [1]. However, there is no clear evidence thus far that this subject has been treated analytically except for in [7] where the authors studied the performance of a single processing gain system.

In this study we evaluate the performance of a hybrid FDM/DS-CDMA system supporting heterogeneous traffic, with calls co-existing at different chip-rates (multiple spreading bandwidths) in overlapping bands. Our analysis is a natural extension of [7], with an evaluation of a more general case for a multi-chip rate multi-processing gain network. In addition, we also investigate the optimal power allocation criteria and admission policies that maximize the system capacity.

Although the conventional CDMA scheme [4][10] is the easiest way to accomplish the objective of multi-rate transmission, it does not utilize the bandwidth efficiently. One may realize that spreading the multi-media traffic over a single wide RF bandwidth can

be wasteful, in particular if the discrepancies between the QoS requirements for these services are large [2]. This is because highest quality requirements have to be guaranteed even for the lowest quality demanding services. The use of spreading results in a protection level to external interferences, and is defined by the processing gain. In a multi-processing gain (single chip-rate) system, this protection level is not constant. Therefore, all the users do not accomplish the same bandwidth efficiency. In order to fully exploit the inherent advantages of CDMA (i.e., better exploitation of multipath diversity), the high rate signals are spread over the entire available bandwidth. However, if we require the same level of protection for all types of heterogeneous traffic (e.g. voice, video), a single processing gain is sufficient [7]. Thus, we say that lower-rate signals are "over-spread" (relative to the high rate signals) especially when both these signals need to be supported with the same QoS.

In the proposed scheme, various source rates will be mapped to different chip rates based on their symbol information rates and quality requirements. Thus users with different rates will have different spreading bandwidths and therefore we can, by the use of frequency division multiplex (FDM), squeeze many such subsystems within the system bandwidth. In other words, with the proposed FDM/DS-CDMA signalling scheme, we attempt to make optimal use of the available resources (i.e., bandwidth) and expect an increase in the spectrum efficiency.

2.1 System Description

The spread-spectrum system model examined in this analysis is similar to that used in [5] and [10], and is depicted in Figure 2.1 for multi-media traffic. A two-rate system model is presented to evaluate the feasibility of our new system. This model can be easily generalized to investigate the performance of a multi-media network with more than two chip rates. For convenience, denote the high data rate signal as *type v* traffic and the lower-data rate traffic as *type s*. The high rate signals are spread over the entire available bandwidth to gain from multipath and interferer diversity. Then, the processing gain G_v for the high data rate signal is given by,

$$G_v = T_v / T_{cv} \tag{2.1}$$

where T_v and T_{cv} represent the bit durations of the *type v* data signals and period of the wideband chip waveform respectively. Similarly for the lower-rate signals (*type s*), the

processing gain is defined as $G_s = T_s/T_{cs}$. Also denote $R_v/R_s = n_s$ and $R_{cv}/R_{cs} = n_{cs}$, with $R_v = 1/T_v$, $R_s = 1/T_s$, $R_{cv} = 1/T_{cv}$ and $R_{cs} = 1/T_{cs}$. Note that if a single processing gain is assumed, then $G_s = G_v$ and $n_{cs} = n_s$.

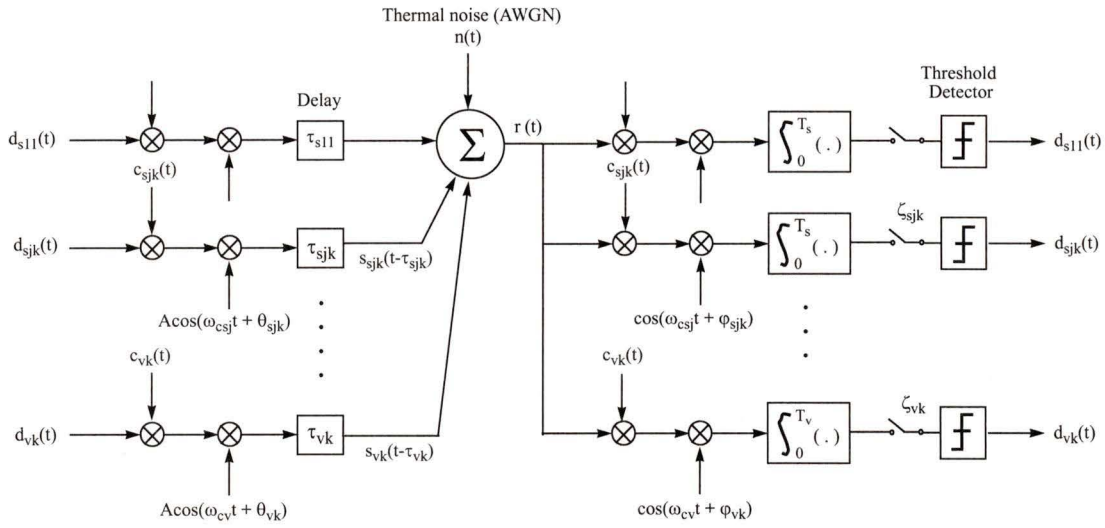

Figure 2.1 DS/SSMA system model.

It is clear that bandwidth $2W_{ss}$ can accommodate R_{cv}/R_{cs} subsystems with rate R_{cs}. To evaluate the performance of the new system, we consider the cases in which $R_{cs} = 2^{1-i}R_{cv}$ $(i = 2, 3, \ldots)$. Thus, $n_{cs} = 2^{i-1}$ subsystems with chip rate R_{cs} can fit in the bandwidth $2W_{ss}$ if the carrier frequencies of the subsystems are suitably chosen. Denote the narrowband subsystems by *subsystem* $[s,j]$ $(j = 1, 2, \ldots, n_{cs})$, then the carrier frequencies of these subsystems f_{csj} are of the form,

$$f_{csj} = f_l + \frac{2j-1}{n_{cs}} W_{ss} \tag{2.2}$$

where f_l is the lower boundary of the system bandwidth and W_{ss} corresponds to the chipping rate of the wideband subsystem. Also denote the subsystem which supports high rate traffic by *subsystem* $[v]$ with carrier frequency $f_{cv} = f_l + W_{ss}$. Hence, the system under investigation consists of $1 + n_{cs}$ subsystems. Figure 2.2 describes the test systems for multi-rate schemes evaluation and the allocation of carrier frequencies for each of these systems.

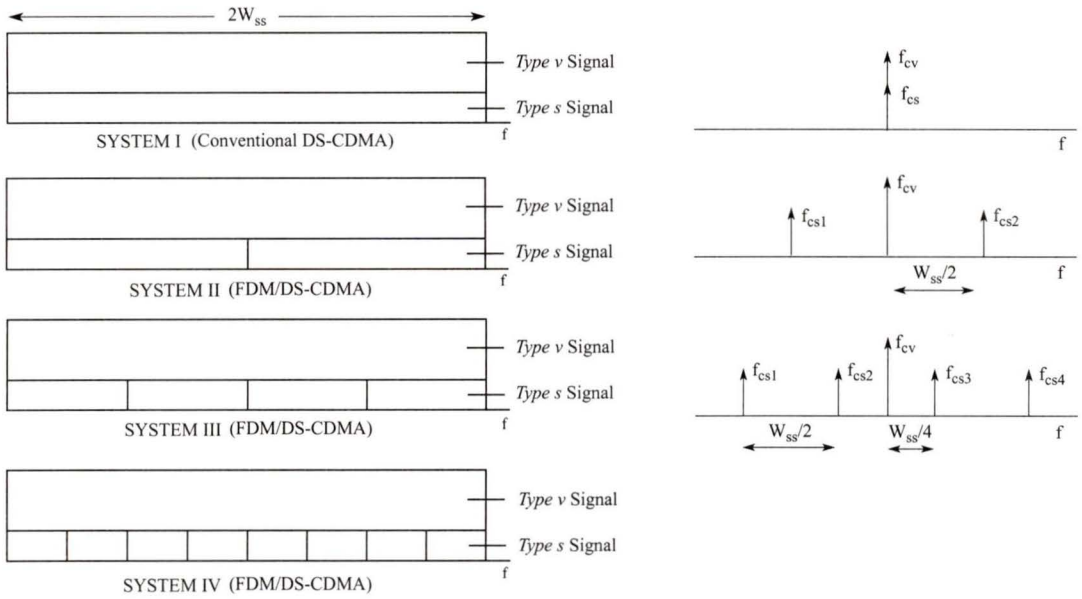

Figure 2.2 System architecture of the test systems for multi-rate schemes evaluation.

Consider a binary direct-sequence CDMA system with a rectangular chip shaping waveform. Let U_v and U_{sj} denote the number of active users in *subsystem* $[v]$ and *subsystem* $[s,j]$ respectively; then the kth transmitted signal of *subsystem* $[v]$, s_{vk} $(1 \le k \le U_v)$, and kth transmitted signal of *subsystem* $[s,j]$, s_{sjk} $(1 \le k \le U_{sj})$ are of the form,

$$s_{vk}(t) = \sqrt{2P_v}\, d_{vk}(t)\, c_{vk}(t) \cos(\omega_{cv} t + \theta_{vk}) \tag{2.3}$$

$$s_{sjk}(t) = \sqrt{2P_s}\, d_{sjk}(t)\, c_{sjk}(t) \cos(\omega_{csj} t + \theta_{sjk}) \tag{2.4}$$

where P_v and P_s denote the transmitted power of the *type v* and *type s* traffic respectively. θ_{vk} and θ_{sjk} are the phase angles introduced by the k-th PSK modulators, and are modeled as i.i.d random variables uniformly distributed over $[0, 2\pi)$. The data waveforms $d_{vk}(t)$ and $d_{sjk}(t)$ consist of sequences of mutually independent rectangular pulses of duration $T_v = 1/R_v$ and $T_s = 1/R_s$ with amplitude taking values from $\{\pm 1\}$ with equal probability. The signature sequences, $c_{vk}(t)$ and $c_{sjk}(t)$ having amplitude {+1,-1} with equal probability, are modelled as mutually independent random binary sequences of duration T_{cv} and T_{cs} respectively. The system is assumed to be synchronous with respect to the chip durations. This assumption can be relaxed and is only made in order to simplify the evaluations.

2.2 Performance Analysis

2.2.1 Wideband DS-CDMA Waveforms

Given $U = U_v + \sum_{j=1}^{n_{cs}} U_{sj}$ active users transmit information simultaneously in an AWGN channel, the received signal at the input of *type v* receiver is [2],

$$r_v(t) = \sum_{k=1}^{U_v} s_{vk}(t-\tau_{vk}) + \sum_{j=1}^{n_{cs}} \sum_{k=1}^{U_{sj}} s_{sjk}(t-\tau_{sjk}) + n(t) \tag{2.5}$$

where τ_{vk} and τ_{sjk} are the k-th signal time delays, and $n(t)$ is a zero-mean white Gaussian noise process with two-sided spectral density $N_0/2$. For coherent reception and correlation receiver matched to the l-th signal, the output is [3][10],

$$g_{vl}(T_v) = \int_0^{T_v} r_v(t)\, c_{vl}(t) \cos(\omega_{cv} t)\, dt \tag{2.6}$$

If $\omega_{cv} \gg 1/T_{cv}$, then a practical spread spectrum receiver is such that the double frequency components of integrand (2.6) can be ignored. Consequently, equation (2.6) can be re-written as [2],

$$g_{vl}(T_v) \equiv \sqrt{\frac{P_v}{2}} T_v (d_{vl}^{(0)} + I_v + \eta_v) \tag{2.7}$$

where $d_{vl}^{(0)}$ is the desired signal in decision interval $[0, T_v]$, η_v is a zero-mean Gaussian random variable with variance $N_0/2E_{bv}$ and I_v is the multiple access interference (MAI) term.

$$I_v = \sum_{k=1,\, k\neq l}^{U_v} \frac{1}{T_v} \int_0^{T_v} C_{vk}(t-\tau_{vk})\, c_{vl}(t) \cos(\varphi_{vk})\, dt \; + \sum_{j=1}^{n_{cs}} \sum_{k=1}^{U_{sj}} \frac{1}{T_v} \sqrt{\frac{P_s}{P_v}} \int_0^{T_v} C_{sjk}(t-\tau_{sjk})\, c_{vl}(t) \cos(\omega_{sj} t + \varphi_{sjk})\, dt \tag{2.8}$$

where $C_{vk}(t)$ and $C_{sjk}(t)$ denote the product of the data and the spreading signature sequences of the wideband and narrowband subsystems respectively, i.e.,

$C_{vk}(t) = d_{vk}(t)\,c_{vk}(t)$ and $C_{sjk}(t) = d_{sjk}(t)\,c_{sjk}(t)$. The random phase angles in (2.8) are given by $\varphi_{vk} = \theta_{vk} - \omega_{cv}\tau_{vk}$ and $\varphi_{sjk} = \theta_{sjk} - \omega_{csj}\tau_{sjk}$ with ω_{sj} expressed as,

$$\omega_{sj} = \omega_{csj} - \omega_{cv} = 2\pi\left[\frac{(2j-1-n_{cs})\,W_{ss}}{n_{cs}}\right] \tag{2.9}$$

We assume the receiver is synchronized with the l-th CDMA signal, so there is no loss in generality in assuming $\tau_{vl} = 0$, $\tau_{sjl} = 0$, $\varphi_{vl} = 0$ and $\varphi_{sjl} = 0$ because we are only concerned with the relative time delays and phase angles. In addition, it is shown in [10] that φ_{vk} and φ_{sjk} are uniformly distributed over $[0, 2\pi)$; τ_{vk} and τ_{sjk} are assumed to be integer multiples of chip waveform periods and uniformly distributed over $[0, T_{cv})$ and $[0, T_{cs})$ respectively. Re-arranging the rectangular pulse functions outside the integration, the expression for I_v in equation (2.8) reduces to,

$$I_v = \sum_{k=1,\,k\neq l}^{U_v} \sum_{g=0}^{G_v-1} \frac{C_{vk,\,(g)}\,c_{vl,\,(g)}\cos\varphi_{vk}}{G_v} + \sum_{j=1}^{n_{cs}} \sum_{k=1}^{U_{sj}} \frac{1}{T_v}\sqrt{\frac{P_s}{P_v}} \sum_{h=0}^{\frac{G_s}{n_s}-1} C_{sjk,\,(h)} \sum_{m=0}^{G_v - n_{cs}\left(\frac{G_s}{n_s}-1\right)-1} c_{vl,\,(n_{cs}h+m)}\,A_{sj,\,(h,m)}(\varphi_{sjk}) \tag{2.10}$$

where $A_{sj,\,(h,m)}(\varphi_{sjk})$ is given by the expression,

$$A_{sj,\,(h,m)}(\varphi_{sjk}) = \int_{(n_{cs}h+m)\,T_{cv}}^{(n_{cs}h+m+1)\,T_{cv}} \cos\omega_{sj}t\cdot\cos\varphi_{sjk} - \sin\omega_{sj}t\cdot\sin\varphi_{sjk}\,dt \tag{2.11}$$

Since $c_{vl}(t)$ is a random signature sequence and the period of $\cos\omega_{sj}t$ and $\sin\omega_{sj}t$ is $n_{cs}T_{cv}/|2j-1-n_{cs}|$, we can replace $A_{sj,\,(h,m)}(\varphi_{sjk})$ with $A_{sj,\,(m)}(\varphi_{sjk})$. Note that $C_{vk,\,(.)}$ take values of +1 or -1 with equal probability, so the statistical properties of the first term in equation (2.10) remain unchanged regardless of which $c_{vl,\,(.)}$ sequences are selected. Hence, this first term and the second term of (2.10) can be re-written as,

$$\delta_v = \sum_{k=1,\,k\neq l}^{U_v} \sum_{g=0}^{G_v-1} \frac{C_{vk,\,(g)}\cos\varphi_{vk}}{G_v} \tag{2.12}$$

$$\Omega_v = \sum_{j=1}^{n_{cs}} \sum_{k=1}^{U_{sj}} \frac{1}{T_v} \sqrt{\frac{P_s}{P_v}} \sum_{h=0}^{\frac{G_s}{n_s}-1} C_{sjk,\,(h)} \sum_{m=0}^{G_v - n_{cs}\left(\frac{G_s}{n_s}-1\right)-1} c_{vl,\,(m)} A_{sj,\,(m)}\,(\varphi_{sjk}) \tag{2.13}$$

where $A_{sj,\,(m)}\,(\varphi_{sjk}) = \int_{mT_{cv}}^{(m+1)\,T_{cv}} \cos\omega_{sj} t \cos\varphi_{sjk} - \sin\omega_{sj} t \sin\varphi_{sjk} dt$.

A prerequisite to the application of Gaussian approximation [10] is the knowledge of the variance of multiple access interference (MAI). It can be easily shown that $E[I_v] = 0$, and thus $Var\{I_v\} = E\left[I_v^2\right] = E\left[\delta_v^2\right] + E\left[\Omega_v^2\right]$ because δ_v and Ω_v are mutually statistically independent random variables and are uncorrelated.

$$E\left[\delta_v^2\right] = \sum_{k=1,\,k\neq l}^{U_v} \sum_{g=0}^{G_v-1} E\left[\left(\frac{\cos\varphi_{vk}}{G_v}\right)^2\right] = \frac{U_v - 1}{2G_v} \tag{2.14}$$

$$E\left[\Omega_v^2\right] = E_\varphi\left\{E_{c_{vl,\,(.)}}\left\{E_{C_{sjk}}\left[\Omega^2 \middle| c_{vl,\,(.)}, \varphi\right]\right\}\right\} \tag{2.15}$$

$$E\left[\Omega_v^2 \middle| c_{vl,\,(.)}, \varphi\right] = \sum_{j=1}^{n_{cs}} \sum_{k=1}^{U_{sj}} \sum_{h=0}^{\frac{G_s}{n_s}-1} \frac{1}{T_v^2} \frac{P_s}{P_v} \left[\sum_{m=0}^{G_v - n_{cs}\left(\frac{G_s}{n_s}-1\right)-1} c_{vl,\,(m)} A_{sj,\,(m)}\,(\varphi_{sjk})\right]^2$$

$$= \sum_{j=1}^{n_{cs}} \sum_{k=1}^{U_{sj}} \sum_{h=0}^{\frac{G_s}{n_s}-1} \frac{P_s}{P_v T_v^2} \sum_{m=0}^{G_v - n_{cs}\left(\frac{G_s}{n_s}-1\right)-1} \left[A_{sj,\,(m)}\,(\varphi_{sjk})\right]^2 +$$

$$2 \sum_{h=0}^{\frac{G_s}{n_s}-1} \sum_{m=0}^{G_v - n_{cs}\left(\frac{G_s}{n_s}-1\right)-2} \sum_{m'=m+1}^{G_v - n_{cs}\left(\frac{G_s}{n_s}-1\right)-1} \left(\frac{P_s c_{vl,\,(m)} c_{vl,\,(m')}}{P_v T_v^2}\right)$$

$$\cdot \left[\sum_{j=1}^{n_{cs}} \sum_{k=1}^{U_{sj}} A_{sj,\,(m)}\,(\varphi_{sjk}) A_{sj,\,(m')}\,(\varphi_{sjk})\right] \tag{2.16}$$

Since $c_{vl,\,(.)}$ is assumed to be a random signature sequence, the second term of equation (2.16) disappears after averaging with respect to $c_{vl,\,(.)}$,

$$E\left[\Omega_v^2 \middle| \varphi\right] = \left(\frac{P_s G_s}{P_v n_s T_v^2}\right) \sum_{j=1}^{n_{cs}} \sum_{k=1}^{U_{sj}} \sum_{m=0}^{G_v - n_{cs}\left(\frac{G_s}{n_s} - 1\right) - 1} \left[A_{sj,\,(m)}\left(\varphi_{sjk}\right)\right]^2 \tag{2.17}$$

Averaging with respect to φ,

$$E\left[\Omega_v^2\right] = \left(\frac{P_s G_s}{P_v n_s T_v^2}\right) \sum_{j=1}^{n_{cs}} \sum_{m=0}^{n_{cs}-1} U_{sj} \left(\frac{\alpha_{sj,\,(m)}^2 + \beta_{sj,\,(m)}^2}{2}\right) \tag{2.18}$$

where $\alpha_{sj,\,(m)}$ and $\beta_{sj,\,(m)}$ are defined as,

$$\alpha_{sj,\,(m)} = \int_{mT_{cv}}^{(m+1)\,T_{cv}} \cos\left(\omega_{sj} t\right) dt \tag{2.19}$$

$$\beta_{sj,\,(m)} = \int_{mT_{cv}}^{(m+1)\,T_{cv}} \sin\left(\omega_{sj} t\right) dt \tag{2.20}$$

Using equations (2.14), (2.18), (2.19) and (2.20), the variance of I_v can be expressed as,

$$Var\left\{I_v\right\} = \frac{U_v - 1}{2G_v} + \frac{P_s G_s}{P_v n_s T_v^2} \sum_{j=1}^{n_{cs}} \sum_{m=0}^{n_{cs}-1} U_{sj} \left(\frac{\alpha_{sj,\,(m)}^2 + \beta_{sj,\,(m)}^2}{2}\right) \tag{2.21}$$

Consequently, the average bit error rate computed via the Gaussian approximation method [10] for *type v* traffic is given by,

$$P_{bv} = Q\left(\sqrt{SNR_v}\right) = Q\left(\sqrt{\left(\frac{2E_{bv}}{N_0}\right)^{-1} + Var\left\{I_v\right\}}\right) \tag{2.22}$$

where $Q(.)$ corresponds to the complementary error function,

$$Q(x) = \frac{1}{\sqrt{2\pi}} \int_x^{\infty} e^{\frac{-u^2}{2}}\, du = \frac{1}{2}\operatorname{erfc}\left(\frac{x}{\sqrt{2}}\right) \tag{2.23}$$

2.2.2 Narrowband DS-CDMA Waveforms

When analyzing the performance of the narrowband DS-CDMA subsystems, we assume that neighboring subsystems do not interfere with each other [see Appendix A]. Then, the MAI is contributed by other users in its own subsystem and that from *subsystem* [*v*].

Hence, the received waveform at the input to the narrowband receiver is given by [2],

$$r_{sj}(t) = \sum_{k=1}^{U_v} s_{vk}(t-\tau_{vk}) + \sum_{k=1}^{U_{sj}} s_{sjk}(t-\tau_{sjk}) + n(t) \tag{2.24}$$

Then the output of the correlation receiver (matched filter) is,

$$g_{sjl}(T_s) = \int_0^{T_s} r_{sj}(t)\, c_{sjl}(t) \cos(\omega_{csj} t)\, dt \equiv \sqrt{\frac{P_s}{2}}\, T_s (d_{sjl}^{(0)} + I_{sj} + \eta_s) \tag{2.25}$$

with the multiple access interference term given by,

$$I_{sj} = \sum_{k=1,\, k\neq l}^{U_{sj}} \frac{1}{T_s} \int_0^{T_s} C_{sjk}(t-\tau_{sjk})\; c_{sjl}(t)\; \cos(\varphi_{sjk})\, dt \;+$$

$$\sum_{k=1}^{U_v} \frac{1}{T_s} \sqrt{\frac{P_v}{P_s}} \int_0^{T_s} C_{vk}(t-\tau_{vk})\, c_{sjl}(t) \cos(-\omega_{sj} t + \varphi_{vk})\, dt \tag{2.26}$$

Following the procedures that we have described above to evaluate the variance of MAI in the wideband subsystem, I_{sj} shown in (2.26) can be re-written as,

$$I_{sj} = \sum_{k=1,\, k\neq l}^{U_{sj}} \sum_{g=0}^{G_s-1} \frac{C_{sjk,\,(g)} \cdot \cos\varphi_{sjk}}{G_s} \;+$$

$$\sum_{k=1}^{U_v} \frac{1}{T_s} \sqrt{\frac{P_v}{P_s}} \sum_{h=0}^{n_s G_v - 1} C_{vk,\,(h)}\, c_{sjl,\,(\lfloor h/n_s \rfloor)}\, B_{sj,\,(h)}(\varphi_{vk}) \tag{2.27}$$

with $B_{sj,\,(h)}(\varphi_{vk}) = \int_{hT_{cv}}^{(h+1)\,T_{cv}} \cos\omega_{sj} t \cos\varphi_{vk} + \sin\omega_{sj} t \sin\varphi_{vk}\, dt$ and $\alpha_{sj,\,(.)}$, $\beta_{sj,\,(.)}$ as defined in (2.19) and (2.20) respectively.

$$E\left[\delta_s^2\right] = \sum_{k=1,\, k\neq l}^{U_{sj}} \sum_{g=0}^{G_s-1} E\left[\left(\frac{\cos\varphi_{sjk}}{G_s}\right)^2\right] = \frac{U_{sj}-1}{2G_s} \tag{2.28}$$

Since $E\left[\Omega_{sj}^2\right]$ is statistically independent of the random signature sequence $c_{sjl}(.)$, then $E\left[\Omega_{sj}^2 \middle| c_{sjl,\,(.)}, \varphi\right] = E\left[\Omega_{sj}^2 \middle| \varphi\right]$.

$$E\left[\Omega_{sj}^2 \middle| \varphi\right] = \left(\frac{P_v}{P_s T_s^2}\right) \sum_{k=1}^{U_v} \sum_{h=0}^{n_s G_v - 1} \left[B_{sj,\,(h)}\,(\varphi_{vk})\right]^2 \tag{2.29}$$

Subsequently averaging (2.29) with respect to φ, we obtain,

$$E\left[\Omega_{sj}^2\right] = \left(\frac{P_v G_v}{2P_s T_s^2}\right) \sum_{h=0}^{n_s - 1} U_v \left(\alpha_{sj,\,(h)}^2 + \beta_{sj,\,(h)}^2\right) \tag{2.30}$$

Using equations (2.28) and (2.30), the variance of I_{sj} can be expressed as,

$$Var\{I_{sj}\} = \frac{U_{sj} - 1}{2G_s} + \left(\frac{P_v G_v}{2P_s T_s^2}\right) \sum_{h=0}^{n_s - 1} U_v \left(\alpha_{sj,\,(h)}^2 + \beta_{sj,\,(h)}^2\right) \tag{2.31}$$

Similar to equation (2.22), the average bit error probability computed via the standard Gaussian approximation method for the *type s* traffic is,

$$P_{bsj} = Q\left(\sqrt{SNR_{sj}}\right) = Q\left(\sqrt{\left(\frac{2E_{bsj}}{N_0}\right)^{-1} + Var\{I_{sj}\}}\right) \tag{2.32}$$

where $Q(.)$ is the complementary error function as defined in (2.23), and SNR_{sj} denotes the average signal-to-noise ratio.

2.2.3 Conventional DS-CDMA

The performance of the conventional single-chip rate DS-CDMA scheme can be obtained from the expressions derived in Sections 2.2.1 and 2.2.2. By substituting $n_{cs} = 1$ in (2.21) and (2.31), the variance for MAI of the *type v* and *type s* traffic can be expressed as,

$$Var\{I_{v\,(conv)}\} = \frac{U_v - 1}{2G_v} + \left(\frac{P_s}{P_v}\right)\frac{U_{sj}}{2G_v} \tag{2.33}$$

$$Var\{I_{s\,(conv)}\} = \frac{U_{sj} - 1}{2G_s} + \left(\frac{P_v}{P_s}\right)\frac{U_v}{2G_s} \tag{2.34}$$

Then the average bit-error rate (BER) expressions for *type v* and *type s* traffic are given by,

$$P_{bv(conv)} = Q\left(\sqrt{\left(\frac{2E_{bv}}{N_0}\right)^{-1} + Var\{I_{v(conv)}\}}\right) \tag{2.35}$$

$$P_{bs(conv)} = Q\left(\sqrt{\left(\frac{2E_{bs}}{N_0}\right)^{-1} + Var\{I_{s(conv)}\}}\right) \tag{2.36}$$

2.3 Optimum Power Distribution

In this section, performance of the integrated services is analyzed and compared under different power control strategies based on equal signal strength (ESS) and equal error probability (EEP) rules. The ESS scheme maintains the power of received signals of all users at a fixed level. One possible choice is to keep the bit energy for all types of users at the same level, i.e.,

$$\frac{P_v}{P_s} = \frac{R_v}{R_s} \tag{2.37}$$

However, the ESS rule does not balance well with the natural dissimilarity between different quality requirements for *type v* and *type s* traffic. Hence, the performance of more vulnerable traffic degrades drastically as the number of active users supported by the network increases. In contrast, the equal error probability rule ensures that the bit-error rate of all the users is maintained at the minimum required level. In [11], it is shown that the optimum power allocation is mainly determined by the quality requirements of the heterogeneous traffic, and a simple way to estimate the optimal power assignment was suggested. Therefore, based on the EEP rule,

$$\frac{P_v}{P_s} = \left(\frac{QR_v}{QR_s}\right)\left(\frac{R_v}{R_s}\right) \tag{2.38}$$

where QR_v and QR_s denote the quality requirement for *type v* and *type s* traffic, respectively.

The performance of different power control strategies described here can be evaluated by substituting appropriate values for the power ratio P_v/P_s, and the bit energy in (2.21), (2.22), (2.31) and (2.32).

2.4 Numerical Results

In this section, we provide some representative numerical curves illustrating the capacities of multi-rate multi-service DS-CDMA systems, based on analytical results derived in the preceding sections. We construct four test systems as shown in Figure 2.2 to evaluate and compare the performance variations between these different multi-rate systems. Notice that *System I* corresponds to the conventional phase-coded spread-spectrum radio interface architecture. It is also assumed that power spectral density for all spread signals in the system is maintained at the same level (i.e., the ESS power control law is employed) for both conventional and new system topologies, unless stated otherwise.

It is apparent from Figure 2.2 (refer to test *System II*) that subsystems [2,1] and [2,2] are symmetric. Consequently, the quality of these subsystems will be identical provided each of them supports the same number of users. In contrast, *System III* and *System IV* consist of a mix of symmetric and nonsymmetric subsystems, and therefore average bit-error probabilities may be different for any two nonsymmetric subsystems with a fixed number of active users in the system. As an example, performance of the nonsymmetric subsystems in test *System IV* have been analyzed and the results are depicted in Figure 2.3. We plot the maximum value of U_v for each given U_s, while ensuring the bit-error rate for all users in the system is below 10^{-3}. For instance, to evaluate the quality of subsystems [4,4] and [4,5], we assign $U_{s1}=U_{s2}=U_{s3}=U_{s6}=U_{s7}=U_{s8}=0$, and $U_{s4}=U_{s5}$ if U_s is even, else $U_{s4}=U_{s5}+1$ when U_s is odd. An interesting point can be derived from this analysis. The results indicate that the larger the carrier frequency offset ω_{sj} (i.e., the farther the carrier frequency of *type s* users in a particular subsystem from the *type v* users' carrier frequency), the lower the magnitude of interference experienced in that particular subsystem, and thus lower the bit-error rate the corresponding subsystem can provide. This is because the $\cos(-\omega_{sj}t + \varphi_{vk})$ term in (2.26) causes different levels of interference for different j. A similar observation was noticed in [7]. Hence by using nonsymmetric channels, flexible quality of service can be achieved even for information of the same rate.

Figures 2.4 and 2.5 illustrate the capacities offered by test *System III* with various distributions of *type s* traffic, for single-bound and multi-bound of bit-error rate respectively. Based on our earlier discussions, the system capacity of the hybrid FDM/DS-CDMA approach is related to the distribution of the *type s* users in the system. Thus, we evaluate the impact of three different allocations of *type s* users on the system capacity:

(a) Uniform (equal) distribution of all the admitted *type s* users to every subsystem.

(b) Allocate the new calls to the appropriate subsystems such that the average interference of the entire system is minimized.

(c) Allocate the new incoming calls first to the subsystems with the carrier frequency farthest away from the *type v* user carrier frequency until the interference threshold limit for that particular subsystem is reached, and then to other subsystems in a similar fashion.

Although higher capacities are observed for all three types of distribution, admission policies based on criteria (b) and (c) mark a significant improvement. Criterion (c) remains optimal (for both cases of single and multiple bit-error rate bounds), in terms of maximizing the number of *type v* users supported by the system for a fixed number of *type s* users occupying the system. On the other hand, criterion (b) ensures that the multi-user interference experienced by all the users in the system is at the minimum level, i.e., provides the best service quality. Hence, the new hybrid scheme in conjunction with any of these two different options for implementing the admission protocol will maximize the system capacity and improve the offered grade of service. Therefore, either of these approaches can be selected based on complexity, ease of implementation (reduced task of the resource manager) or other relevant factors. Furthermore, the capacity improvement is more pronounced in a multi-service scenario. This suggests that the proposed hybrid radio interface topology is capable of facilitating different QoS contracts for multi-media networks.

In Figure 2.6, the average bit-error probability of *System III (b)* is plotted as a function of E_b/N_0 for fixed numbers of *type v* and *type s* users occupying the system. It is evident that the new system architecture outperforms the traditional spreading approach by providing a higher grade of service for all the users in the system. Subsequently in Figure 2.7, the number of *type s* active users in test *System III (c)* is plotted as a function of E_{bv}/N_0, for different values of *type v* users. The performance of the conventional single chip-rate scheme is also shown for comparison. From this analysis, we can conclude that the capacity of the new system is more robust to variations in the ratio of E_{bv}/E_{bs} than the latter, and therefore is less susceptible to power control errors. In addition, an estimate for the optimum power assignment in *System I* suggested by [11] (described in (2.38)) is also apparent from this figure. We confirm that this simple estimation is also valid for our new multi-chip rate system.

Notice that results presented in Figures 2.3-2.7 correspond to the performance of a single processing gain network architecture. However, systems with multiple chip-rates and processing gain values are anticipated to exist in future, in particular because they offer greater flexibility in designing an integrated network. Besides, such network topology may also exist in the ISM band with different applications supported via different bandwidths in overlapping bands. Moreover, it would be interesting to find out how the interference in between these subsystems may affect the system capacity and transmission quality while moving away from this single processing gain restriction. These results are illustrated in Figures 2.8-2.11.

Figure 2.8 compares the performance of *System I-IV* with a single quality of service requirement both traffic types, whereas in Figure 2.9, the grade of service for the high-rate traffic is more stringent than the lower-rate traffic. Subsequently, the system capacities for different multi-rate system architectures are illustrated in Figure 2.10 when the bit-error rate requirements for these two traffic classes are interchanged. Results presented in Figures 2.8, 2.9 and 2.10 suggest that the capacity gain increases as we increase the number of narrowband CDMA subsystems but gets saturated afterwards. Therefore, *system III* will be preferred for the system parameters considered in this analysis because it yields a good trade-off between performance and system complexity. Consequently, increasing the number of subsystems beyond the five subsystems topology makes the system design less profitable.

Figure 2.11 depicts the performance of test *System I-IV* carrying multimedia traffic with optimized power assignment. As expected, the system capacity and grade of service are further enhanced by employing the EEP power control strategy. Furthermore, comparison between results exhibited in Figure 2.9 and Figure 2.11 implies that ESS rule do not balance well the natural dissimilarities between the different quality requirements for the heterogeneous traffic. While maintaining the received energy per bit to be equal (based on ESS strategy) for all the users, performance of more vulnerable traffic degrades drastically as the number of simultaneous users supported by the network increases. In contrast, the EEP rule ensures that the bit-error rate of all the users is maintained at the minimum required level.

2.5 Conclusions

In summary, we have presented a hybrid signalling scheme which simultaneously minimizes interference and provides variable quality of service (QoS) contracts for the heterogeneous traffic in a DS-CDMA network. Using the Gaussian approximation method, we have derived the average bit-error rate expressions, and estimate the number of users that can simultaneously transmit without exceeding a predetermined performance measure for each different class of traffic. The analysis presented in this paper is essential in view of the gradual evolution of an IWAN architecture which is anticipated in the very near future. In particular, we have investigated how user distributions in various subsystems affect the system capacity and transmission quality. Subsequently, two different options for implementing the admission policy were suggested to maximize the system capacity. Different power control strategies based on ESS and EEP rules were presented and analyzed. The EEP rule offers higher capacity provided that resources and interference budgets are not exceeded. It has been shown that the proposed FDM/DS-CDMA network architecture is superior to the conventional single chip-rate system, both in terms of system capacity and flexibility in facilitating different service requirements in a multi-media scenario, regardless which type of power control strategy is employed. Our results recommend the multiple chip rates radio interface as an attractive alternative to achieve the goal of improving spectrum utilization of the future multi-rate multi-service CDMA personal communication systems.

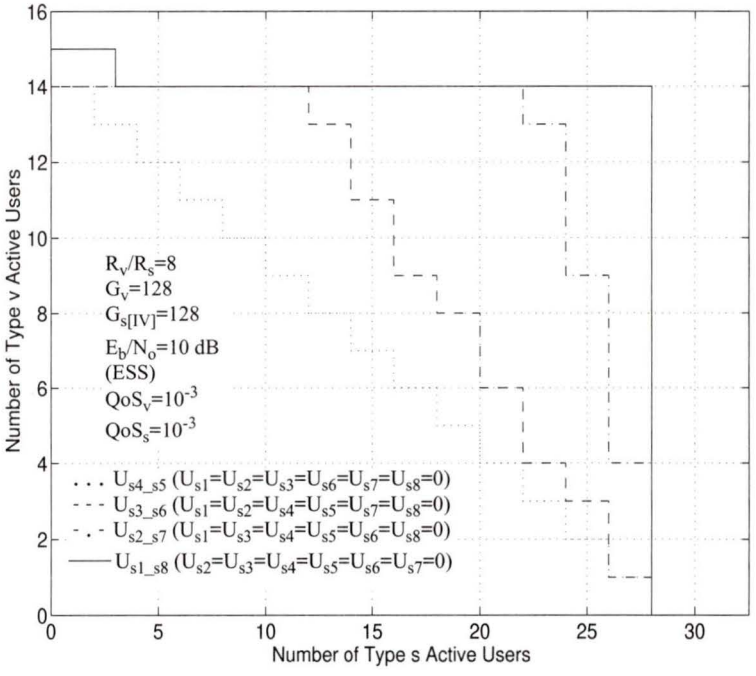

Figure 2.3 Performance of non-symmetric subsystems in the test system IV.

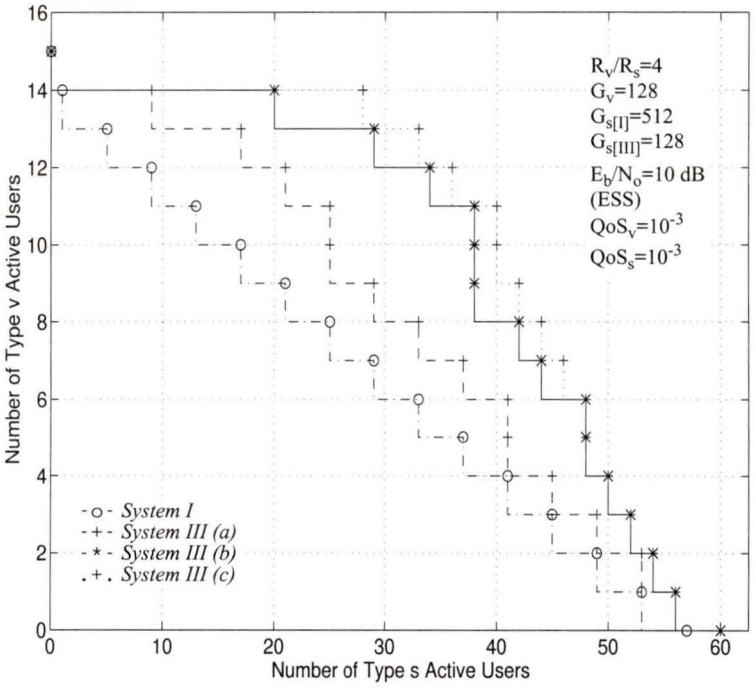

Figure 2.4 The effect of different admission policies (various criteria for allocating the *type s* users to the narrowband subsystems) on the test System III capacity.

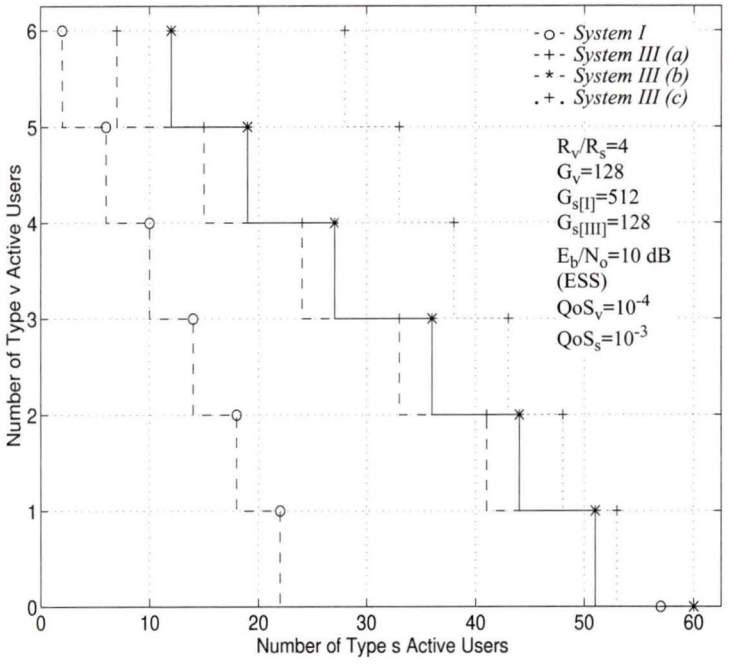

Figure 2.5 Capacity comparison between System I and System III with different admission policies for multiple bit-error rate bounds (multi-service scenario).

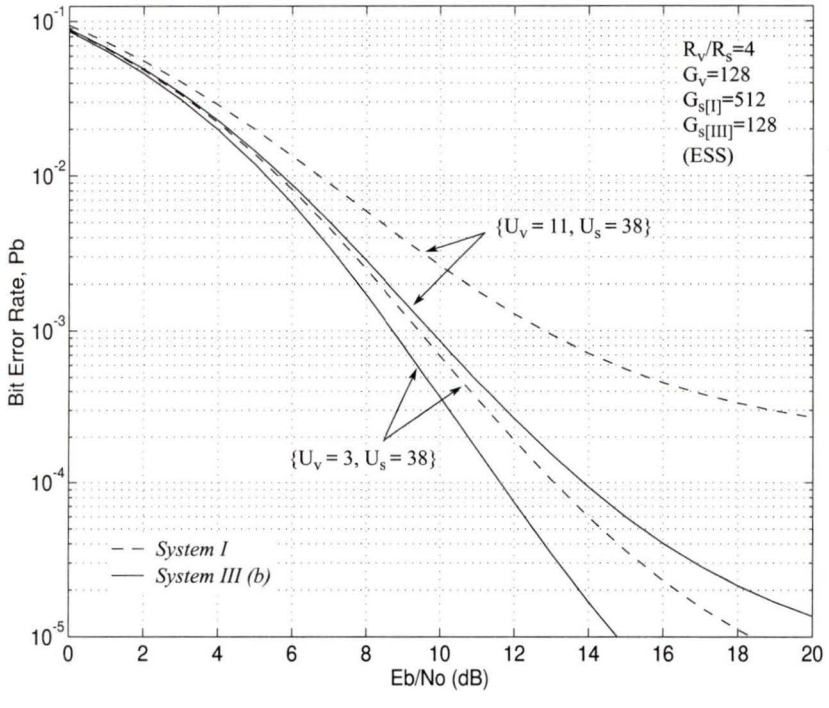

Figure 2.6 Average bit-error probability of System I and III as a function of bit energy per noise ratio E_b/N_o, for fixed numbers of *type v* and *type s* users occupying the system.

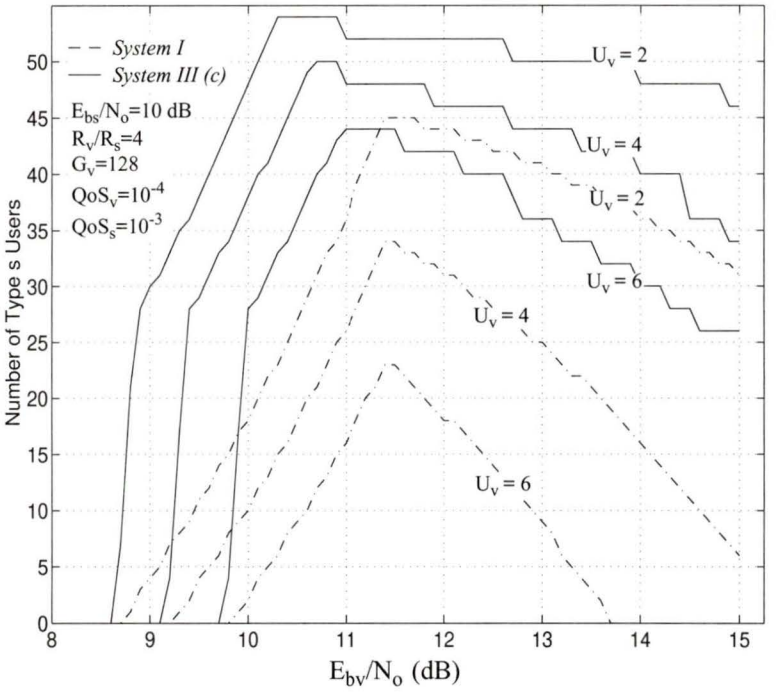

Figure 2.7 Analysis of optimal power allocation and the impact of variations in E_{bv}/E_{bs} on the system capacity.

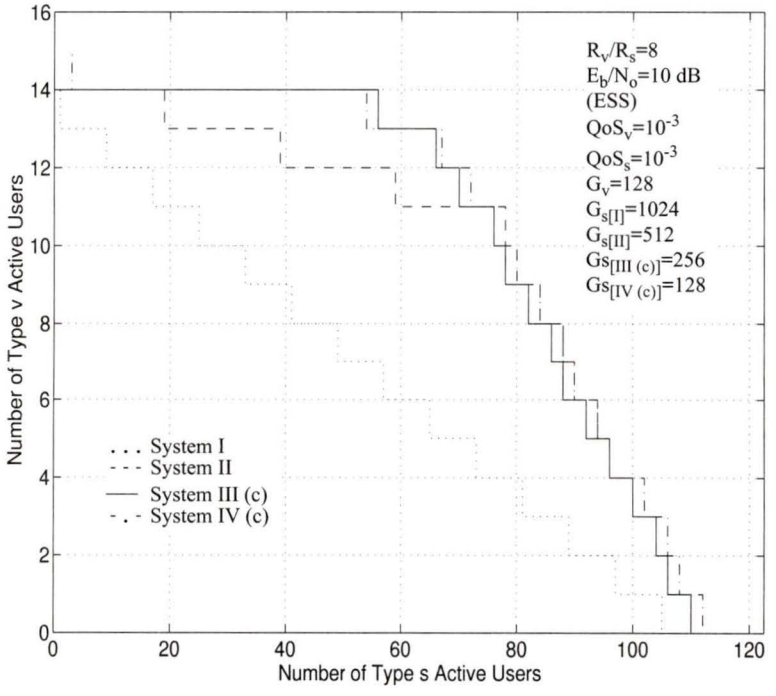

Figure 2.8 Capacity comparison between various flexible system configurations (multiple chip rates and processing gain values) with a single QoS requirement.

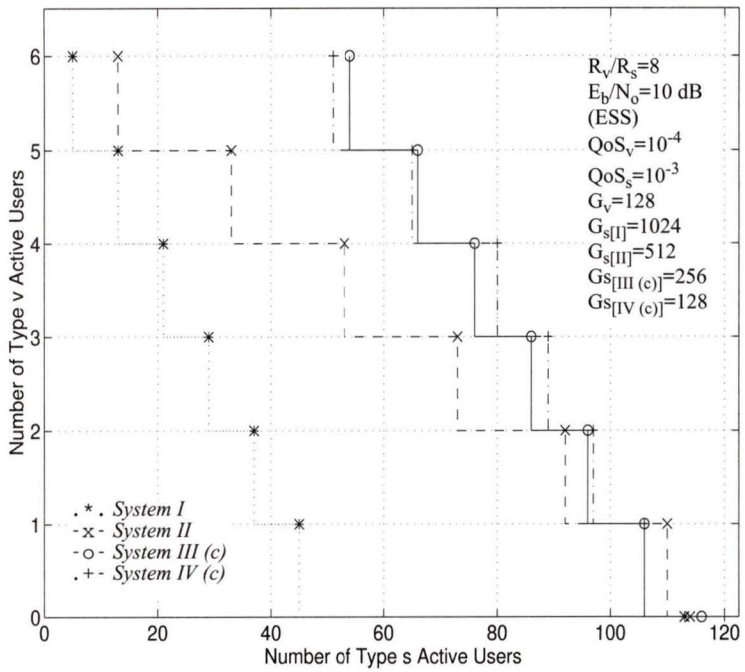

Figure 2.9 Performance of System I-IV (operating at multiple chip rates and processing gain values) in an integrated network with multiple QoS requirements.

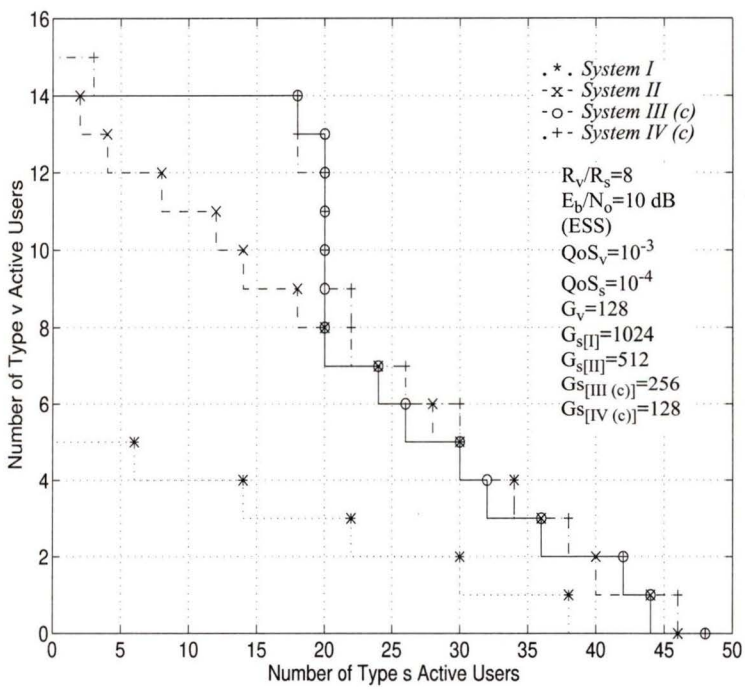

Figure 2.10 Performance of System I-IV carrying multi-media traffic with different QoS requirements, and power control strategy based on ESS criteria.

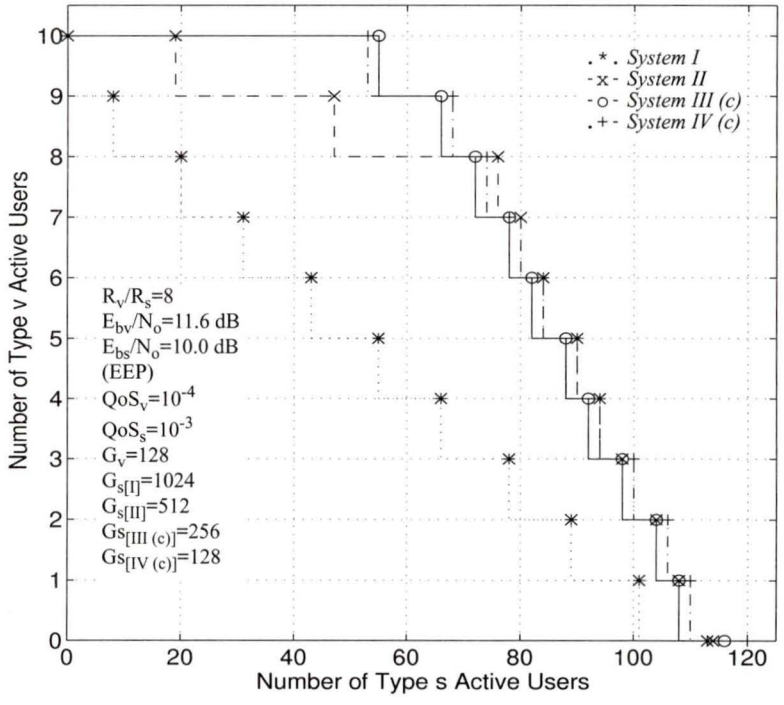

Figure 2.11 Performance of System I-IV carrying multi-media traffic (multi-rate multi-service requirements) with optimized power allocation (EEP power control strategy).

Chapter 3

Micro-diversity Reception Techniques for Phase Coded Spread-Spectrum Signals

Diversity reception has long been recognized as an effective technique for combatting the detrimental effects of channel fading. The underlying premise is that if several uncorrelated replicas of a signal are received over multiple diversity branches with comparable strengths, then it is improbable that these signals will experience simultaneous deep fades. Diversity methods can be employed either at the base station (macroscopic diversity or macro-diversity) or at the mobile (microscopic diversity or micro-diversity), although the antenna separation required differs for each case [31]. In practice, micro-diversity reception combats the fast fading variations in the received signal strength caused by multipath fading, whereas macro-diversity combats the slower fading variations caused by shadowing [12].

To capitalize on the improvement in signal statistics due to diversity, several combining techniques have been proposed, and they can be categorized into two main groups, namely switched combining and gain combining. Among these approaches, selecting the best diversity reception is the simplest and perhaps the most frequently used form of diversity combining [21]. It is also worth mentioning here that the improvements achieved through diversity reception are usually at the expense of increased system complexity. For instance, in a signal-to-noise ratio based diversity scheme, some type of SNR measuring device is required or a pilot tone calibration scheme may be employed [12]. Therefore, techniques of improving the system performance without incurring a substantial penalty in terms of implementation complexity or cost are of practical interest.

The conventional selection diversity system measures the signal-to-noise plus interference ratio (SNIR) at each branch (i.e., antenna) and chooses the branch with the highest SNIR value for data recovery. Thus, if Mth order diversity is employed and the mean

noise power is assumed to be identical for all branches, then the decision criterion reduces to $\max[\alpha_i]$, $i = 1, \ldots, M$, where α_i is the channel gain from the ith branch [14]. However in practice, measurements of SNIR may be difficult or expensive [12], especially for high data rate transmissions. To be most effective, the system should be able to make its selection in a period of time equal to or less than the interval of the shortest signal that will be transmitted. Consequently, the branch with the largest amplitude of the received composite signal is chosen.

In a related work [14], *Chyi et. al.* evaluated the performance of two receiver structures for M-ary orthogonal signalling over a frequency non-selective Rayleigh fading channel. They have shown that the traditionally accepted analysis which selects the branch with the highest SNR produces inferior performance indication of an S+N selection system. Subsequently in [17], an explanation for this observation was furnished, with the reason being that the conventional selection diversity model does not take into account the stochastic nature of the noise. In [15], we studied the performance of two different selection diversity schemes for slotted DS/CDMA packet radio communications over a frequency-selective Rayleigh fading channel. A simple and practical selection combining rule has been proposed, in which the amplitude of the received composite signal is used in the selection diversity process. The scheme lends itself to a low-complexity receiver structure [15], and is particularly attractive for high signalling rates.

In this chapter, we first analyze the performance of various pre-detection diversity techniques in a Nakagami multipath fading channel. Nakagami's m-distribution is a versatile statistical model, which can accurately fit experimental data for many physical propagation channels. Computationally efficient formulas are derived to evaluate the average bit error probability of a phase-coded spread-spectrum receiver with antenna (spatial) diversity reception. In addition to the SNIR and S+I-selection methods, performance of an optimum linear diversity combiner is also evaluated for comparison. Emphasis is placed on simpler models that yield to analysis and that allow for unique insights, without being too unrealistic. We show that these insights apply to actual systems. The analysis presented here is also valid for frequency and time-diversity schemes. Subsequently, we investigate the effects of unequal mean signal strengths on the bit-error rate performance.

3.1 System Description

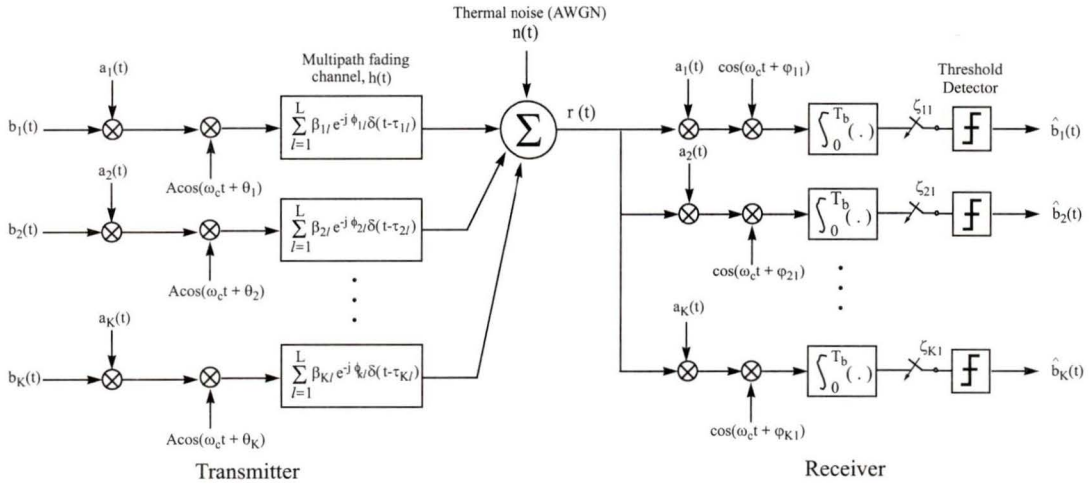

Figure 3.1 System model for a DS/CDMA network operating over a frequency-selective multipath fading channel.

3.1.1 Transmitter Model

The system model to be considered consists of K active users transmitting binary data simultaneously to a central-station (the first user being the reference user whose performance is to be evaluated), as depicted in Figure 3.1. Each transmitter or user is assigned a unique long PN sequence which modulates the data waveform along with the carrier. Then the transmitted signal of the kth user can be expressed as,

$$s_k(t) = \sqrt{2P_k}\, b_k(t)\, a_k(t) \cos(\omega_c t + \theta_k) \tag{3.1}$$

where $b_k(t)$ is the data sequence of unit amplitude, antipodal rectangular pulses of duration T_b and $a_k(t)$ corresponds to the spreading waveform which consists of periodic antipodal binary sequences of duration T_c. P_k and ω_c denote the transmitted power by the kth user and common angular carrier frequency respectively. θ_k is the phase angle introduced by the kth PSK modulator and is modeled as an i.i.d. random variable uniformly distributed over $[0, 2\pi)$. The data signal of the kth user may be written as,

$$b_k(t) = \sum_{j=-\infty}^{\infty} b_{k,j} P_{T_b}(t - jT_b) \tag{3.2}$$

and the spreading signature waveform as,

$$a_k(t) = \sum_{j=-\infty}^{\infty} a_{k,j} P_{T_c}(t - jT_c) \tag{3.3}$$

where $b_{k,j}$ and $a_{k,j}$ denote the jth bit from the kth user's source and signature waveforms respectively, and are assumed to be mutually independent antipodal binary sequences with amplitude taking values from $\{\pm 1\}$ with equal probability. We assume the chip waveform P_{T_x} to be a rectangular pulse, i.e., $P_{T_x} = 1$ for $0 \le t \le T_x$, $P_{T_x} = 0$ otherwise.

3.1.2 Channel Model

Here we characterize the link between a transmitter and its receiver as a Nakagami multipath fading channel. The Nakagami's m-distribution [24] is a generalized statistical distribution which can model different fading environments. This analytical model assumes that the received signal is a sum of vectors with random strengths and phases. As a consequence, this distribution provides greater flexibility and accuracy in matching some experimental data statistics [24]. For example, Suzuki [25] and Braun and Dersch [27] have shown that Nakagami distributions fit some urban radio multipath channel data better than Rayleigh, Rice, or lognormal distributions. It also has the advantage of including the Rayleigh and one-sided Gaussian distribution as special cases. Furthermore, it can be used to model fading conditions that are less or more severe than those modelled by the Rayleigh distribution [13].

The multipath fading channel is modelled as frequency selective in that the chip rate $1/T_c$ is higher than the channel coherence bandwidth. In this case, the discrete multipath components in the received signal are resolvable with a resolution in time delay of T_c, the chip duration. The maximum number of resolvable paths is,

$$L = \lfloor T_m / T_c \rfloor + 1 \tag{3.4}$$

where T_m is the maximum multipath delay spread. T_m is assumed to be less than the symbol duration to avoid intersymbol interference [18]. The complex low-pass equivalent impulse response of the channel for the link between the kth user transmitter and its receiver is,

$$h_k(t) = \sum_{l=1}^{L} \beta_{kl} \exp(j\phi_{kl}) \, \delta(t - \tau_{kl}) \tag{3.5}$$

where $\delta(.)$ is the Dirac impulse response while β_{kl}, τ_{kl}, ϕ_{kl} are the lth path gain, time delay and phase delay respectively of the kth user. In (3.5), ϕ_{kl} and τ_{kl} are assumed to be uniform in $[0, 2\pi)$ and $[0, T_b)$ respectively. This will naturally result in a worst-case scenario, rendering the results conservative [20]. We assume β_{kl} is a Nakagami random variable, and has probability density function (p.d.f.) in the form,

$$f_{\beta}(R) = \frac{2m^m R^{2m-1}}{\Gamma(m)\,\Omega^m} \exp\left(\frac{-mR^2}{\Omega}\right) u(R) \tag{3.6}$$

where $u(.)$ denotes the unit-step function and $\Gamma(.)$ corresponds to the Gamma function. The scalar parameter m in (3.6) is defined as the ratio of moments, called the fading figure [24],

$$m = \frac{\Omega^2}{E\left[(R^2-\Omega)^2\right]} \geq \frac{1}{2} \tag{3.7}$$

where $\Omega = E[R^2]$, and $E[.]$ represents the mean function. The Rayleigh p.d.f. is obtained for $m = 1$, and $m = 0.5$ gives the p.d.f. for one-sided Gaussian random variables. The nonfading case corresponds to $m = \infty$. The average power of the desired signal is given by $\Omega/2$.

The output signal $y(t)$ produced by the multipath fading channel model consists of a sum of delayed, phase shifted, attenuated replicas of the input signal, and therefore can be expressed as,

$$y_k(t) = \sum_{l=1}^{L} Re\{\beta_{kl}\, s_k(t-\tau_{kl}) \exp(j\phi_{kl})\} \tag{3.8}$$

where $Re\{.\}$ denotes the real part.

3.1.3 Receiver Model

The channel output $y(t)$ is further corrupted by multiple access interference as well as system thermal noise, which is modeled as additive white Gaussian noise $n(t)$ with two-sided spectral density $N_o/2$. Therefore, the received signal at the base-station is given by (see Figure 3.1),

$$
\begin{aligned}
r(t) &= \sum_{k=1}^{K} y_k(t) + n(t) \\
&= \sum_{k=1}^{K} \sum_{l=1}^{L} \sqrt{2P_k}\,\beta_{kl}\, a_k(t-\tau_{kl})\, b_k(t-\tau_{kl}) \cos(\omega_c t + \varphi_{kl}) + n(t)
\end{aligned}
\tag{3.9}
$$

where $\varphi_{kl} = \theta_k + \phi_{kl} - \omega_c \tau_{kl}$. In our analysis, we have assumed a correlation receiver (matched filter) as in [19]-[20]. It is worth noting that any diversity combining technique employed to combine the multipaths will also enhance the overall performance of our system.

For coherent reception, we can assume that the reference Receiver 1 can recover the carrier phase and ideally delay lock onto the first arriving signal path. For mathematical simplification and with no loss in generality, let us also assume $\tau_{11} = 0$ and $\varphi_{11} = 0$, because we are only concerned with relative time delays and phase angles. After the correlation operation that collapses the wideband coded signal into a narrowband modulated signal and the demodulation process, a signal sample at the receiver low-pass filter output can be expressed as,

$$
\zeta_{11} = \beta_{11}\sqrt{\frac{P}{2}}\,T_b\, b_{1,0} + \sqrt{\frac{P}{2}}\,T_b\,(I_m + F_m) + \eta \tag{3.10}
$$

where $b_{1,0}$ is the polarity of the data bit that needs to be detected, and $\eta = \int_0^{T_b} n(t)\, a_1(t) \cos(\omega_c t)$. I_m corresponds to the multiuser interference,

$$
I_m = \sum_{k=2}^{K} \beta_{k1} \left[\frac{b_{k,-1}\, R_{k,1}(k, \tau_{k1}) + b_{k,0}\, \hat{R}_{k,1}(k, \tau_{k1})}{T_b} \right] \cos(\varphi_{k1}) \tag{3.11}
$$

and F_m is due to multipath interference,

$$
F_m = \sum_{k=1}^{K} \sum_{l=2}^{L} \beta_{kl} \left[\frac{b_{k,-1}\, R_{k,1}(k, \tau_{kl}) + b_{k,0}\, \hat{R}_{k,1}(k, \tau_{kl})}{T_b} \right] \cos(\varphi_{kl}) \tag{3.12}
$$

Here $b_{k,-1}$ and $b_{k,0}$ denote the previous and current data bit of the kth user, respectively. $R_{ki}(\tau)$ and $\hat{R}_{ki}(\tau)$ are the continuous time partial cross-correlation functions, and are defined as in [10].

$$R_{k,i}(k,\tau) = \int_0^{\tau} a_i(t)\, a_k(t-\tau)\, dt \tag{3.13}$$

$$\hat{R_{k,i}}(k,\tau) = \int_{\tau}^{T_b} a_i(t)\, a_k(t-\tau)\, dt \tag{3.14}$$

In arriving at (3.10), we have assumed that average power control is employed, which means that on the average, the same power is received from each active user. The first term in equation (3.10) represents the desired signal to be detected while the final term is a Gaussian random variable with zero mean and variance (power) $N_0 T_b/4$, due to AWGN.

3.2 Error Probability Analysis

In this section, analytical expressions are derived to evaluate the bit error probabilities of a correlation receiver with antenna diversity reception, by modelling the multiple access interference (MAI) as a Gaussian process. The efficacy of selection diversity is studied by considering two different combining rules, namely SNIR and S+I selection diversity. Performance of an optimum linear diversity combiner is also evaluated for comparison. The standard Gaussian approximation method for MAI is very attractive due to its simplicity. It also yields reasonably accurate results, especially for high bit-error rates (BER), small signal-to-noise ratio (SNR) and processing gain values, and if SNR is conditioned on fading random variable [20].

A prerequisite to the application of Gaussian approximation is the knowledge of the variance of multiple access interference. Variance of the cross-correlation function for Gold codes has been derived in [10], and is given by,

$$E\left\{\frac{\left[\alpha_{-1} R(\tau) + \alpha_0 \hat{R}(\tau)\right]^2}{T_b^2}\right\} = \frac{2}{3N} \tag{3.15}$$

where $\alpha_y \in \{\pm 1\}$, $y = \{-1, 0\}$, are independent and identically distributed binary random variables. N denotes the system processing gain, and therefore each bit is encoded with N chips. Following the central limit theorem, the total interference is assumed to be Gaussian distributed with zero mean, and variance equal to the sum of variances of all the terms that contribute to multiple access interference in (3.10).

$$Var\{MAI\} = \sigma^2 = \frac{PT_b^2}{2}\left(\frac{(K-1)}{3N}E\left[\beta_{k1}^2\right] + \frac{K}{3N}\sum_{l=2}^{L}E\left[\beta_{kl}^2\right]\right) + \frac{N_0 T_b}{4} \tag{3.16}$$

Hence, the signal-to noise plus interference ratio is given by,

$$SNIR = \frac{\beta_{11}^2}{\frac{1}{3N}\left[(K-1)E\left[\beta_{k1}^2\right] + K\sum_{l=2}^{L}E\left[\beta_{kl}^2\right]\right] + \frac{N_0}{2E_b}} = 2\gamma_b \tag{3.17}$$

where γ_b denotes the received signal-to-noise ratio (usually referred as SNR per bit [13]).

The sample (decision statistic) of the received composite signal described in (3.10) can be further simplified and re-written in a more compact form,

$$\zeta_j \equiv \alpha_j b_0 + n_j \tag{3.18}$$

where $\alpha_j = \sqrt{P/2}\,T_b\beta_j$ is the fading sample, n_j is the MAI (multipath and multi-user interference plus AWGN noise) sample with variance σ_j^2, and b_0 is the polarity of the data bit being detected. Also, α_j and n_j are assumed to be independent and identically distributed Nakagami and Gaussian random variables, respectively. Subscript j corresponds to the jth copy of a signal available at the receiver for detection, $j \in \{1, 2, \ldots, M\}$, where M denotes the diversity order.

3.2.1 SNIR-Selection Diversity

The conventional selection diversity model specifies that of M diversity branches, the one providing the largest signal-to-noise plus interference ratio (SNIR) be selected for data recovery. Improvement in signal reception is achieved by the uncorrelated nature of the signals from the multiple antennas, i.e., the likelihood that all of the M signals fade simultaneously is much lower than the fading probability of any signal from a single branch. If we assume that $b_0 = +1$ was transmitted, then the conditional error probability is given by,

$$Prob\{\zeta_j < 0 \mid b_0 = +1\} = \sum_{j=1}^{M} Prob\left\{\alpha_j + n_j < 0\,,\ \frac{\alpha_j^2}{\sigma_j^2} > \frac{\alpha_i^2}{\sigma_i^2}\,,\ \text{for } i \neq j\right\} \tag{3.19}$$

In [18], statistics from the self-interference, multiple-access interference, and Gaussian noise are assumed to be same on each diversity branch. Consequently, the selection

diversity process is simplified by considering the largest path gain as the best estimate of the transmitted signal, $\beta_{max} = max\{\beta_{1j}\}, 1 \le j \le M$.

With the assumption that all β_{1j}, $j \in \{1, 2, \ldots, M\}$, are independent and identically distributed Nakagami random variables, the probability density function of β_{max} can be evaluated by,

$$f_{\beta_{max}}(x) = M f_{\beta}(x)\left(\int_0^x f_{\beta}(y)\,dy\right)^{M-1} \tag{3.20}$$

where f_{β} is described in (3.6), and its cumulative distribution function is given by,

$$\begin{aligned}\int_0^x f_{\beta}(y)\,dy &= \frac{2}{\Gamma(m)}\left(\frac{m}{\Omega}\right)^m \int_0^x y^{2m-1}\exp\left(\frac{-my^2}{\Omega}\right)dy \\ &= 1-\exp\left(\frac{-mx^2}{\Omega}\right)\left[\sum_{k=0}^{m-1}\frac{1}{k!}\left(\frac{mx^2}{\Omega}\right)^k\right], \quad m \in \{integer\}\end{aligned} \tag{3.21}$$

Assuming that the data bits are equiprobable, and owing to the statistical symmetry property of the decision variable, we can compute the bit error rate as follows,

$$P_b = Prob\{\zeta_j < 0 \mid b_0 = +1\} = \int_0^{\infty} Q\left(\sqrt{2\gamma_b}\right) f_{\beta_{max}}(\beta_{11})\,d\beta_{11} \tag{3.22}$$

where γ_b and $f_{\beta_{max}}$ are described in (3.17) and (3.20), respectively. $Q(.)$ denotes the complementary error function, which is defined as,

$$Q(x) = \frac{1}{\sqrt{2\pi}}\int_x^{\infty}\exp\left(\frac{-u^2}{2}\right)du = \frac{1}{2}\mathrm{erfc}\left(\frac{x}{\sqrt{2}}\right) \tag{3.23}$$

If the effects of unequal mean signal strengths are taken into account, then the average bit error rate can be evaluated by [see Appendix B],

$$\begin{aligned}P_b = \sum_{j=1}^{M}\int_0^{\infty} Q\left(\sqrt{\gamma_j}\right)\frac{m^m \gamma_j^{m-1}}{\Gamma(m)\,\bar{\gamma}_j^m}\exp\left(\frac{-m\gamma_j}{\bar{\gamma}_j}\right) \\ \cdot \prod_{i=1, i\neq j}^{M}\left[1-\exp\left(\frac{-m\gamma_j}{\bar{\gamma}_i}\right)\sum_{k=0}^{m-1}\frac{1}{k!}\left(\frac{m\gamma_j}{\bar{\gamma}_i}\right)^k\right] d\gamma_j\end{aligned} \tag{3.24}$$

where $\gamma_j = \alpha_j^2/\sigma_j^2$ and $\bar{\gamma}_j$ denote the instantaneous received signal-to-noise plus interference ratio (SNIR) of the jth diversity branch and its mean value, respectively.

3.2.2 S+I Selection Diversity

In an S+I selection scheme, the branch with the largest amplitude of the received composite signal is chosen for data recovery. Consequently, the scheme lends itself to a low-complexity receiver structure, and is particularly attractive for high data rate traffic. It should be noted that in our scheme, selection diversity is employed at the bit level to increase the reliability of the signal being detected. While using the signals from each diversity branch alone might not enable the receiver to recover the transmitted data, combining these replicas enhances the probability of this recovery. Then the average probability of bit error is given by,

$$\begin{aligned} P_b &= 1 - \sum_{j=1}^{M} Prob\{\zeta_j > 0 \,|\, b_0 = +1, |\zeta_j| > |\zeta_i|,\ i \neq j\} \\ &= 1 - \sum_{j=1}^{M} \int_0^{\infty} f_\zeta(\zeta_j) \prod_{i=1, i\neq j}^{M} \left[\int_{-\zeta_j}^{\zeta_j} f_\zeta(\zeta_i)\, d\zeta_i \right] d\zeta_j \end{aligned} \tag{3.25}$$

where $f_\zeta(x)$ denotes the probability density function of the decision variable ζ_j. To facilitate the analysis, the transformation $z_j = \zeta_j/\sigma_j$, $j = 1, 2, \ldots, M$, is considered, without affecting the results. Consequently, equation (3.25) can be re-stated as,

$$P_b = 1 - \sum_{j=1}^{M} \int_0^{\infty} g_\zeta(z_j) \prod_{i=1, i\neq j}^{M} \left[\int_{-\frac{\sigma_j}{\sigma_i} z_j}^{\frac{\sigma_j}{\sigma_i} z_j} g_\zeta(z_i)\, dz_i \right] dz_j \tag{3.26}$$

Assuming that $b_0 = +1$ was transmitted, the random variable z_j is the sum of a Gaussian random variable and a Nakagami distributed random variable. Therefore, the p.d.f. of $g_\zeta(x)$ can be easily obtained through convolution of their individual density functions,

$$g_\zeta(z_j) = \int_0^{\infty} \frac{1}{\sqrt{2\pi}} \exp\left(\frac{-(z_j - x)^2}{2} \right) \frac{2m^m x^{2m-1}}{\Gamma(m) \left[\Omega_j/\sigma_j^2 \right]^m} \exp\left(\frac{-mx^2}{\Omega_j/\sigma_j^2} \right) dx \tag{3.27}$$

After some mathematical manipulations, equation (3.27) can be re-written as [refer to Appendix C],

$$g_\zeta(z_j) = \frac{2m^m \Gamma(2m)}{\sqrt{2\pi}\,\Gamma(m)\,\bar{\gamma}_j^{\,m}} \left(\frac{2m + \bar{\gamma}_j}{\bar{\gamma}_j} \right)^{-m} \exp\left(\frac{-z_j^2 (4m + \bar{\gamma}_j)}{4(2m + \bar{\gamma}_j)} \right) D_{-2m}\left(-z_j \sqrt{\frac{\bar{\gamma}_j}{2m + \bar{\gamma}_j}} \right) \tag{3.28}$$

where $D_{-v}(z)$ is the function of the parabolic cylinder [29] of order v and argument z. It is worth noting that $D_{-2m}(z)$ can be computed efficiently using the following recurrence relationship,

$$D_{p+1}(z) - zD_p(z) + pD_{p-1}(z) = 0 \tag{3.29}$$

with specific cases $D_{-1}(z)$ and $D_{-2}(z)$ given by (3.30) and (3.31), respectively.

$$D_{-1}(z) = \sqrt{\frac{\pi}{2}} \exp\left(\frac{z^2}{4}\right) \operatorname{erfc}\left(\frac{z}{\sqrt{2}}\right), \tag{3.30}$$

$$D_{-2}(z) = \exp\left(-\frac{z^2}{4}\right) - z \exp\left(\frac{z^2}{4}\right) \sqrt{\frac{\pi}{2}} \operatorname{erfc}\left(\frac{z}{\sqrt{2}}\right). \tag{3.31}$$

A numerical integration (Gaussian quadrature [23]) technique is applied to compute the average probability of bit error described in (3.26).

3.2.3 Maximum-Ratio Diversity

Maximum-ratio combining is known to be optimum in the sense that it yields the best statistical reduction of fading in any linear diversity combiner. In this technique, the M diversity branches are first co-phased and then weighted proportional to their signal level before summing. The output of the maximum-ratio combiner can be expressed as a single decision variable in the form,

$$U = \left(\sum_{j=1}^{M} \frac{\alpha_j^2}{\sigma_j^2} \right) b_0 + \sum_{j=1}^{M} \frac{\alpha_j n_j}{\sigma_j^2} \tag{3.32}$$

For a fixed set of $\{\alpha_j\}$, the decision variable U is Gaussian with mean, $E[U] = \sum_{j=1}^{M} \alpha_j^2 / \sigma_j^2 = \gamma$. Subsequently, the average probability of bit error can be expressed as [see Appendix D],

$$\begin{aligned} P_b &= \int_0^\infty Q\left(\sqrt{\gamma}\right) f_{\gamma_{mrc}}(\gamma)\, d\gamma \\ &= \sum_{j=1}^{M} \sum_{k=1}^{m} A_{jk} \left[\frac{1}{2}(1-\mu_j)\right]^k \sum_{i=0}^{k-1} \binom{k-1+i}{i} \left[\frac{1}{2}(1+\mu_j)\right]^i \end{aligned} \tag{3.33}$$

where $\mu_j = \sqrt{\bar{\gamma}_j / (2m + \bar{\gamma}_j)}$, and A_{jk} is defined as,

$$A_{jk} = \frac{(-m)^{m-k}}{(m-k)!\,\bar{\gamma}_j^{\,m-k}} \frac{d^{m-k}}{dx^{m-k}} \left[\prod_{i \neq j} \left(1 - \frac{\bar{\gamma}_i x}{m} \right)^{-m} \right] \Bigg|_{x = \frac{m}{\bar{\gamma}_j}} \tag{3.34}$$

If we assume that α_j and n_j, $j = 1, 2, \ldots, M$, are statistically mutually independent and identically distributed Nakagami and Gaussian random variables respectively, then equation (3.33) can be simplified as,

$$P_b = \left[\frac{1}{2}(1-\mu) \right]^{mM} \sum_{i=0}^{mM-1} \binom{mM-1+i}{i} \left[\frac{1}{2}(1+\mu) \right]^{i} \tag{3.35}$$

where $\mu = \sqrt{\bar{\gamma} / (2m + \bar{\gamma})}$, and $\bar{\gamma}$ is the mean SNIR (which is the same on every branch). For the particular case of $m = 1$ and $M = 1$, (3.35) reduces to the familiar expression for P_b in a Rayleigh fading channel with no diversity. Also notice that when $m = 1$, the bit error rate for M-diversity maximum ratio combiner in Rayleigh fading is equivalent to the expression given in Proakis [12, 14-4-15].

3.3 Numerical Results and Discussions

In this section, we provide some representative numerical curves illustrating the performance of a DS/CDMA network over a Nakagami multipath fading channel, based on the analytical results derived in the preceding sections. Figure 3.2 illustrates the probability of error of binary PSK signals with fading figure m as a parameter. Recall that $m = 1$ corresponds to Rayleigh fading. The system performance improves as m increased above unity, which is indicative of the fact that fading is less severe. We have also verified that when the average signal power is zero (i.e., $\bar{\gamma}_b = 0$ or $\bar{\gamma}_b\,(in\ dB) \rightarrow -\infty$), the probability of bit-error is 0.5 (not shown in this figure), which is anticipated for BPSK signals.

We now discuss the system performance with micro-diversity reception. First consider Figure 3.3, which compares the bit-error rate (BER) performance of BPSK signals with different combining techniques and varying diversity order M={1, 2, 3, 4}, over a Rayleigh fading channel. Obviously, all of the diversity combining methods yield identical results for a single diversity branch. It is also apparent from this figure that the largest diversity gain is obtained using 2-branch diversity and diminishing returns are obtained

with increasing order of M. This is typical for all diversity techniques. Another interesting point to note is that the proposed S+I selection rule outperforms the traditional selection scheme. The explanation for this observation has been furnished in [17]. This result is also intuitively satisfying because there is opportunity for at least one of the samples to be less noisy than the mean of the samples, owing to the stochastic nature of the noise. As an example, the differences in required SNR per bit predicted by the S+I selection model with respect to the conventional selection scheme for dual-diversity and four-fold diversity systems are 0.9 dB and 1.4 dB respectively, at an average BER of 10^{-3}. As we can see, the difference becomes more evident with a larger number of diversity branches. This may be attributed to the increased number of choices among statistically independent Gaussian-distributed multiple access interference samples.

Figure 3.4 depicts the bit error performance for binary PSK signals over a Nakagami fading channel with fading figure $m = 2$. Similar trends as in the Rayleigh fading case were observed here, with an exception that the results are slightly better. Also notice that the results in these figures clearly illustrate the advantage of diversity as a means of overcoming the severe penalty in SNR/bit caused by fading. A few important conclusions can be drawn by comparing Figures 3.3 and 3.4. First, the fade distribution affects the diversity gain. The relative advantage of diversity is greater for Rayleigh than Rician fading because as the fading figure m increases, there is less difference between the instantaneous receiver SNR on the various diversity branches. However, the performance is always better with Rician fading than Rayleigh fading for a given average received signal-to-noise ratio and diversity order. Next, the discrepancy between the SNIR and S+I selection systems becomes more pronounced in environments that have strong specular paths (larger m). Finally it is observed that the performance of an S+I scheme is much closer to the maximum-ratio diversity than the conventional selection scheme for small diversity orders. This observation becomes more noticeable in good channel conditions. However, the reverse is true when the number of diversity branches grows (refer to Figure 3.7).

It is worth noting that the results presented in Figures 3.3 and 3.4 are directly applicable for the noise-limited environments, whereas Figures 3.5 and 3.6 correspond to the interference limited scenarios. For the Nakagami multipath fading model, we assume that the number of the resolvable paths L to be 3, having relative path strengths (0 dB, -9.5 dB, -12 dB) as suggested in [28]. This 3-ray model (based on channel measurements in downtown Ottawa) is applicable for system bandwidths of 5 MHz in an urban outdoor

microcellular or 20 MHz in an indoor microcellular. Figure 3.5 and Figure 3.6 illustrate the average bit error rate performance of a micro-diversity DS/SSMA network in different fading environments. The normalized background (thermal) noise and processing gain are assumed to be 15 dB and 63, respectively. Once again, the largest diversity gain is achieved with 2-branch diversity and diminishing returns are realized with increasing M. Other main conclusions drawn from Figures 3 and 4 are also apparent by looking at these figures.

Figure 3.6 shows that the dual diversity S+I system supports almost as many active users as the optimum linear diversity combiner with the same order at the average BER of 10^{-3} or lower. Also notice that the same qualitative result can be obtained from Figure 3.4 in terms of average SNR/bit. This is particularly interesting in that the dual-diversity systems are by far the more common in current applications. However for higher orders of the diversity, maximum-ratio combiner remains optimum in terms of performance. Next in Figure 3.7, we illustrate the performance trend for the three diversity combining techniques, as the number of diversity branches increases. To create this plot, an average SNR/bit of 7 dB was chosen as being representative of the mobile communications environment. Notice that when fading becomes lighter, the performance improvement with the traditional selection diversity saturates much faster than the S+I-selection or maximum-ratio combining counterparts, as the diversity order grows.

We shall now describe the effects of unequal mean signal strengths among the statistically independent diversity branches on the error performance of a DS/CDMA network. To facilitate this analysis, we introduce a simple tolerance model that adds a small amount of perturbation ε to the average sum of the SNIR $\bar{\gamma}$. Consequently, the mean SNIR of the j th branch is given by,

$$\bar{\gamma}_j = \begin{cases} \bar{\gamma} & \text{if } j = \lceil M/2 \rceil \text{ and } M \text{ odd} \\ (1-\varepsilon)\bar{\gamma} & \text{if } j < \lceil M/2 \rceil \text{ and } M \text{ odd} \\ (1+\varepsilon)\bar{\gamma} & \text{if } j > \lceil M/2 \rceil \\ (1-\varepsilon)\bar{\gamma} & \text{if } j \le M/2 \quad \text{and } M \text{ even} \end{cases} \tag{3.36}$$

where $\bar{\gamma}_j = \Omega_j/\sigma_j^2$ and $\bar{\gamma} = \left(\sum_{j=1}^{M} \bar{\gamma}_j \right) / M$.

It is important in our study to investigate the effect of variations in the average long-term noise power σ^2 and unequal mean received signal power Ω separately. One may anticipate some difference in the performance of an S+I selection scheme, in particu-

lar realizing that the ratio σ_i/σ_j in (3.26) is different for both cases. As expected, there is some loss in diversity gain due to unequal mean signal strengths. The penalty is more apparent in channels that experience severe deep fades. Similar trends were also observed for higher orders of M. From Table 3.1, it appears that S+I selection is more vulnerable to the variations in the long-term average noise and interference power σ^2 than the SNIR-selection scheme. Consequently, the discrepancy between S+I and traditional selection diversity diminishes as ε becomes larger. If ε is allowed to be very large (e.g., $\varepsilon = \pm 75\%$) beyond the cross-over tolerance, then it is found that S+I system exhibits poorer performance than the SNIR-selection model. As an example, for dual-diversity S+I system, the cross-over tolerance is 53% in a Rayleigh fading channel.

In summary, our results indicate that the S+I selection rule outperforms the traditional selection model if the differences in mean signal strength among the independent diversity branches are small. However, when the variation is extremely large, a very noisy branch can easily upset the system performance because it introduces ambiguity in the selection process. Fortunately in practice, the variation in mean signal strength is relatively small for micro-diversity reception (the assumption of constant noise power in all diversity branches is valid at most instances, and the deviation in the mean signal power is usually small). Consequently, the proposed S+I-selection scheme will always perform better than the conventional selection diversity when realistic practical conditions are considered for the microscopic diversity reception. In contrast, this conclusion may not necessarily hold true at all times for packet radio communications with packet combining because the interference level experienced by each of the combined packets may vary substantially due to the time-varying nature of the multi-user interference.

Comparison between Table 3.2 and Table 3.1 reveals an interesting insight about the selection diversity systems. It was observed that S+I selection scheme is less susceptible to the variations in the mean received signal power levels compared to the fluctuations of the average long-term noise power. In contrast, the conventional selection diversity performs identically to the variations in σ^2 or Ω, which is anticipated.

3.4 Concluding Remarks

The efficacy of selection diversity has been studied by comparing the performance of two receiver structures employing BPSK signalling over a Nakagami multipath fading channel. First, an accurate analytical expression to evaluate the performance of a practical S+I-selection diversity scheme on various mobile radio environments has been presented. An attractive feature of the S+I-selection rule is that it is much easier and cheaper to implement in practice. Further, it has been shown that the new scheme outperforms the conventional selection diversity model. The difference becomes more evident with a larger number of diversity branches and in environments that do not experience severe fading. Next we have examined the effects of unequal mean signal strengths on the bit error rate performance. The difference between the S+I and SNIR selection techniques diminishes as the variation in the mean signal strengths among the diversity branches becomes larger. It was also observed that the S+I selection scheme is less susceptible to the variations in the mean received signal power levels compared to the fluctuations of the average long-term noise power. Finally, our results indicate that the proposed S+I selection scheme exhibits comparable performance with that of an optimum linear diversity combiner in environments where a strong specular path is available, and for small diversity orders. This is particularly interesting in that the dual-diversity systems are by far more common in current applications.

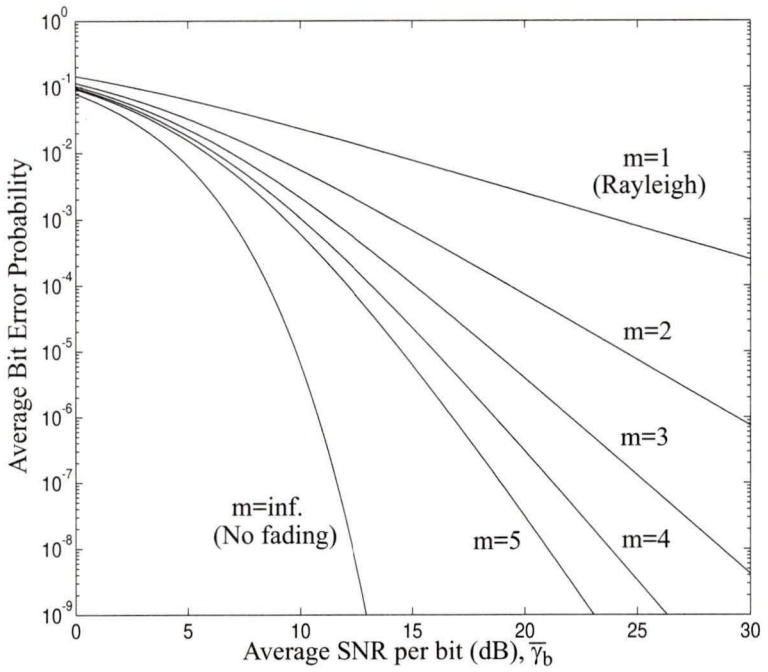

Figure 3.2 Average error probability for binary PSK symbol in nondiversity reception (M=1).

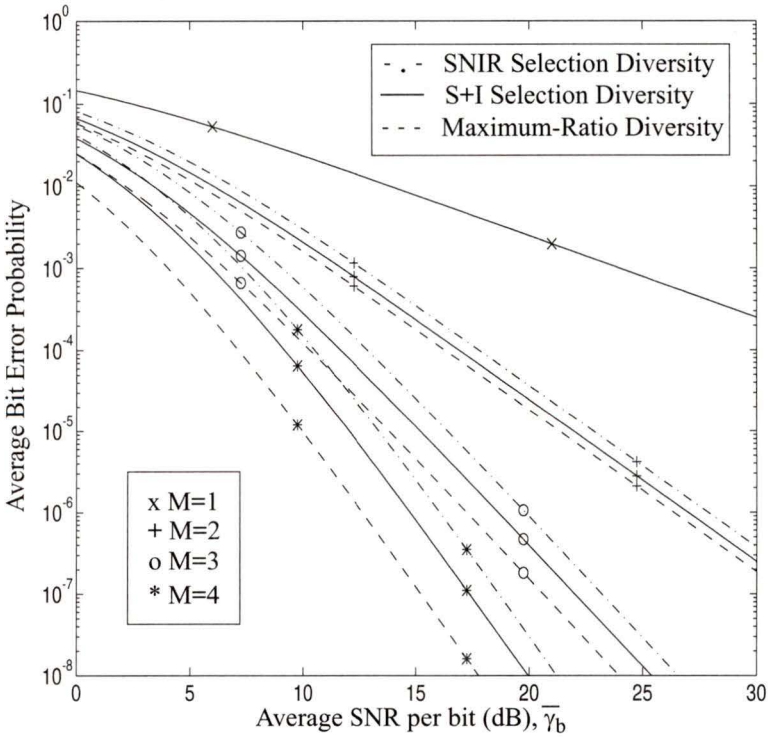

Figure 3.3 Performance comparison of different diversity combining techniques and varying diversity order (M=1, 2, 3 and 4) for 2-PSK signals over a Rayleigh fading channel (m=1).

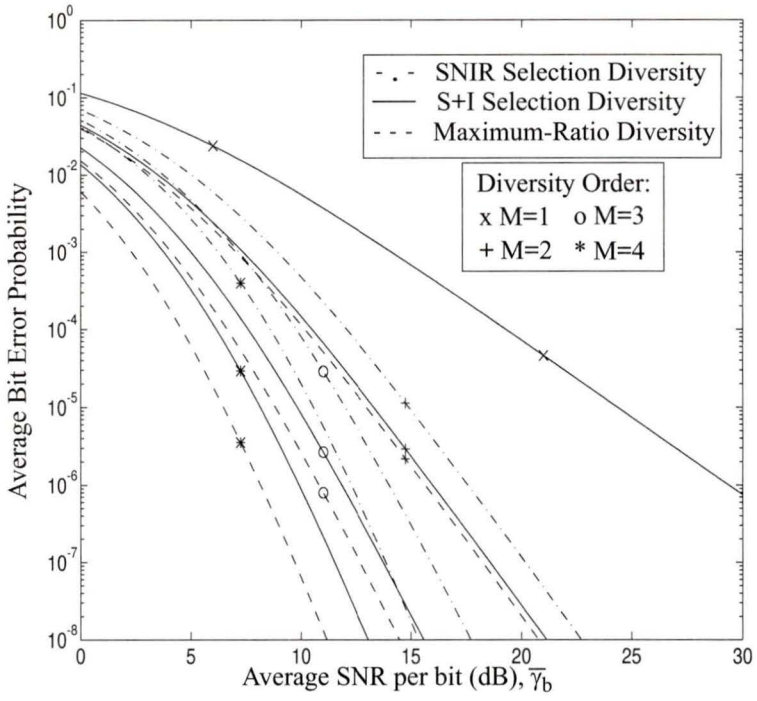

Figure 3.4 Bit error rate performance for binary PSK signals over a Nakagami fading channel with fading figure m=2, as a function of mean received signal-to-noise ratio.

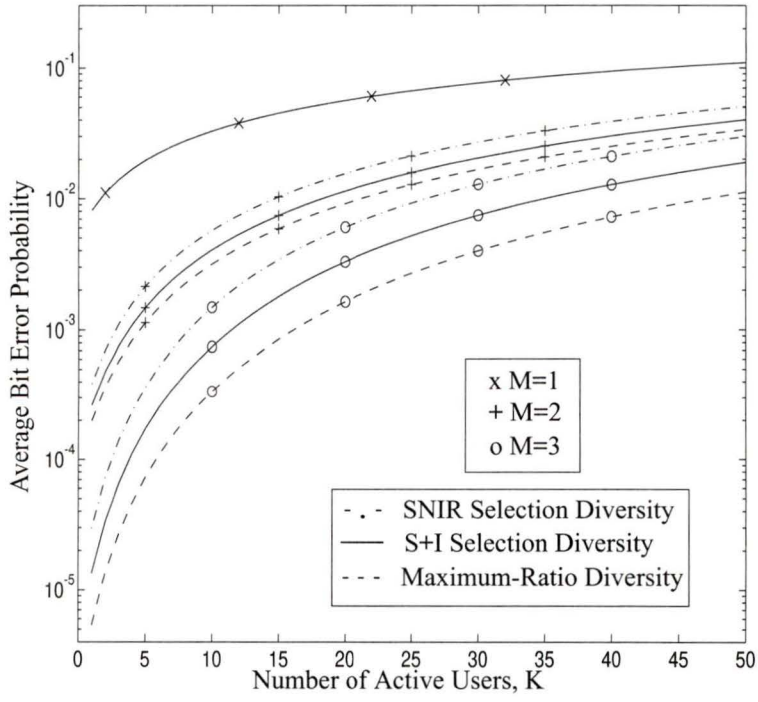

Figure 3.5 Error probability comparison of three different combining techniques as a function of number of active users K, for Rayleigh fading channels (m=1).

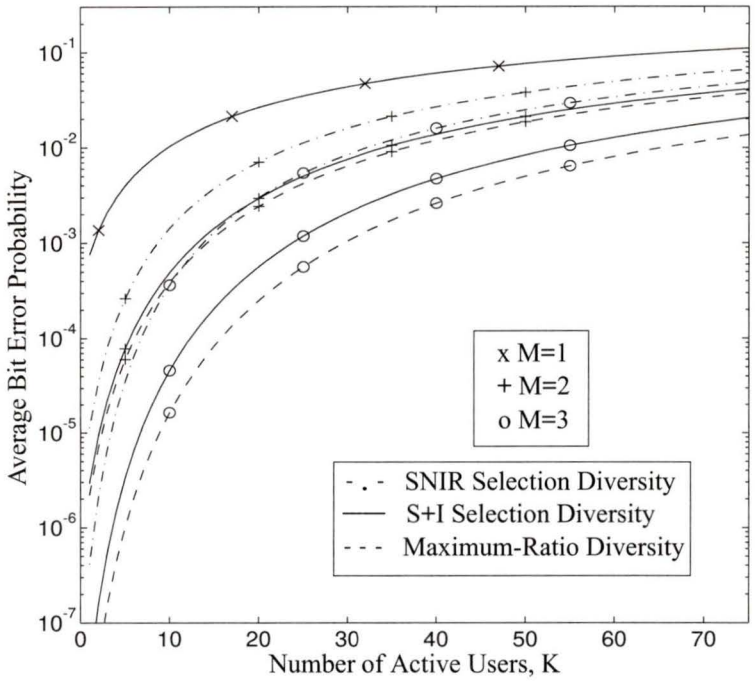

Figure 3.6 Average bit error probability of a binary phase-coded spread-spectrum system over a Nakagami multipath fading channel with fading figure m=2.

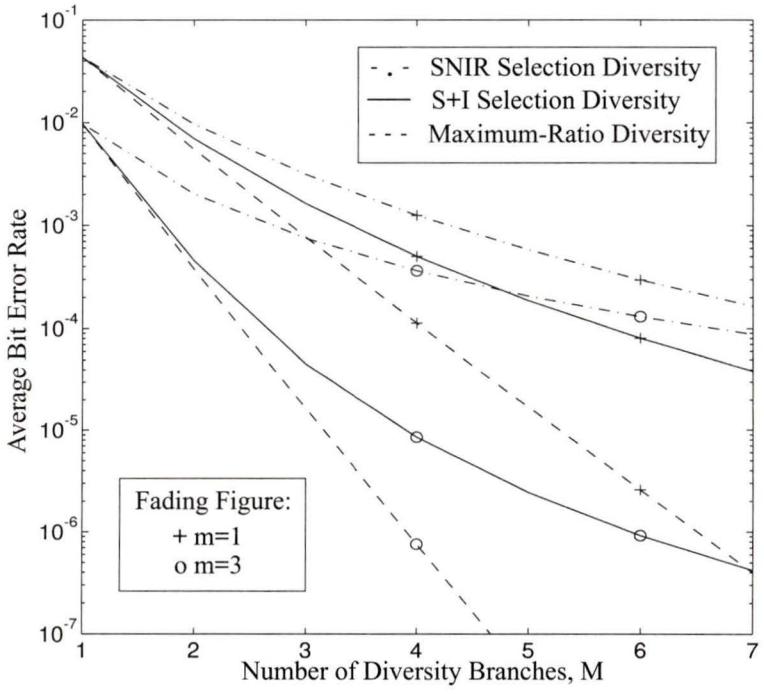

Figure 3.7 Illustration of the average bit error rate trend for BPSK receiver structures, plotted for mean SNR/bit γ_b = 7 dB, as the number of diversity branches grows.

Diversity Order	Variation in $\bar{\gamma}_j$ due to σ^2	Average Bit-Error Probability, P_b					
		m = 1 (Rayleigh)		m = 2		m = 3	
		SNIR	S+I	SNIR	S+I	SNIR	S+I
M=2	0 %	9.669×10^{-3}	6.966×10^{-3}	3.387×10^{-3}	1.276×10^{-3}	2.021×10^{-3}	4.554×10^{-4}
	±10 %	9.731×10^{-3}	7.084×10^{-3}	3.411×10^{-3}	1.314×10^{-3}	2.031×10^{-3}	4.733×10^{-4}
	±20 %	9.922×10^{-3}	7.458×10^{-3}	3.484×10^{-3}	1.436×10^{-3}	2.061×10^{-3}	5.319×10^{-4}
	±30 %	1.026×10^{-2}	8.151×10^{-3}	3.609×10^{-3}	1.672×10^{-3}	2.111×10^{-3}	6.496×10^{-4}
	±50 %	1.150×10^{-2}	1.116×10^{-2}	4.045×10^{-3}	2.845×10^{-3}	2.258×10^{-3}	1.295×10^{-3}
	±60 %	1.253×10^{-2}	1.433×10^{-2}	4.371×10^{-3}	4.298×10^{-3}	2.343×10^{-3}	2.194×10^{-3}
	±75 %	1.499×10^{-2}	2.516×10^{-2}	4.999×10^{-3}	1.056×10^{-2}	2.429×10^{-3}	6.728×10^{-3}
M=3	0 %	3.123×10^{-3}	1.630×10^{-3}	1.141×10^{-3}	1.762×10^{-4}	7.484×10^{-4}	4.560×10^{-5}
	±10 %	3.141×10^{-3}	1.666×10^{-3}	1.146×10^{-3}	1.837×10^{-4}	7.494×10^{-4}	4.835×10^{-5}
	±20 %	3.193×10^{-3}	1.781×10^{-3}	1.161×10^{-3}	2.084×10^{-4}	7.519×10^{-4}	5.780×10^{-5}
	±30 %	3.283×10^{-3}	2.002×10^{-3}	1.186×10^{-3}	2.598×10^{-4}	7.550×10^{-4}	7.863×10^{-5}
	±50 %	3.607×10^{-3}	3.070×10^{-3}	1.264×10^{-3}	5.673×10^{-4}	7.574×10^{-4}	2.255×10^{-4}

Table 3.1 Average error probability taking into account of the variation in the long-term average noise power σ_j^2 among the statistically independent diversity branches. It is assumed that the mean SNR/bit $\bar{\gamma}_b$ = 7 dB, and Ω_j are identical on every diversity branch.

Diversity Order	Variation in $\bar{\gamma}_j$ due to $\Omega = E[\alpha^2]$	Average Bit-Error Probability, P_b					
		m = 1 (Rayleigh)		m = 2		m = 3	
		SNIR	S+I	SNIR	S+I	SNIR	S+I
M=2	±10 %	9.731×10^{-3}	7.016×10^{-3}	3.411×10^{-3}	1.291×10^{-3}	2.031×10^{-3}	4.618×10^{-4}
	±20 %	9.922×10^{-3}	7.172×10^{-3}	3.484×10^{-3}	1.336×10^{-3}	2.061×10^{-3}	4.818×10^{-4}
	±30 %	1.026×10^{-2}	7.449×10^{-3}	3.609×10^{-3}	1.417×10^{-3}	2.111×10^{-3}	5.181×10^{-4}
	±40 %	1.077×10^{-2}	7.876×10^{-3}	3.794×10^{-3}	1.545×10^{-3}	2.178×10^{-3}	5.759×10^{-4}
	±50 %	1.150×10^{-2}	8.506×10^{-3}	4.045×10^{-3}	1.738×10^{-3}	2.258×10^{-3}	6.651×10^{-4}
	±75 %	1.499×10^{-2}	1.187×10^{-2}	4.999×10^{-3}	2.858×10^{-3}	2.429×10^{-3}	1.211×10^{-3}
M=3	±10 %	3.141×10^{-3}	1.641×10^{-3}	1.146×10^{-3}	1.780×10^{-4}	7.494×10^{-4}	4.620×10^{-5}
	±20 %	3.193×10^{-3}	1.675×10^{-3}	1.161×10^{-3}	1.837×10^{-4}	7.519×10^{-4}	4.807×10^{-5}
	±30 %	3.283×10^{-3}	1.734×10^{-3}	1.186×10^{-3}	1.938×10^{-4}	7.550×10^{-4}	5.146×10^{-5}
	±40 %	3.418×10^{-3}	1.824×10^{-3}	1.221×10^{-3}	2.097×10^{-4}	7.567×10^{-4}	5.691×10^{-5}
	±50 %	3.607×10^{-3}	1.957×10^{-3}	1.264×10^{-3}	2.337×10^{-4}	7.574×10^{-4}	6.544×10^{-5}

Table 3.2 Average error probability taking into account of the variations in the mean received signal power Ω_j. It is assumed that the mean SNR/bit $\bar{\gamma}_b$ = 7 dB, and σ_j^2 are identical on every diversity branch.

Chapter 4

Adaptive Retransmission Diversity with Packet Combining for Wireless Data Networks

In Chapter 3, various post-demodulation diversity combination techniques have been investigated for a phase-coded spread-spectrum system, operating in a generalized fading channel. In particular, the results are tailored for the analysis of micro-diversity reception (spatial diversity) either in the mobile unit or at the base-station, although the antenna separation required to achieve statistically independent diversity branches differ in both cases. By contrast, in this chapter we shall focus on another form of diversity reception in packet radio communications, namely adaptive retransmission with packet combining. In particular, we are interested in computing the lower bounds for the throughput of a slotted DS/CDMA ALOHA with packet combining.

In recent years, many researchers have highlighted the advantages of spread-spectrum techniques in the context of wireless data communication scenarios [44][45][46]. An excellent review can be found in [44]. One of the key attractions of spread-spectrum for such new services is its potential for operation at low power density, which may permit overlay communication in currently allocated frequency bands [46]. For instance, in [45] the authors have suggested providing subscriber access to a metropolitan area network (MAN) via a spread-spectrum based radio link, as a solution to the "last-mile" problem that still exists in data communications. Also, for packet data communication, the comparison with FDMA (Frequency Division Multiple Access) approaches may be more favorable than for voice services due to a combination of factors: (a) the source coding penalty associated with digital voice (i.e., 3 kHz analog to 32 or 64 kbps digital) no longer applies; (b) low-delay channel access is provided in CDMA without incurring the access protocol overheads; and (c) packet CDMA systems with retransmission capability can be designed to operate at higher bit-error rates, more closely approaching true capac-

ity than circuit-assigned systems for voice (which require relatively low bit-error rates).

As we attempt to make wireless technology available for a broader range of applications and due to the anticipated growth in consumer demands, the next generation wireless systems, namely Personal Communication Services (PCS), endeavor to provide ubiquitous communications of packetized multi-media data. This imposes many new challenges to designers, one of which is ensuring the integrity of data is sustained during transmission. In order to cope with the detrimental effects of channel fading and multi-user interference, some form of diversity reception is needed. As an example, packet data with retransmission capability can be designed to operate at higher bit error rates, while ensuring a reliable communication. Such a scheme is well suited for services that impose stringent bit-error rate requirements but are relatively insensitive to delay.

Time diversity has received much attention in mobile digital radio communications due to its simplicity in terms of implementation and because it does not require multiple antennas at the receiver [12]. However, its main drawback is that it transmits data blocks even in the absence of errors. On the other hand, when a basic automatic-repeat request (ARQ) scheme is applied to mobile radio that operates in a fading environment, the number of retransmissions before receiving a packet correctly is increased, thereby decreasing the throughput of the system. These issues can be mitigated by packet combining — a technique that utilizes current and previous transmissions of packets in decisions on data content. The combining operation can be performed at the level of individual channel outputs, at the level of code symbols, or at higher levels. Chase [40] has suggested combining the noise corrupted packets at the codeword level to form a single more reliable packet, thus minimizing the average number of retransmissions required before a packet is received successfully. The analysis was extended in [32] by considering a type-II hybrid ARQ scheme in conjunction with codeword combining. A significant improvement in the system performance was observed but at the expense of increased cost and implementation complexity. In contrast, in our analysis combining occurs at the bit level, and the resulting decisions are produced by employing selection diversity at the output of the correlator. This approach can be viewed as a modified time diversity scheme using an adaptive number of diversity branches. The main thrust of the proposed packet combining technique is to improve the system capacity and reliability while ensuring a simple and low-cost receiver structure. Further, the scheme can be readily applied to CDMA packet radio networks, especially for data transmission and communications without stringent latency requirements.

Emphasis is placed on simpler models that are amenable to analysis and that allow for unique insights without being too unrealistic. We assume a correlation receiver (matched filter) instead of a RAKE because our objective here is to investigate the performance of adaptive retransmission diversity rather than multipath diversity gains. However, it is worth noting that any form of diversity combining techniques employed to combine the multipaths will also enhance the overall performance of our system.

4.1 Theoretical Multipath Models

In the previous chapter, theoretical expressions have been derived to evaluate the average bit error probabilities of two types of selection diversity, namely SNIR and S+I selection schemes, for direct-sequence code division multiple access communications on a frequency selective Nakagami fading channel. However in this chapter, we are only concerned with multipath Rayleigh fading channels, which corresponds to fading figure $m = 1$. Consequently, the probability density function for β_{kl} described in (3.6) can be re-stated as,

$$f_{\beta}(x) = \frac{x}{\sigma_l^2} \exp\left(\frac{-x^2}{2\sigma_l^2}\right) u(x) \tag{4.1}$$

where $u(x)$ is the unit step function and $2\sigma_l^2$ corresponds to the power of the scattered components, i.e., $2\sigma_1^2 = E\left[\beta_{k1}^2\right]$.

In this section, analytical expressions are presented to compute the average bit error probability of a correlation receiver by modelling the multiple access interference (MAI) either as a Gaussian or an improved Gaussian process. The standard Gaussian approximation (GA) method for MAI is very attractive due to its simplicity. It also yields reasonably accurate results, especially for high bit-error rate (BER), small signal-to-noise ratio (SNR) and processing gain values, and if SNR is conditioned on fading random variable [20]. The accuracy of this approximation is verified by comparing its performance with a more accurate model based on Improved Gaussian Approximation (IGA). Unlike in Chapter 3, where the multipath powers are based on channel measurements in downtown Ottawa, here we consider two widely used analytical multipath models.

4.1.1 Constant Multipath Intensity Profile

If we assume that all multipaths have equal variances, i.e., $\sigma_l^2 = \sigma_1^2$, then the signal-to-noise plus interference ratio (SNIR) is given by,

$$SNIR = \frac{\frac{PT_b^2}{2}\beta_{11}^2}{\frac{PT_b^2}{6N}(KL-1)E\left[\beta_{11}^2\right] + \frac{N_0 T_b}{4}} = \frac{\beta_{11}^2}{\frac{(KL-1)}{3N}\left(2\sigma_1^2\right) + \frac{N_0}{2E_b}} \tag{4.2}$$

and its average value is,

$$\overline{SNIR} = \left(\frac{(KL-1)}{3N} + \frac{N_0}{2E_b\left[2\sigma_1^2\right]} \right)^{-1} \tag{4.3}$$

Under an energy-sharing communication environment, the total transmitted energy for a symbol is shared among all of its multipaths [13]. Let σ_T^2 denote the sum of variances of all the multipaths for user k, then the variance corresponding to the first multipath component is,

$$\sigma_1^2 = \frac{1}{2L}\sum_{l=1}^{L} E\left[\beta_{kl}^2\right] = \frac{\sigma_T^2}{L} \tag{4.4}$$

Using the Gaussian approximation (GA) method, the average probability of bit-error of a non-diversity receiver is,

$$P_b = \int_0^\infty Q\left(\sqrt{SNIR}\right) f_\beta(\beta_{11})\, d\beta_{11} = \frac{1}{2}\left[1 - \sqrt{\frac{\gamma_0}{1+\gamma_0}}\right] \tag{4.5}$$

where $SNIR$ and $f_\beta(x)$ are defined in (4.2) and (4.1), respectively. γ_0 is equal to half the mean signal-to-noise plus interference ratio, i.e., $\gamma_0 = \overline{SNIR}/2$, and $Q(.)$ is the complementary error function.

$$Q(x) = \frac{1}{\sqrt{2\pi}}\int_x^\infty e^{\frac{-u^2}{2}}\, du = \frac{1}{2}\mathrm{erfc}\left(\frac{x}{\sqrt{2}}\right) \tag{4.6}$$

An improved Gaussian approximation (IGA) for MAI was presented in [41] and [42], and it was shown that this approximation provides accurate values for the probability of bit-error for asynchronous DS/CDMA using random sequences in AWGN channel.

The analysis was extended in [43] for a Ricean fading channel, where the discrepancy between the bit-error rate performance obtained by modelling MAI as Gaussian process and improved Gaussian process was highlighted. For the sake of completeness, we extend this work and present numerical results to establish the accuracy of Gaussian approximation in both frequency selective and non-selective Rayleigh fading channels. Interestingly, we provide a few important observations and trends which were not cited in [43]. After some algebraic manipulations of equations (39)-(41) in [43], the average probability of bit-error for a correlation receiver on a multipath Rayleigh fading channel can be expressed as,

$$P_b = \frac{1}{3}\left[1-\sqrt{\frac{\gamma_0}{1+\gamma_0}}\right]+\frac{1}{12}\left[1-\sqrt{\frac{\gamma_1}{1+\gamma_1}}\right]+\frac{1}{12}\left[1-\sqrt{\frac{\gamma_2}{1+\gamma_2}}\right] \tag{4.7}$$

where γ_0 is equal to half the mean signal-to-noise plus interference ratio,

$$\gamma_1 = \left(\frac{2(KL-1)}{3N}+\frac{2\sqrt{3}\sigma_\psi}{N^2}+\frac{N_0}{E_b\left[2\sigma_1^2\right]}\right)^{-1} \tag{4.8}$$

$$\gamma_2 = \left(\frac{2(KL-1)}{3N}-\frac{2\sqrt{3}\sigma_\psi}{N^2}+\frac{N_0}{E_b\left[2\sigma_1^2\right]}\right)^{-1} \tag{4.9}$$

with σ_ψ^2 in this case is given by,

$$\sigma_\psi^2 = (KL-1)\left[\frac{7N^2+2N-2}{20}-\frac{N^2}{9}+(KL-2)\frac{N-1}{36}\right] \tag{4.10}$$

4.1.2 Exponential Multipath Intensity Profile

In arriving at (4.3), we have assumed that the variance for the path gain is the same for all multipaths and users. In most physical situations, one should expect a reduction in the average path power [36]. If spread-spectrum modulation is used with a chip duration less than the delay spread of the channel, the multipath power is partially reduced by the correlation operation in the receiver. In addition, extensive measurements of indoor wireless channel characteristics have shown that the average power of the multipath components decreases exponentially with increasing delay [37][38][39]. Assuming that the channel has exponential MIP with L resolvable multipaths, the variance for path l can be estimated as,

$$2\sigma_{kl}^2 = E\left[\beta_{k1}^2\right] e^{-\varepsilon(l-1)} = 2\sigma_1^2 e^{-\varepsilon(l-1)} \quad \text{for } 1 \le l \le L \tag{4.11}$$

where ε is a decay constant, and β_{k1} corresponds to the amplitude of the first arriving path which we assume without loss of generality to have a delay $\tau_{k1} = 0$. Thus, the signal-to-noise plus interference ratio for the exponential MIP profile is given by,

$$\begin{aligned} SNIR &= \frac{\beta_{11}^2}{\frac{K}{3N}\left[\sum_{l=2}^{L} 2\sigma_1^2 e^{-\varepsilon(l-1)}\right] + \frac{K-1}{3N}\left(2\sigma_1^2\right) + \frac{N_0}{2E_b}} \\ &= \frac{\beta_{11}^2}{\frac{K\Omega}{3N}\left(2\sigma_1^2\right) + \frac{K-1}{3N}\left(2\sigma_1^2\right) + \frac{N_0}{2E_b}} \end{aligned} \tag{4.12}$$

where $\Omega = \sum_{l=2}^{L} e^{-\varepsilon(l-1)} = \frac{1-e^{-\varepsilon(L-1)}}{e^{\varepsilon}-1}$.

Then, the average value of SNIR is,

$$\overline{SNIR} = \left(\frac{K\Omega}{3N} + \frac{K-1}{3N} + \frac{N_0}{2E_b\left[2\sigma_1^2\right]}\right)^{-1} \tag{4.13}$$

and the variance for the first multipath term as a fraction of the sum of all multipath variances is,

$$\sigma_1^2 = \frac{\sigma_T^2}{\sum_{l=1}^{L} e^{-\varepsilon(l-1)}} = \left(\frac{1-e^{-\varepsilon}}{1-e^{-\varepsilon L}}\right)\sigma_T^2 \tag{4.14}$$

where $2\sigma_T^2 = \sum_{l=1}^{L} E\left[\beta_{kl}^2\right]$.

4.2 Mean Bit-Error Rate Analysis

In a traditional slotted DS/CDMA system [41], the erroneous packet will be discarded, and decoding of a newly received copy is attempted at the receiver without using any prior knowledge from previously received copies (which were not recovered successfully). However, ignoring the previously received packets when the retransmission rate is

high seems to wasteful, especially when one realizes that a portion of the packet may have been received correctly. Therefore, in our scheme, selection diversity is employed at the bit level to form a more reliable block (representing the best estimate of the transmitted packet data) once a duplicate of that packet is received. While using each copy alone might not enable the receiver to recover the transmitted packet, combining these copies enhances the probability of this recovery.

Following the central limit theorem, the decision variable of the received composite signal described in (3.10) can be re-stated in the following form,

$$\zeta_j \equiv \alpha_j b_0 + n_j \tag{4.15}$$

where $\alpha_j = \sqrt{P/2}\, T_b \beta_j$ is the fading sample, n_j is the MAI (multipath and multi-user interference plus AWGN noise) sample and b_0 is the polarity of the data bit being detected. Subscript j corresponds to the jth copy of a packet (time diversity branch) available at the receiver for detection, $j \in \{1, 2, \ldots, M\}$ where M is the diversity order. We assume that α_j and n_j are independent and identically distributed Rayleigh and Gaussian random variables, respectively. The detector makes a wrong decision if ζ_j is negative while $b_0 = +1$, or if ζ_j is positive when $b_0 = -1$ was transmitted.

4.2.1 Conventional Selection Diversity

In [18], the SNIR-selection diversity process is simplified by considering the largest path gain for each user as the best estimate of the transmitted data, which has a probability density function in the form,

$$f_{\beta_{max}}(x) = M \sum_{k=0}^{M-1} \binom{M-1}{k} \frac{(-1)^k x}{\sigma_1^2} \exp\left(-\frac{x^2 (k+1)}{2\sigma_1^2}\right) u(x) \tag{4.16}$$

as shown in equation (5.2-7) of [12]. Following the steps as outlined in Section 3.2.1, the average probability of bit error for this case is given by [15][18],

$$P_b(K) = \left[\frac{M}{2}\right] \sum_{k=0}^{M-1} \binom{M-1}{k} \frac{(-1)^k}{k+1} \left\{1 - \sqrt{\frac{\gamma_0}{1+k+\gamma_0}}\right\} \tag{4.17}$$

where γ_0 is as defined in (4.5).

4.2.2 S+I Selection Diversity

In this proposed combining scheme, the branch with the largest amplitude of the received composite signal is chosen for data recovery. Consequently, the scheme lends itself to a low-complexity receiver structure, and is particularly attractive for high data rate traffic. Then the average probability of bit error is given by (3.26), which can be computed numerically.

With the assumption that α_k and n_k are i.i.d. Rayleigh and Gaussian random variables respectively, and for equal mean strengths, the average error probability depicted in (3.26) can be simplified as [15],

$$P_b(K) = 1 - M\int_0^{\infty} [G_\zeta(\zeta) - G_\zeta(-\zeta)]^{M-1} g_\zeta(\zeta)\, d\zeta \tag{4.18}$$

where $G_\zeta(x) = \int_{-\infty}^{x} g_\zeta(\tau)\, d\tau$. Since the probability density function of the sum of two statistically independent random variables is the convolution of their individual density functions, $g_\zeta(x)$ can easily be obtained through convolution of probability density functions of a Gaussian random variable and a Rayleigh random variable.

$$g_\zeta(z) = \int_0^{\infty} \frac{1}{\sqrt{2\pi}} \exp\left\{\frac{-(z-x)^2}{2}\right\} \frac{2x}{\Lambda} \exp\left\{\frac{-x^2}{\Lambda}\right\} dx \tag{4.19}$$

where $z = \zeta/\sigma$, and $\Lambda = E[\alpha^2]/\sigma^2 = 2\gamma_0$. After some mathematical manipulations, (4.19) reduces to [refer to Appendix E],

$$g_\zeta(z) = \frac{1}{\sqrt{2\pi}(1+\gamma_0)} \exp\left(\frac{-z^2}{2}\right) + \left[\operatorname{erfc}\left\{-z\sqrt{\frac{\gamma_0}{2(\gamma_0+1)}}\right\} \frac{z}{2(1+\gamma_0)} \sqrt{\frac{\gamma_0}{1+\gamma_0}} \exp\left\{\frac{-z^2}{2(1+\gamma_0)}\right\}\right] \tag{4.20}$$

Subsequently, the average bit error rate described by (4.18) is evaluated numerically via Gaussian quadrature integration technique [23]. Using the closed-form expression for the probability density function of random variable ζ depicted in (4.20), we present a time-efficient computational approach for evaluating (4.18) (only need to evaluate a single integral numerically).

4.3 Delay-Throughput Analysis

In this section, the system throughput and delay characteristics of a time slotted DS/CDMA network that operates in a random access mode (slotted DS/SSMA ALOHA) are evaluated. Since the users in this system are required to wait until the beginning of some time slot to transmit or re-transmit their packets, there is no loss in generality in assuming a constant number of interfering transmissions throughout the entire packet. We also assume that the feedback channel is noiseless, and therefore the status signals from the receiver to transmitter are assumed to always arrive correctly.

First, we will outline the operation of our hybrid ARQ scheme. The transmitter buffers previously transmitted frames until an ACK or NACK is received. An acknowledgment (ACK) signal is always transmitted in the return channel while the received data block is not an uncorrectable error pattern. On the other hand, when a decoded message block is detected in error, a negative acknowledgment (NACK) status signal is sent to request the transmitter to resend a duplicate of this packet. In a traditional slotted DS-CDMA system, the erroneous packet will be discarded, and decoding of a newly received copy is attempted at the receiver without using any prior knowledge from previously received copies (which were not recovered successfully). Simply discarding the noisy packet seems to be wasteful in particular when one realizes that a portion of the packet may have been received correctly. Therefore, we propose to improve the throughput performance, delay characteristics and reliability of the system by using a simple packet combining approach. To do so, selection diversity is employed at the bit level to form a more reliable block by using the erroneous copies of that packet, which were retained at the receiver. While using each copy alone might not enable the receiver to recover the transmitted packet, combining these copies enhances the probability of this recovery. As we will show shortly, the new scheme provides a considerable advantage over the conventional slotted DS-CDMA ALOHA without incurring a substantial penalty in terms of cost or complexity.

In our analysis, we assume that the system is occupied by a large number of subscribers, and both the origination and backlog mode terminals have the same packet generation statistics. Consequently, the composite packet arrival (offered load) distribution $f_G(m)$ is Poisson,

$$f_G(m) = \frac{G^m}{m!}e^{-G} \tag{4.21}$$

where G denotes the offered traffic (average number of attempted transmission per slot). Forward error correction (FEC) is employed, which can correct up to t erroneous bits in each packet. It is also assumed that the fading statistics are uncorrelated from bit to bit, and remain constant during the transmission of each bit.

Exact evaluation of the throughput performance for systems with packet combining is very difficult, specifically because the packet success probability is dependent not only on the most recently received packet but is also related to previously received copies of that packet. In particular, the time-varying nature of the multi-user interference (since the number of interfering users may be different during the transmission of each of the combined packets) imposes considerable analytical and computational difficulties. Thus, we resort to bounding techniques to investigate the system performance.

Let $D^{(i)}(m_1, m_2, \ldots\ldots, m_i)$ be the event that after combining i copies of the same packet, the new decoded data block still contains an uncorrectable error pattern, conditioned on m_j simultaneous users during transmission of the jth copy, $j = 1, 2, \ldots, i$. The probability of this event is upper-bounded by,

$$\begin{aligned} p\{D^{(i)}(m_1, m_2, m_3, \ldots\ldots, m_i)\} &\le p\{D^{(i)}(m, m, m, \ldots\ldots, m)\} \\ &= \sum_{j=t+1}^{N_p} \binom{N_p}{j} \left(P_b^{(i)}(m)\right)^j \left(1 - P_b^{(i)}(m)\right)^{N_p - j} \\ &= 1 - \sum_{j=1}^{t} \binom{N_p}{j} \left(P_b^{(i)}(m)\right)^j \left(1 - P_b^{(i)}(m)\right)^{N_p - j} \end{aligned} \tag{4.22}$$

where $m = max(m_1, m_2, \ldots\ldots, m_i)$ and $P_b^{(i)}(m)$ are calculated as in the previous sections. The right hand side of (4.22) is the case where there are $m \ge m_j$, $j = 1, 2, \ldots, i$, simultaneous users during the transmission of each copy.

Let $R_{av}(m_1, m_2, \ldots)$ denote the average number of transmissions necessary to transmit a given packet successfully when m_i other users are transmitting simultaneously during the ith transmission of this packet. $R_{av}(m_1, m_2, m_3, \ldots)$ is given by [15][48],

$$R_{av}(m_1, m_2, m_3, \ldots) = 1 + p\{D^{(1)}(m_1)\} + p\{D^{(1)}(m_1), D^{(1)}(m_2), D^{(2)}(m_1, m_2)\} + p\{D^{(1)}(m_1), D^{(1)}(m_2), D^{(2)}(m_1, m_2), D^{(1)}(m_3), D^{(3)}(m_1, m_2, m_3)\} + \ldots\ldots \quad (4.23)$$

where

$$p\{D^{(1)}(m_1), D^{(1)}(m_2), D^{(2)}(m_1, m_2), \ldots, D^{(1)}(m_i), D^{(i)}(m_1, m_2, \ldots, m_i)\} \leq p\{D^{(i)}(m_1, m_2, \ldots\ldots, m_i)\}. \quad (4.24)$$

Subsequently, (4.23) can be upper bounded by,

$$R_{av}(m_1, m_2, \ldots) \leq 1 + \sum_{i=1}^{\infty} p\{D^{(i)}(m_1, m_2, \ldots\ldots, m_i)\} \quad (4.25)$$

The unconditional average number of transmissions is obtained by averaging (4.25) over (4.21),

$$R_{av} \leq 1 + \sum_{i=1}^{\infty} \left[\sum_{m_1=0}^{\infty} f_G(m_1) \sum_{m_2=0}^{\infty} f_G(m_2) \sum_{m_3=0}^{\infty} f_G(m_3) \ldots\ldots \sum_{m_i=0}^{\infty} f_G(m_i) \right] \times p\{D^{(i)}(m_1 + 1, m_2 + 1, m_3 + 1, \ldots\ldots, m_i + 1)\} \quad (4.26)$$

After some mathematical manipulations, equation (4.26) can be expressed as [see Appendix F],

$$R_{av} \leq 1 + \sum_{i=1}^{\infty} \sum_{m=0}^{\infty} \left[(f_G(m) + g_G(m))^i - (g_G(m))^i \right] \times p\{D^{(i)}(m + 1, m + 1, m + 1, \ldots\ldots, m + 1)\} \quad (4.27)$$

where $p\{D^{(i)}(m + 1, m + 1, \ldots\ldots, m + 1)\}$, $f_G(m)$ and $g_G(m)$ are given by (4.22), (4.21) and (4.28), respectively.

$$g_G(m) = \left(\sum_{t=0}^{m-1} \frac{G^t}{t!} \right) e^{-G} \quad (4.28)$$

Since the average portion of a packet which is received successfully for each transmission is $1/R_{av}$, and G is the average number of packets generated during each time slot, the system throughput is,

$$T = \left(\frac{G}{R_{av}}\right)\left(\frac{k}{n}\right) \tag{4.29}$$

where (k/n) corresponds to the FEC code rate. The normalized throughput is therefore defined as throughput divided by the system processing gain, T/N. Using (4.21), (4.22), (4.27), (4.28) and (4.29), we can compute the lower bound for throughput of our slotted DS/CDMA network with packet combining.

4.4 Numerical Results and Discussions

In this section, we provide some representative numerical curves illustrating the performance of a slotted DS/CDMA switched packet radio network, based on the analytical results derived in the preceding sections.

First we compare the average probability of bit-error obtained via the improved Gaussian approximation (IGA) method with the result of the standard Gaussian approximation (GA). From Table 4.1, it appears that P_b(GA) is a good approximation for bit-error probability even for a small number of active users in the system. Notice that the Gaussian approximation is conservative for Rayleigh fading channels, but the discrepancy becomes smaller as the spreading factor increases or for a decreasing number of active users in the system. These insights were not found in [43]. However, a similar trend was also observed in [35], where an accurate approximation for bit-error rate was obtained via the characteristics function method. Further, there is little improvement to be gained by increasing the number of chips per data bit N (which corresponds to increasing the bandwidth). This is because the primary reason for poor performance on the channel is the Rayleigh fading rather than the intersymbol interference due to multipath.

Table 4.2 illustrates the bit-error rate as a function of number of multipaths and active users occupying the system. As expected, the probability of bit-error increases as L increases because the unresolved multipaths add to the multiple access interference term. The bit-error rate performance for different values of E_b/N_o is described in Table 4.3. Again, it is interesting to note that the discrepancy between the results obtained by modelling MAI as Gaussian and improved Gaussian process is more evident at higher E_b/N_o values. Unlike in an environment where a strong specular path exists (e.g., Rician

channel), the Gaussian approximation yields slightly conservative results for the system parameters considered in our analysis.

Next, the throughput performance and delay characteristics of an asynchronous DS/CDMA packet radio network are presented. Each packet consists of $N_p = 255$ bits, and FEC is assumed of correcting up to $t = 10$ bits in each packet, i.e., a (255,179,10) BCH code. It is also assumed that the number of resolvable multipaths for each copy of a packet is $L = 3$, unless stated otherwise. Figure 4.1 illustrates the throughput curves of a slotted asynchronous DS/SSMA network with the assumption of uniform multipath intensity profile. It is evident from this figure that the basic ALOHA random access protocol is inherently unstable. For instance, the throughput curve (without packet combining) tends to zero as the load increases beyond a threshold value. In the operation of this protocol, from time to time the load becomes heavy which causes the interference level to be the dominating factor of the correct packet reception probability. Consequently retransmissions rise, adding to the load and further reducing throughput. Employing a simple combining scheme as proposed here improves the throughput performance considerably, which also helps to sustain a stable network for a wider range of offered traffic (mitigates the stability problem to some extent). In this figure, the conventional selection scheme which focuses on selecting the diversity branch with the largest SNIR has been considered. It is also apparent from this figure that packet combining is more effective in poor channel conditions. For example, we can achieve at least 2-fold and 6-fold increase in the maximum throughput value (with respect to basis ARQ scheme) at E_b/N_o=50dB and E_b/N_o=15dB, respectively.

The throughput curves for the practical S+I-selection method are presented in Figure 4.2. Comparison with Figure 4.1 clearly indicates that both schemes yield identical results for the case without packet combining, as anticipated. On the other hand, when packet combining is considered, the S+I selection model performs slightly better than the conventional selection diversity method. These observations are well supported by noting the discrepancy in the average bit error rate curves in Figure 3.3. Figure 4.3 depicts the delay characteristics of the system under consideration for different selection combining rules and various E_b/N_o values. Two interesting points can be drawn from this figure. First, packet combining is a very effective method of improving the average time delay before a packet is received successfully. This is because the average number of retransmissions increases more gradually (with respect to the increase in the offered traffic) in comparison with the traditional basic ARQ scheme. Secondly, by exploiting the knowl-

edge of the previously transmitted copies of a packet (which were also detected in error) with a simple combining mechanism at the bit-level yields a more robust system against variations in the background noise, or alternatively E_b/N_o. At least this is true for the system parameters considered in our analysis. For example, the average number of transmissions required to transmit a packet successfully increase more than an order of magnitude for a basic ARQ scheme, whereas only one additional retransmission is required for the packet combining scenario, at an offered traffic rate of 10 packets/slot and when the E_b/N_o parameter varies from 20dB to 15dB.

The throughput and delay characteristics of a phase-coded spread-spectrum system having an exponential multipath intensity profile are shown in Figures 4.4 and 4.5, respectively. Similar trends with a uniform MIP model were observed, and therefore the main conclusions drawn from Figures 4.1, 4.2 and 4.3 are also valid for this model with an exception that the results are slightly better. A key reason for this observation is because the unresolved multipaths contribute less interference, as the interfering multipaths' signal powers are assumed to decay exponentially corresponding to their time delays. Further, signal power in the resolved multipath of an exponential MIP model is slightly higher than the constant MIP case because the parameter $2\sigma_T^2$ is kept constant for both scenarios. However the contribution due to this reason is not very substantial.

In Figure 4.6, the system throughput is analyzed for various multipath power decaying rates. Here the S+I-selection rule is employed to combine the multiple copies of a packet (which were not recovered successfully) at the receiver end. As explained before, the throughput is higher as the channel becomes less dispersive (larger decaying factors). Also notice that as the decay factors become smaller, the results converge towards the uniform MIP situation. It is important to mention here that if multipath diversity is exploited to improve the system performance [36][21], then as ε becomes smaller, the channel becomes more dispersive and L-th order diversity gain is achieved. Our results contradict this fact because we treat all the unresolved multipaths as interference, as in [35][20]. Finally, the efficacy of FEC has been examined in Figure 4.7. The average number of transmissions versus the normalized throughput curves are plotted for uncoded and coded systems. It should be stressed that the E_b/N_o value for the uncoded system has been adjusted (E_b/N_o of the coded system divided by the FEC code rate) to make a fair comparison. An important conclusion that can be drawn from this figure is that the application of FEC is crucial to achieve a reasonable system performance. The stability problem is also apparent from this figure.

4.5 Concluding Remarks

First, we have presented some numerical results to verify the accuracy of Gaussian approximation for multiple access interference in both frequency-selective and non-selective Rayleigh fading channels. It is observed that for Rayleigh fading channels, the bit-error rate obtained via Gaussian approximation is still valid even for a small number of active users in the system. We would like to highlight that the Gaussian approximation is conservative for Rayleigh fading channels, but the discrepancy becomes smaller as the spreading factor increases or for a decreasing number of active users in the system. Similar trends were also cited in [35]. However, the expression (4.7) provided here computes an accurate bit-error probability more efficiently than the expression found in [35].

Next, we have examined the throughput performance and delay characteristics of a slotted asynchronous DS/CDMA packet radio operating over a multipath Rayleigh fading channel. The receiver retains and processes all the retransmissions of a single data block using predetection diversity combining, instead of discarding those which are detected in error. To facilitate the analysis, we have derived simple and time-efficient formulas for evaluating the mean bit-error rate of the practical S+I-selection scheme and the computation of the average number of transmissions for the packet combining scenario. Two forms of selection diversity have been investigated. It is evident that in an interference limited environment, the proposed S+I selection scheme outperforms the conventional SNIR-selection model. This is particularly interesting in that the proposed packet combining scheme (which focuses on selecting the bit with the largest amplitude of the received composite signal) lends itself to a low-cost and reduced complexity receiver structure. This scheme is also well suited for high data-rate transmissions because accurate measurements of the signal-to-noise ratio becomes difficult or expensive. Our numerical results show that the proposed adaptive retransmission scheme with this simple packet combining method enhances the system performance significantly, and ensures a more stable network. Also, it was observed that packet combining is more effective when the retransmission rate is high (poor channel conditions). Finally, we have shown that application of FEC is crucial to achieve a reasonable system performance in a direct sequence CDMA network.

	K=2		K=5		K=10		K=15	
	P_b (GA)	P_b (IGA)	P_b (GA)	P_b (IGA)	P_b (GA)	P_b (IGA)	P_b (GA)	P_b (IGA)
N=31	0.01697	0.01681	0.03088	0.03033	0.05162	0.05060	0.06984	0.06851
N=63	0.01449	0.01445	0.02159	0.02145	0.03278	0.03248	0.04321	0.04280
N=127	0.01326	0.01325	0.01685	0.01682	0.02267	0.02259	0.02828	0.02816
N=255	0.01265	0.01265	0.01446	0.01445	0.01742	0.01741	0.02034	0.02031

Table 4.1 Comparison of the probability of bit-error for a DS/SSMA based on standard Gaussian approximation P_b (GA) and improved Gaussian approximation P_b (IGA) methods, over a nonselective Rayleigh fading channel (L=1, Eb/No=20dB, $E\{\beta_{11}^2\}=2\sigma_1^2$=-7dB).

	K=2		K=5		K=10		K=15	
	P_b (GA)	P_b (IGA)	P_b (GA)	P_b (IGA)	P_b (GA)	P_b (IGA)	P_b (GA)	P_b (IGA)
L=1	0.00263	0.00259	0.01027	0.01010	0.02224	0.02191	0.03338	0.03292
L=2	0.00776	0.00764	0.02224	0.02191	0.04377	0.04321	0.06263	0.06192
L=3	0.01273	0.01253	0.03338	0.03292	0.06263	0.06192	0.08699	0.08616
L=4	0.01756	0.01729	0.04377	0.04321	0.07933	0.07853	0.10769	0.10680

Table 4.2 Bit-error rate for asynchronous DS/CDMA systems with different number of active users and multipaths, over a Rayleigh fading channel (N=63, Eb/No=50dB, $E\{\beta_{11}^2\}=2\sigma_1^2$=-7dB).

	K=2		K=5		K=10		K=15	
	P_b (GA)	P_b (IGA)	P_b (GA)	P_b (IGA)	P_b (GA)	P_b (IGA)	P_b (GA)	P_b (IGA)
E_b/N_o=10dB	0.09876	0.09869	0.11053	0.11034	0.12803	0.12771	0.14336	0.14297
E_b/N_o=15dB	0.04564	0.04550	0.06252	0.06219	0.08690	0.08637	0.10761	0.10697
E_b/N_o=20dB	0.02389	0.02372	0.04321	0.04280	0.07076	0.07011	0.09386	0.09309
E_b/N_o=25dB	0.01634	0.01615	0.03655	0.03610	0.06525	0.06455	0.08919	0.08838
E_b/N_o=50dB	0.01273	0.01253	0.03338	0.03292	0.06263	0.06192	0.08699	0.08616
E_b/N_o= ∞	0.01272	0.01252	0.03337	0.03291	0.06263	0.06191	0.08699	0.08615

Table 4.3 Probability of bit-error for asynchronous DS/SSMA over a frequency-selective Rayleigh fading channel, as a function of Eb/No and number of active users in the system (L=3, N=63, $E\{\beta_{11}^2\}=2\sigma_1^2$=-7dB).

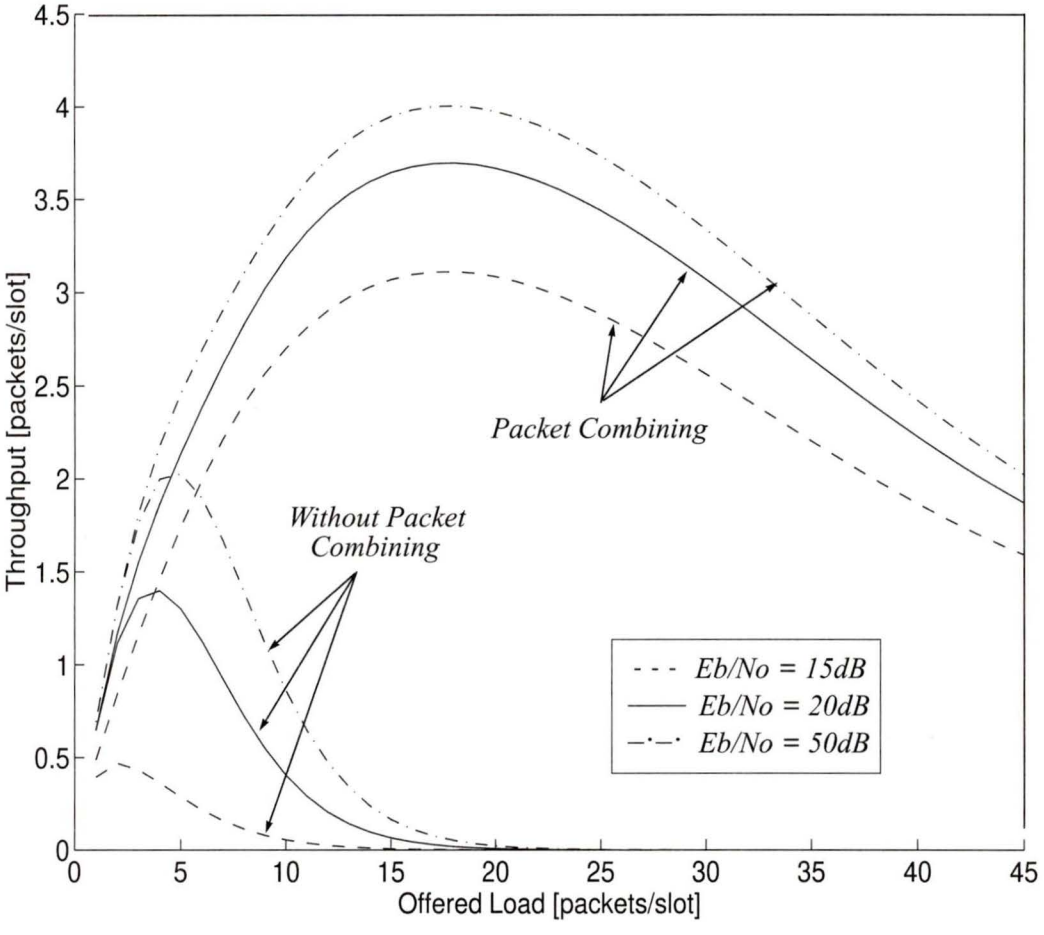

Figure 4.1 Throughput performance of a slotted asynchronous DS/CDMA as a function of offered traffic and Eb/N_0. Packet combining is achieved using conventional selection diversity (SNIR) approach at the bit level. Constant MIP is assumed. System parameters: N_p=255 bits, L=3, N=63, σ_1^2=-10 dB, (255,179,10) BCH FEC code.

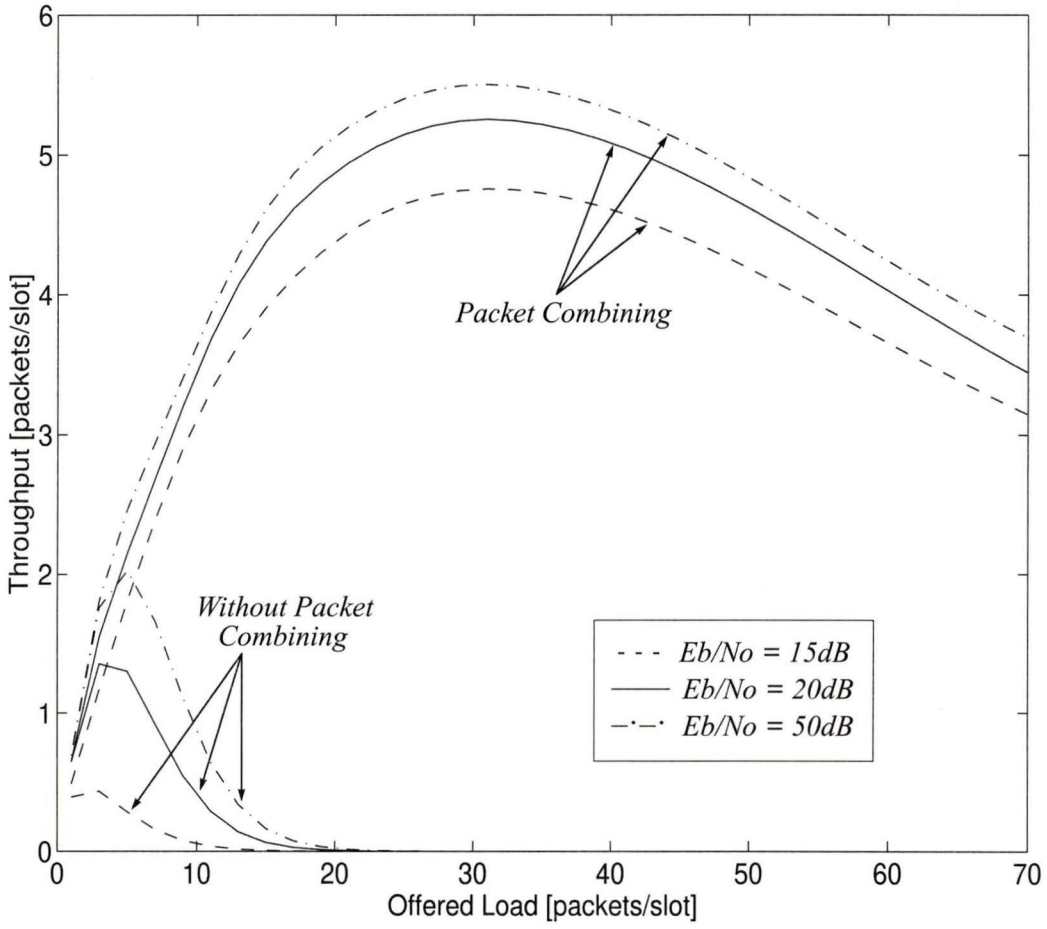

Figure 4.2 Throughput performance of a slotted asynchronous DS/CDMA network with correlation receiver, as a function of offered traffic and Eb/N_0. Packet combining is achieved using S+I selection diversity combining rule at the bit level. Constant MIP is assumed. System parameters: N_p=255 bits, L=3, N=63, σ_1^2=-10 dB, (255,179,10) BCH FEC code.

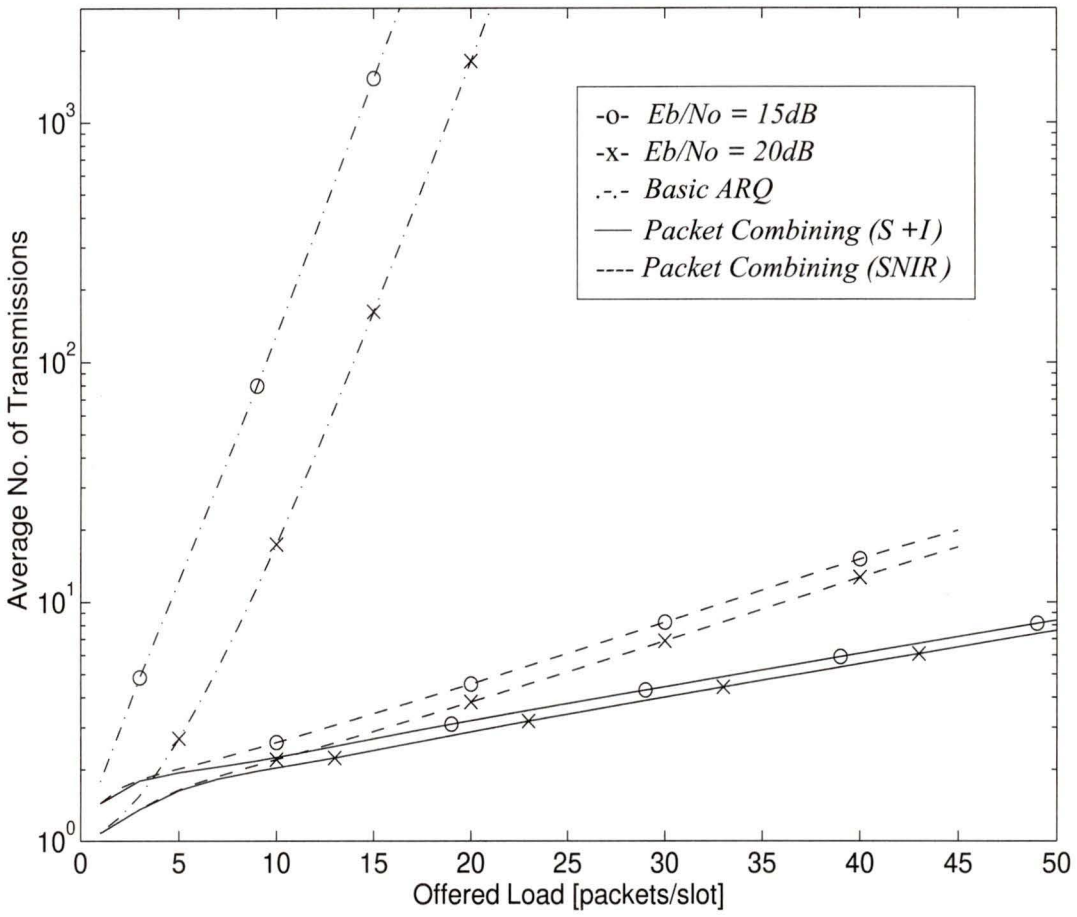

Figure 4.3 Delay characteristics of a slotted ALOHA DS/CDMA with and without packet combining. Different selection diversity rules are illustrated as a function of offered traffic and E_b/N_0. Uniform MIP is assumed. System parameters: N_p=255 bits, L=3, N=63, σ_1^2=-10 dB, (255,179,10) BCH FEC code.

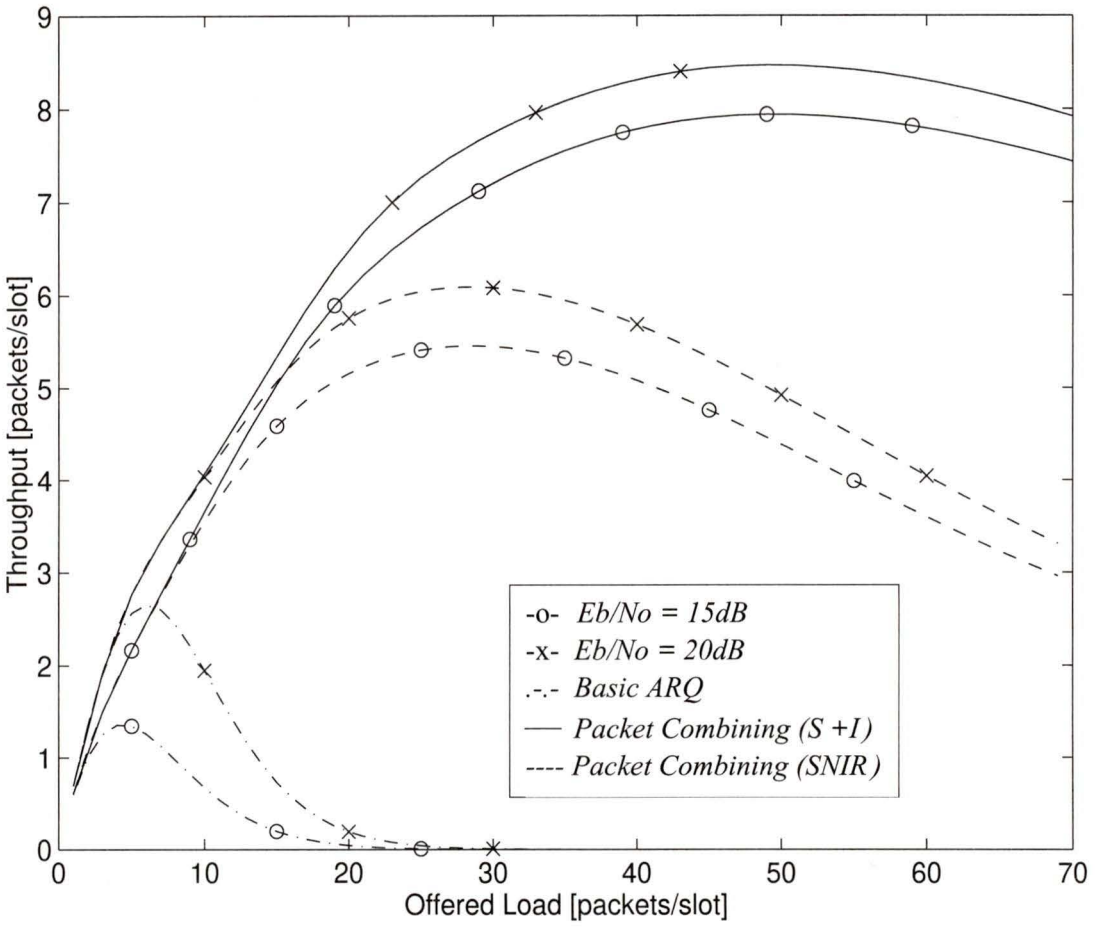

Figure 4.4 System throughput as a function of offered traffic and Eb/N_0. Exponential MIP is assumed. Packet combining is achieved by predetection selection diversity (SNIR and S+I schemes are considered) at the bit level. System parameters: N_p=255 bits, L=3, N=63, ε=0.5, σ_T^2= -5.229 dB, (255,179,10) BCH FEC code.

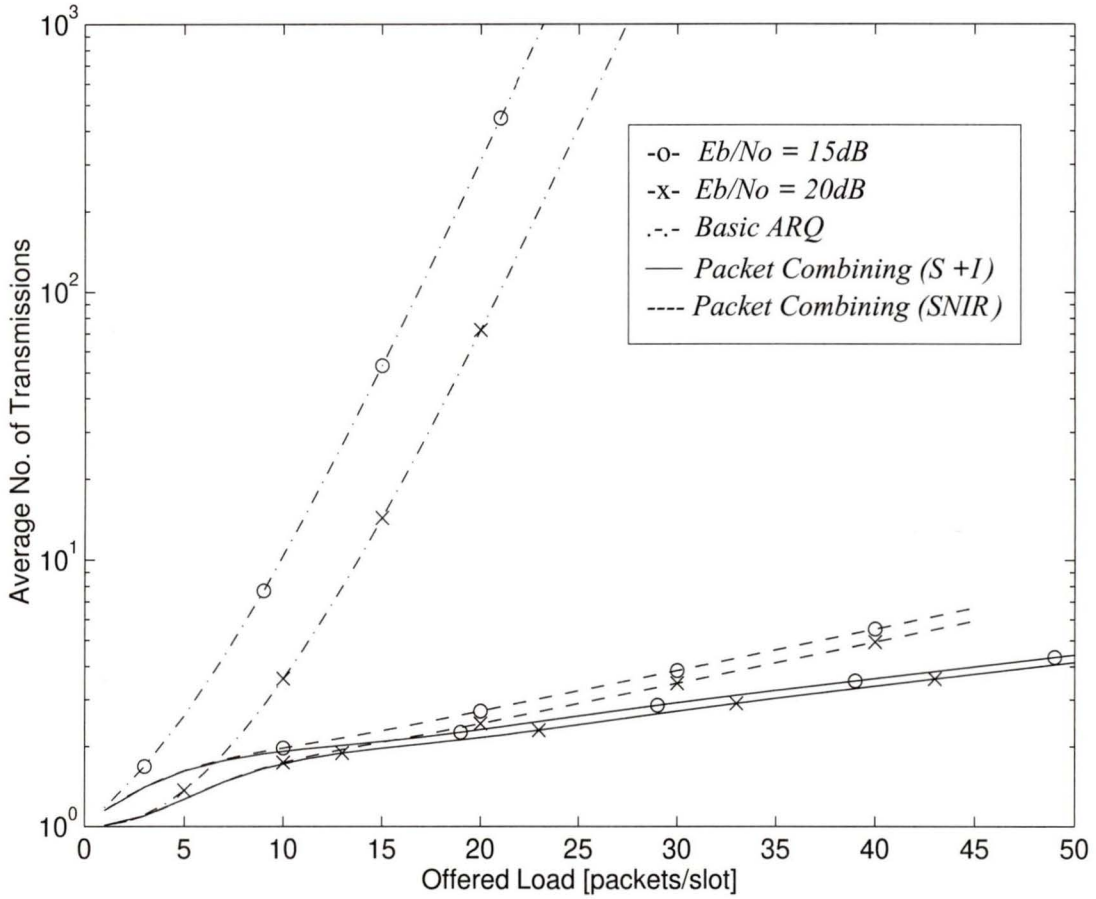

Figure 4.5 Delay characteristics of a slotted DS/CDMA ALOHA with and without packet combining, as a function of offered traffic and E_b/N_0. Exponential MIP is assumed. System parameters: N_p=255 bits, L=3, N=63, ε=0.5, σ_T^2= -5.229 dB, (255,179,10) BCH FEC code.

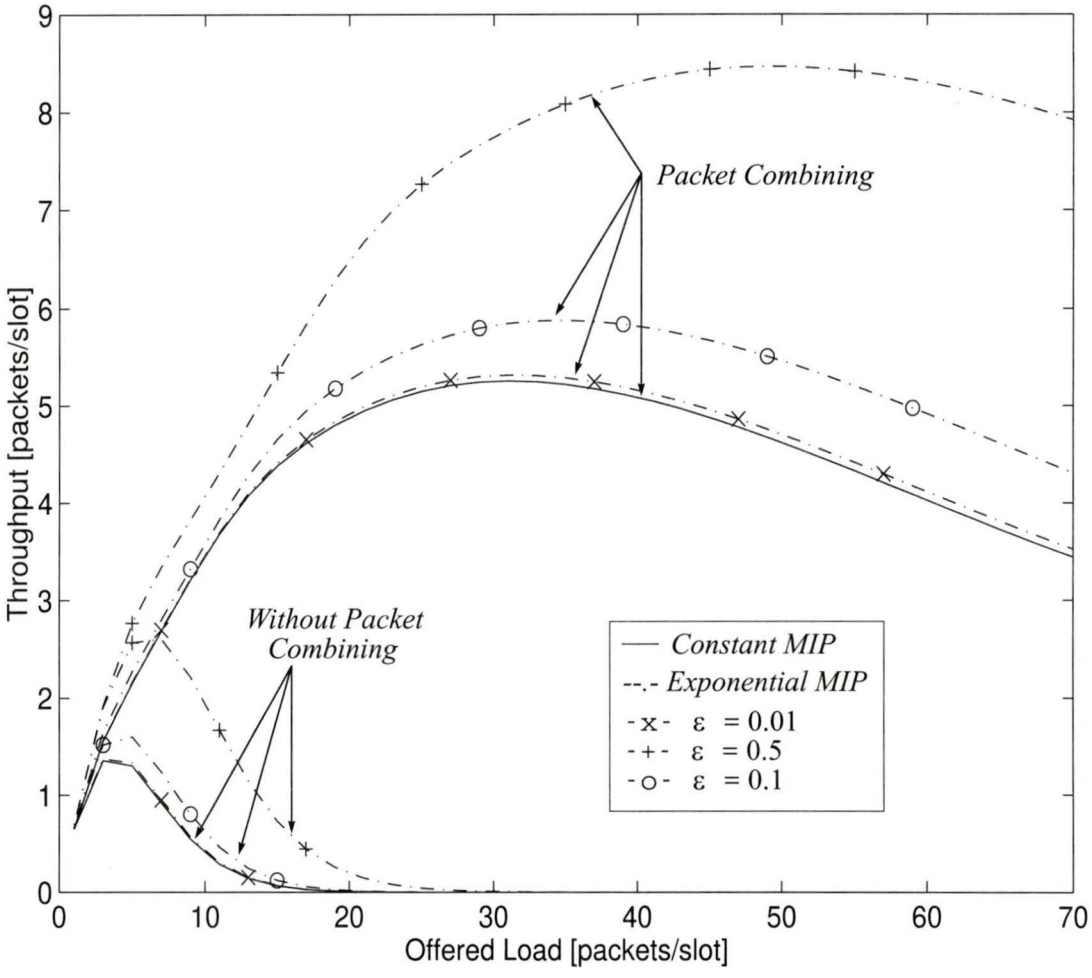

Figure 4.6 System throughput as a function of offered traffic for various multipath power decaying rates. S+I selection rule is employed to combine multiple copies of the same packet available at the receiver end. System parameters: N_p=255 bits, L=3, N=63, E_b/N_o=20 dB, σ_T^2= -5.229 dB, (255,179,10) BCH FEC code.

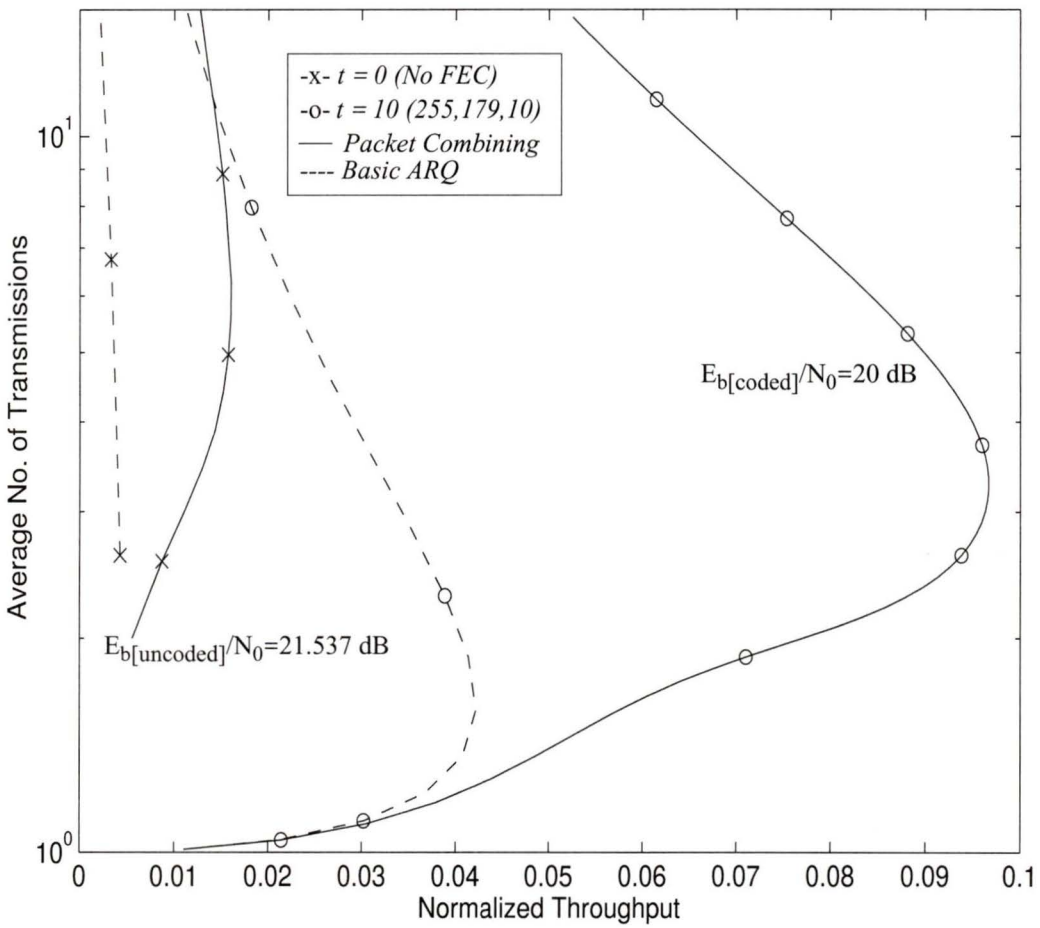

Figure 4.7 Average number of transmissions before a packet is received successfully versus the normalized throughput for the cases with and without FEC and packet combing (SNIR selection scheme). System parameters: N_p=255 bits, L=3, N=63, ε=0.5, σ_T^2= -5.229 dB.

Chapter 5

Conclusions

This dissertation focuses on efficient integration of multimedia traffic and error combatting techniques for future third generation wireless systems. We resort to numerical analysis and bounding techniques whenever we encounter difficulty in computing the exact closed-form formulas. Examples are furnished to help quantify the performance improvements achievable.

In Chapter 2, we have derived a general expression for computing average probability of bit error for a flexible network topology with multiple chip rates and processing gain values. These equations are obtained by modelling the multiple access interference as a Gaussian process. In this analysis, we have also assumed that the channel is perturbed only by additive white Gaussian noise and multiuser interference, as in [5], [7] and [10]. With the above assumptions, the multi-chip rate topology can offer substantial improvements in terms of system capacity, and/or service quality. The improvements owe to the reduction in the interference level by introducing a larger carrier frequency offset (between the different classes of traffic) in conjunction with a proper admission control. However, in a multipath fading environment, as the number of subsystems increases, narrowband subsystems become more vulnerable to multipath interference, resulting in a lower capacity. Thus, it can be conjectured that there exists an optimum system configuration that maximizes the user capacity for a given bit-error rate requirement and the fading figure. This issue has not been considered in this thesis, and will be a subject of our future study.

It was also observed that user distributions have a strong influence on the achievable system capacity. Consequently, we provide two different admission policies that will maximize the number of simultaneous users that can be accommodated by the system, or alternatively improve the grade of service for a fixed number of users. Proper power allo-

cation to various classes of traffic will also help to increase the system capacity, especially because the conventional power control law based on the ESS rule (by maintaining equal energy per bit) only combats the near/far problem and does not balance well the natural dissimilarities between different QoS requirements in a multimedia scenario.

Next in Chapter 3, we have studied the efficacy of selection diversity on a generalized fading channel model. Performance of an optimum linear diversity combiner is also presented for comparison. Here we have provided an accurate analytical expression to evaluate the performance of a practical S+I-selection diversity scheme on various mobile radio environments. An attractive feature of the S+I-selection rule is that it is much easier and cheaper to implement in practice. Further, it has been shown that the new scheme outperforms the conventional selection diversity model. The difference becomes more evident with a larger number of diversity branches and in environments that do not experience severe fading.

Subsequently, we have examined the effects of unequal mean signal strengths on the bit error rate performance. The difference between the S+I and SNIR selection techniques diminishes as the variation in the mean signal strengths among the diversity branches becomes larger. It was also observed that the S+I selection scheme is less susceptible to the variations in the mean received signal power levels compared to the fluctuations of the average long-term noise power. Finally, our results indicate that the proposed S+I selection scheme exhibits comparable performance with that of the optimum maximal-ratio combiner in environments where a strong specular path is available, and for small diversity orders. This is particularly interesting in that the dual-diversity systems are by far more common in current applications. We also would like to point out that the application of antenna diversity reception becomes even more crucial for portable units with low-mobility (such as in indoor wireless communications) because in such scenarios, the coding with interleavers approach will not work effectively to combat multipath fading. This is because the interleaving time span should cover independent fades, and therefore require a very large memory (interleaving span).

Finally, we have investigated the throughput and delay performance of a slotted DS-CDMA ALOHA with packet combining over a frequency selective Rayleigh fading channel. Notice that exact evaluation of the throughput performance for systems with packet combining is very difficult, specifically because the packet success probability is dependent not only on the most recently received packet but is also related to previously

received copies of that packet. In particular, the time-varying nature of the multi-user interference (since the number of interfering users may be different during the transmission of each of the combined packets) imposes considerable analytical and computational difficulties. Thus, we have resorted to bounding techniques to investigate the system performance. It is observed that even with a simple packet combining scheme, the system performance can be greatly enhanced and yields a more stable network.

Since the exact throughput performance cannot be estimated by the analytical results presented in this dissertation, it is highly desirable to verify the tightness of the lower bound via simulation techniques. Moreover, it is evident from Chapter 3 that if the variations in the mean signal strengths of the combined packets are very large (because the interference level experienced by each of the combined packets may vary substantially due to the time-varying nature of the multi-user interference), then S+I selection may not necessarily outperform the conventional selection approach. However, we predict the probability of such occurrences to be relatively small. Besides, in an interference limited network (the system is fully loaded) the variance of the multiple access interferences does not change drastically with the varying number of active users. Consequently, in such situations the proposed S+I selection will always perform better than the traditional SNIR selection diversity.

5.1 Suggestions for Further Work

The following are interesting topics which may be pursued for future work.

1. System Architecture and Bandwidth Management:

   - Extension of current analysis for multipath fading channels, in particular to obtain the optimum number of subsystems that will maximize the system capacity for a given BER and fading figure.
   - Analyze the effectiveness of the proposed system configuration in a multi-cell scenario (cellular applications).

2. Diversity Techniques for Wireless Packet Data Networks:

   - Verify the tightness of the bounds presented in this thesis via simulation.
   - Exact throughput estimation with different packet combining strategies via simulation taking into account more realistic hardware and channel conditions. For

instance, performance improvement by exploiting the multipaths (by utilizing a RAKE receiver), with different power decay delay profiles will be of interest. Factors such as packet correlation and Doppler spread should be incorporated, to accurately estimate the system capacity.

- Investigate the effect of limited buffer size on the throughput performance of slotted and unslotted DS-CDMA ALOHA with different packet combining mechanisms. Emphasis should be placed various methods of tackling the buffer overflow situation. This issue does not arise in the selection combining scheme, but has a significant impact on maximum-ratio combining approach.

Bibliography

[1] A. Baier, U. -C. Fiebig, W. Granzow, W. Koch, P. Teder, J. Thielecke, "Design Study for a CDMA-Based Third Generation Mobile Radio System," *IEEE J. Select. Areas Commun., Vol. 12, No. 4*, pp. 733-743, May 1994.

[2] A. Annamalai, V. K. Bhargava, "Some Results on FDM/DS-CDMA Signalling Scheme for Wireless Communication Networks," *Proc. IEEE International Conference on Personal Wireless Communications*, pp. 116-122, February 1996.

[3] Y. Egawa, L. B. Milstein, "On the capacity of a CDMA network which is overlaying narrowband BPSK waveforms," *Proc. Conf. on Information Sciences and Systems,* pp. 529-531, March 1991.

[4] M. -H. Fong, V. K. Bhargava, Q. Wang, "Concatenated Orthogonal/PN Spreading Sequences and Their Applications to Cellular DS-CDMA Systems with Integrated Traffic," *IEEE J. Select. Areas Commun., Vol. 14, No. 3*, pp. 547-558, April 1996.

[5] T. M. Lok, J. S. Lehnert, "Error Probabilities for Generalized Quadriphase DS/ SSMA with Random Signature Sequences," *IEEE Trans. Commun., Vol. 44*, pp. 876-885, July 1996.

[6] P. Mermelstein, S. Kandala, "Capacity Estimates for Mixed-rate Traffic on Integrated Wireless Access Network," *Proc. IEEE PIMRC'95*, pp. 228-232, Sept. 1995.

[7] T. -H. Wu, E. Geraniotis, "CDMA with Multiple Chip Rates for Multi-Media Communications," *Proc. Conf. on Information Sciences and Systems,* pp. 992-997, 1994.

[8] R. Prasad, J. A. M. Nijhof, H. I. Cakil, "Hybrid TDMA/CDMA Multiple Access Protocol for Multimedia Communications," *Proc. IEEE ICPWC'96*, pp. 123-128, Feb. 1996.

[9] A. Annamalai, V. K. Bhargava, "Evaluation of Direct-Sequence CDMA Communications with Multiple Chip Rates in an Integrated Network," (to be submitted).

[10] M. B. Pursley, "Spread-spectrum multiple-access communications," in *Multi-User Communication Systems*, G. Longo Ed. New York: Springer-Verlag, 1981, pp. 139-199.

[11] J. Zou , V. K. Bhargava, ''Optimized Power Allocation for Mixed Rate Traffic in a DS-CDMA Cellular System,'' *IEE Electronics Letters, Vol. 31, No. 22*, pp. 1902-1903, October 1995.

[12] W. C. Jakes, *Microwave Mobile Communications,* American Telephone and Telegraph Company, 1974 (Reissued by IEEE Press, Piscataway, NJ, 1993).

[13] J. G. Proakis, *Digital Communications,* (Third Edition), McGraw-Hill, NY, 1995.

[14] G. Chyi, J. G. Proakis, C. M. Keller, "On the Symbol Error Probability of Maximum Selection Diversity Reception Schemes over a Rayleigh Fading Channel," *IEEE Trans. Commun., Vol. 37,* pp. 79-83, Jan. 1989.

[15] A. Annamalai, V. K. Bhargava, "Performance of Selection Combining Time-Diversity ARQ in Slotted DS/CDMA Wireless Packet Radio Networks," *Proc. International Symposium on Information Theory and Its Applications*, pp. 460-463, September 1996.

[16] A. Annamalai, V. K. Bhargava, "Micro-Diversity Reception of Spread Spectrum Signals on Nakagami Fading Channels," (to be submitted).

[17] E. A. Neasmith, N. C. Beaulieu, "A New Look at Selection Diversity," *Proc. WIRELESS '96*, pp. 191-206, 8-10 July, 1996.

[18] M. Kavehrad, P. J. McLane, "Performance of Low-Complexity Channel Coding and Diversity for Indoor Wireless Communications," *AT&T Tech. Journal, Vol. 64*, pp. 1927-1965, Oct. 1985.

[19] M. B. Pursley, "Performance Evaluation for Phase-Coded Spread-Spectrum Multiple Access Communications - Part-I: System Analysis," *IEEE Trans. Commun., Vol. 25*, pp 795-799, Aug. 1977.

[20] E. Geraniotis, M. B. Pursley, "Performance of Coherent Direct-Sequence Spread-Spectrum Communications Over Specular Multipath Fading Channels," *IEEE Trans. Commun., Vol. 33*, pp 502-508, June 1985.

[21] A. Paulraj, "Diversity Techniques" in *Mobile Communications Handbook,* in J. D. Gibson (Ed.), CRC Press, 1996, pp. 166-176.

[22] F. E. Bond, H. F. Meyer, "The Effect of Fading on Communication Circuits Subject to Interference," *Proc. IRE, Vol. 45*, pp. 636-642, May 1957.

[23] W. Press, S. Teukolsky, W. Vetterling, B. Flannery, *Numerical Recipes in C: The Art of Scientific Computing*, (Second Edition), Cambridge University Press, 1992.

[24] M. Nakagami, "The m-distribution - A General Formula of Intensity Distribution of Fading," in *Statistical Methods in Radio Wave Propagation*, W. C. Hoffman, Ed. Oxford, England: Pergamon, 1960.

[25] H. Suzuki, "A statistical model for urban radio propagation," *IEEE Trans. Commun., Vol. 25*, pp. 673-680, July 1977.

[26] N. C. Beaulieu, A. Abu-Dayya, "Analysis of Equal Gain Diversity on Nakagami Fading Channels," *IEEE Trans. Commun., Vol. 39*, pp 225-234, February 1991.

[27] W. R. Braun, U. Dersch, "A Physical Mobile Radio Channel Model," *IEEE Trans. Vehic. Tech., Vol. 40*, pp 472-482, February 1991.

[28] G. Wu, A. Jalali, P. Mermelstein, "On Channel Models for Microcellular CDMA Systems," *Proc. IEEE VTC '94*, pp. 205-209, June 1994.

[29] I. S. Gradshteyn, I. M. Ryzhik, *Table of Integrals, Series and Products,* Academic Press, 1980.

[30] Staff of Research and Education, *Handbook of Mathematical, Scientific, and Engineering: Formulas, Tables, Functions, Graphs, Transforms,*" Research and Education Association, Piscataway, New Jersey, 1989.

[31] A. J. Mueller, *Issues in Diversity and Error Control Coding for Wireless Communications,* M.A.Sc. Thesis, University of Victoria, British Columbia, Canada, 1995.

[32] S. Kallel, "Analysis of a Type II Hybrid ARQ Scheme with Code Combining," *IEEE Trans. Commun., Vol. 38,* pp. 1133-1137, Aug. 1990.

[33] A. Annamalai, V. K. Bhargava, "Adaptive Retransmission Diversity with Packet Combining for Slotted DS-CDMA Packet Radio Networks," (to be submitted).

[34] M. B. Pursley, Dilip V. Sarwate, "Performance Evaluation for Phase-Coded Spread-Spectrum Multiple Access Communications - Part-II: Code Sequence Analysis," *IEEE Trans. Commun., Vol. 25*, pp 800-804, Aug. 1977.

[35] E. Geraniotis, "Direct-Sequence Spread-Spectrum Multiple-Access Communications Over Nonselective and Frequency-Selective Rician Fading Channels," *IEEE Trans. Commun., Vol. 34*, pp 756-764, Aug. 1986.

[36] M. Kahvehrad, B. Ramamurthi, "Direct-Sequence Spread Spectrum with DPSK Modulation and Diversity for Indoor Wireless Communications," *IEEE Trans. Commun., Vol. 35*, pp 224-236, Feb. 1987.

[37] D. Devasirvatham, "Multipath Time Delay Spread in Digital Portable Radio Environment," *IEEE Commun. Mag., Vol. 25*, pp 13-21, June 1987.

[38] T. S. Rappaport, "Indoor Radio Communications for Factories of the Future," *IEEE Commun. Mag., Vol. 27*, pp 15-24, May 1989.

[39] R. Bultitude, "Propagation Characteristics in Microcellular Urban Mobile Radio Channels at 910 MHz," *IEEE J. Selected Areas Commun., Vol. 7*, pp 31-39, Jan. 1989.

[40] D. Chase, "Code combining - A Maximum-Likelihood Decoding Approach for Combining an Arbitrary Number of Noisy Packets," *IEEE Trans. Commun., Vol. 33*, pp 385-393, May 1985.

[41] R. Morrow, J. Lehnert, "Packet Throughput in Slotted ALOHA DS/SSMA Radio Systems with Random Signature Sequences," *IEEE Trans. Commun., Vol. 40*, pp. 1223-1230, July 1992.

[42] J. M. Holtzman, "A Simple, Accurate Method to Calculate Spread-Spectrum Multiple-Access Error Probabilities," *IEEE Trans. Commun., Vol. 40*, pp. 461-465, March 1992.

[43] C. Trabelsi, A. Yongacoglu, "Bit Error Rate Performance for Asynchronous DS-CDMA over Multipath Fading Channels," *IEE Proc. Commun., Pt. F, Vol. 142*, pp. 307-314, Oct. 1995.

[44] M. B. Pursley, "The Role of Spread Spectrum in Packet Radio Network," *Proc. IEEE, Vol. 75*, pp. 116-134, January 1987.

[45] K. Joseph, D. Raychaudhuri, "Performance Evaluation of Cellular Packet CDMA Networks with Transmit Power Constraints," *Proc. IEEE International Conference on Communications 1991*, pp. 1614-1620.

[46] L. B. Milstein, D. L. Schilling, R. L. Pickholtz, V. Erceg, M. Kullback, E. G. Kanterakis, D. S. Fishman, W. H. Biederman, D. C. Salerno, "On the Feasibility of a CDMA Overlay for Personal Communications Networks," *IEEE J. Select. Areas Commun., Vol. 10, No. 4*, pp. 655-668, May 1992.

[47] D. T. Magill, F. D. Natali, G. P. Edwards, "Spread Spectrum Technology for Commercial Applications," *Proc. IEEE, Vol. 82*, pp. 572-584, April 1994.

[48] A. Bigloo, T. A. Gulliver, V. K. Bhargava, "Slotted DS/SSMA ALOHA with Packet Combining in a Rayleigh Fading Channel," *Proc. IEEE International Conference on Vehicular Technology 1996*, pp. 1710-1714.

[49] J. T. Taylor, J. K. Omura, "Spread Spectrum Technology: A Solution to the Personal Communications Services Frequency Allocation Dilemma," *IEEE Communications Magazine, Vol. 75*, February 1991.

[50] V. K. Bhargava, D. Haccoun, R. Matyas, P. Nuspl, *Digital Communications by Satellite,* A Wiley-Interscience Publication, 1981.

Appendix A

Validation of Equation (2.24)

In this appendix, we show that the received composite signal expression in the narrowband subsystems can be simplified as described by equation (2.24). Therefore, there is no loss in generality with our assumption that the neighbouring subsystems do not interfere with each other.

The received composite signal at the input of narrowband receiver in subsystem $[s, j]$ can be expressed as,

$$r_{sj}(t) = \sum_{k=1}^{U_v} s_{vk}(t-\tau_{vk}) + \sum_{k=1}^{U_{sj}} s_{sjk}(t-\tau_{sjk}) + \sum_{i=1, i\neq j}^{n_{cs}} \sum_{k=1}^{U_{si}} s_{sik}(t-\tau_{sik}) \qquad \text{(A.1)}$$

Then the output of the correlation receiver is,

$$g_{sjl}(T_s) = \int_0^{T_s} r_{sj}(t)\, c_{sjl}(t) \cos(\omega_{csj} t)\, dt \equiv \sqrt{\frac{P_s}{2}} T_s (d_{sjl}^{(0)} + I_{sj} + \eta_s) \qquad \text{(A.2)}$$

with multiple access interference (MAI) term represented by,

$$\begin{aligned} I_{sj} = & \sum_{k=1}^{U_v} \frac{1}{T_s} \sqrt{\frac{P_v}{P_s}} \int_0^{T_s} C_{vk}(t-\tau_{vk})\, c_{sjl}(t) \cos(-\omega_{sj} t + \varphi_{vk})\, dt + \\ & \sum_{k=1, k\neq l}^{U_{sj}} \frac{1}{T_s} \int_0^{T_s} C_{sjk}(t-\tau_{sjk})\, c_{sjl}(t) \cos(\varphi_{sjk})\, dt + \\ & \sum_{i=1, i\neq j}^{n_{cs}} \sum_{k=1}^{U_{si}} \frac{1}{T_s} \int_0^{T_s} C_{sik}(t-\tau_{sik})\, c_{sjl}(t) \cos(\omega_{ij} t + \varphi_{sik})\, dt \end{aligned} \qquad \text{(A.3)}$$

where $\omega_{ij} = \omega_{csi} - \omega_{csj} = 4\pi W_{ss}(i-j)/n_{cs}$, and $C_{sjk}(t)$, $C_{sik}(t)$, $C_{vk}(t)$ and ω_{sj} are as defined in (2.8) and (2.9).

Let ζ denote the third term of (A.3). Then,

$$\zeta = \sum_{i=1, i\neq j}^{n_{cs}} \sum_{k=1}^{U_{si}} \frac{1}{T_s} \sum_{g=0}^{G_s-1} C_{sik,\,(g)}\, c_{sjl,\,(g)}\, \chi_{s,\,(g)} \tag{A.4}$$

where $\chi_{s,\,(g)} = \int_{gT_{cs}}^{(g+1)T_{cs}} \cos\omega_{ij}t \cos\varphi_{sik} + \sin\omega_{ij}t \sin\varphi_{sik}\, dt.$

$$Var\{\zeta^2\} = E[\zeta^2] = \sum_{i=1, i\neq j}^{n_{cs}} \frac{U_{si}}{T_s^2} \sum_{g=0}^{G_s-1} E[\chi_{s,\,(g)}^2] \tag{A.5}$$

First by computing the expected value for $\chi_{s,\,(g)}^2$, and then substituting the result into (A.5), the variance of ζ can be easily shown to be zero.

$$Var\{\zeta^2\} = \sum_{i=1, i\neq j}^{n_{cs}} \frac{U_{si}}{T_s^2} \sum_{g=0}^{G_s-1} \frac{\mu_{(g)}^2 + \varepsilon_{(g)}^2}{2} = 0 \tag{A.6}$$

where $\mu_{(g)} = \int_{gT_{cs}}^{(g+1)T_{cs}} \cos(\omega_{ij}t)\, dt$ and $\varepsilon_{(m)} = \int_{gT_{cs}}^{(g+1)T_{cs}} \sin(\omega_{ij}t)\, dt$.

Hence, expression (A.1) representing the received signal at the input of a narrowband receiver, $r_{sj}(t)$, can be reduced to expression (2.24).

Appendix B

Mean Bit-Error Rate Expression for a Conventional Selection Diversity with Unequal Mean Signal Strengths

If α is characterized statistically by the Nakagami-m distribution, then the random variable $\gamma_b = \alpha^2 \xi_b / N_0$ has the probability density function [13],

$$p(\gamma_b) = \frac{m^m}{\Gamma(m)\bar{\gamma}_b^m} \gamma_b^{m-1} \exp\left(\frac{-m\gamma_b}{\bar{\gamma}_b}\right) \tag{B.1}$$

where $\bar{\gamma}_b = E[\alpha^2]\xi_b / N_0$. Consequently, if the branch with the largest signal-to-noise is chosen, then the bit-error rate can be expressed as,

$$P_b = \sum_{j=1}^{M} \int_0^\infty Q\left(\sqrt{\gamma_j}\right) f_{\gamma_j}(\gamma_j) \prod_{i=1, i\neq j}^{M} F_{\gamma_i}(\gamma_j)\, d\gamma_j \tag{B.2}$$

where

$$f_{\gamma_j}(y) = \frac{m^m}{\Gamma(m)\bar{\gamma}_j^m} y^{m-1} \exp\left(\frac{-my}{\bar{\gamma}_j}\right), \tag{B.3}$$

$$\begin{aligned} F_{\gamma_j}(x) &= \frac{m^m}{\bar{\gamma}_j^m \Gamma(m)} \int_0^x y^{m-1} \exp\left(\frac{-my}{\bar{\gamma}_j}\right) dy \\ &= 1 - \exp\left(\frac{-mx}{\bar{\gamma}_j}\right) \sum_{k=0}^{m-1} \frac{1}{k!} \left(\frac{mx}{\bar{\gamma}_j}\right)^k, \quad m \in \{integer\} \end{aligned} \tag{B.4}$$

and γ_j is the instantaneous signal-to-noise plus interference ratio of the jth branch. Average bit error probability described in (3.24) is obtained simply by substituting (B.3) and (B.4) into (B.2).

Appendix C

Transformation of Eq. (3.27) into (3.28)

In this appendix, we describe the important intermediate steps involved in the transformation of equation (3.27) into (3.28). Let us denote $\bar{\gamma}_j = \Omega_j/\sigma_j^2$, then (3.27) can be restated as,

$$\begin{aligned} g_\zeta(z_j) &= \int_0^\infty \frac{1}{\sqrt{2\pi}} \exp\left(\frac{-(z_j-x)^2}{2}\right) \frac{2m^m x^{2m-1}}{\Gamma(m)\bar{\gamma}_j^{\,m}} \exp\left(\frac{-mx^2}{\bar{\gamma}_j}\right) dx \\ &= \frac{2m^m}{\sqrt{2\pi}\,\Gamma(m)\bar{\gamma}_j^{\,m}} \exp\left(\frac{-z_j^2}{2}\right) \int_0^\infty x^{2m-1} \exp\left[-\frac{(2m+\bar{\gamma}_j)}{2\bar{\gamma}_j}x^2 + z_j x\right] dx \end{aligned} \tag{C.1}$$

We recognize that the definite integral in (C.1) can be expressed in terms of the parabolic cylinder function using the following identity [27, pp. 337],

$$\int_0^\infty x^{v-1} \exp\left(-bx^2 - cx\right) dx = (2b)^{-v/2}\,\Gamma(v) \exp\left(\frac{c^2}{8b}\right) D_{-v}\left(\frac{c}{\sqrt{2b}}\right), \quad b>0, v>0 \tag{C.2}$$

and $D_{-n-1}(.)$ for any non-negative integer n is given by,

$$D_{-n-1}(z) = \sqrt{\frac{\pi}{2}}\frac{(-1)^n}{n!} \exp\left(-\frac{z^2}{4}\right) \frac{d^n}{dz^n}\left[\exp\left(\frac{z^2}{2}\right)\operatorname{erfc}\left(\frac{z}{\sqrt{2}}\right)\right], \quad n = 0, 1, 2, \ldots \tag{C.3}$$

After some algebraic manipulations, we obtain $g_\zeta(z_j)$ as illustrated in (3.28). Further, we would like to point out that by computing the derivatives of the parabolic cylinder function, recurrence relationship described in (3.29) can be easily verified. Consequently, $D_{-v}(.)$ can be computed efficiently using this recurrence relationship, with $D_{-1}(z)$ and

$D_{-2}(z)$ obtained using (C.3).

For the particular case of $m = 1$ (Rayleigh fading channel), equation (3.28) reduces to,

$$g_{\zeta}(z_j) = \frac{2}{\sqrt{2\pi}\,\bar{\gamma}_j}\left(\frac{2+\bar{\gamma}_j}{\bar{\gamma}_j}\right)^{-1}\exp\left(\frac{-z_j^2(4+\bar{\gamma}_j)}{4(2+\bar{\gamma}_j)}\right)D_{-2}\left(-z_j\sqrt{\frac{\bar{\gamma}_j}{2+\bar{\gamma}_j}}\right) \tag{C.4}$$

Expression described in (C.4) can be re-stated as,

$$g_{\zeta}(z_j) = \frac{2}{\sqrt{2\pi}\,(2+\bar{\gamma}_j)}\exp\left(-\frac{z_j^2}{2}\right) + \operatorname{erfc}\left[-z_j\sqrt{\frac{\bar{\gamma}_j}{2(2+\bar{\gamma}_j)}}\right]\frac{z_j}{2+\bar{\gamma}_j}\sqrt{\frac{\bar{\gamma}_j}{2+\bar{\gamma}_j}}\exp\left(\frac{-z_j^2}{2+\bar{\gamma}_j}\right) \tag{C.5}$$

which is equivalent to the expression given in [15].

Appendix D

Average Bit-Error Probability Expression for an Optimum Linear Diversity Combiner

A closed form analytical expression to evaluate the average bit error rate for maximum-ratio combiner is derived in this appendix. Let us denote $\gamma_n = \alpha_n^2/\sigma_n^2$, having probability density function as described in (B.1). Following (3.32), the signal-to-noise plus interference ratio at the output of the maximum ratio combiner is equal to $\gamma_{mrc} = \sum_{n=1}^{M} \gamma_n$. If we assume that the branch fading as well as the branch noises to be mutually statistically independent, then the characteristic function for the sum of γ_n, $n = 1, 2, \ldots, M$, is simply the product of their individual characteristic functions, i.e.,

$$\psi_{\gamma_{mrc}}(jv) = \prod_{n=1}^{M} \frac{1}{\left(1 - jv\frac{\bar{\gamma}_n}{m}\right)^m} = \sum_{n=1}^{M} \sum_{k=1}^{m} \frac{A_{nk}}{(1 - jv\bar{\gamma}_n)^k} \tag{D.1}$$

where A_{nk} is defined in (3.34).

The inverse Fourier transform of the characteristic function in (D.1) yields the probability density function of γ_{mrc} in the form,

$$f_{\gamma_{mrc}}(\gamma_n) = \sum_{n=1}^{M} \sum_{k=1}^{m} A_{nk} \frac{m^k \gamma_n^{k-1}}{\Gamma(k)\,\bar{\gamma}_n^k} \exp\left(\frac{-m\gamma_n}{\bar{\gamma}_n}\right) \tag{D.2}$$

Hence, the average bit error probability is given by,

$$P_b = \sum_{n=1}^{M} \sum_{k=1}^{m} A_{nk} \int_0^{\infty} Q\left(\sqrt{\gamma_n}\right) \frac{m^k \gamma_n^{k-1}}{\Gamma(k)\, \bar{\gamma}_n^{k}} \exp\left(\frac{-m\gamma_n}{\bar{\gamma}_n}\right) d\gamma_n \tag{D.3}$$

The definite integral in (D.3) has a known closed-form solution [13],

$$\int_0^{\infty} Q\left(\sqrt{\gamma_n}\right) \frac{m^k \gamma_n^{k-1}}{\Gamma(k)\, \bar{\gamma}_n^{k}} \exp\left(\frac{-m\gamma_n}{\bar{\gamma}_n}\right) d\gamma_n$$

$$= \left[\frac{1}{2}(1-\mu_n)\right]^k \sum_{i=0}^{k-1} \binom{k-1+i}{i} \left[\frac{1}{2}(1+\mu_n)\right]^i \tag{D.4}$$

where $\mu_n = \sqrt{\bar{\gamma}_n / (2m + \bar{\gamma}_n)}$, and therefore (3.33) is readily shown.

Appendix E

Closed-Form Probability Density Function for the Random Variable ζ

In this appendix, we describe the important intermediate steps involved in the transformation of equation (4.19) into (4.20). Let us denote $\Gamma = \Lambda/(\Lambda+2)$, then (4.19) can be restated as,

$$g_\zeta(z) = \frac{2}{\Lambda\sqrt{2\pi}} \int_0^\infty x \exp\left(\frac{z^2(\Lambda/2) - x\Lambda z + [(\Lambda/2)+1]x^2}{-\Lambda}\right) dx \tag{E.1}$$

$$= \frac{2}{\Lambda\sqrt{2\pi}} \int_0^\infty x \exp\left\{\frac{-z^2[\Gamma-\Gamma^2]}{2\Gamma}\right\} \exp\left\{\frac{-(x-\Gamma z)^2}{2\Gamma}\right\} dx \tag{E.2}$$

$$= \frac{\exp\left\{\frac{z^2[\Gamma-\Gamma^2]}{-2\Gamma}\right\}}{(\Lambda/2)\sqrt{2\pi}} \left[\int_0^\infty (x-\Gamma z) \exp\left\{\frac{(x-\Gamma z)^2}{-2\Gamma}\right\} dx + \Gamma z \int_0^\infty \exp\left\{\frac{(x-\Gamma z)^2}{-2\Gamma}\right\} dx\right]$$

$$= \frac{2}{\Lambda\sqrt{2\pi}} \exp\left\{\frac{z^2[\Gamma-\Gamma^2]}{-2\Gamma}\right\} \left[\Gamma \exp\left(\frac{-\Gamma^2 z^2}{2\Gamma}\right) + \frac{\Gamma z\sqrt{2\pi\Gamma}}{2} \operatorname{erfc}\left(\frac{-\Gamma z}{\sqrt{2\Gamma}}\right)\right] \tag{E.3}$$

Equation (E.3) can be further simplified as follows,

$$g_\zeta(z) = \frac{1}{\sqrt{2\pi}}\left(\frac{2}{\Lambda+2}\right)\exp\left(\frac{-z^2}{2}\right)$$

$$+ \left[\operatorname{erfc}\left\{-z\sqrt{\frac{\Lambda}{2(\Lambda+2)}}\right\} \frac{z}{(\Lambda+2)} \sqrt{\frac{\Lambda}{\Lambda+2}} \exp\left(\frac{-z^2}{\Lambda+2}\right)\right] \tag{E.4}$$

Finally by substituting $\Lambda = 2\gamma_0$ in (E.4), this expression reduces to (4.20).

Appendix F

Computationally Efficient Formula for Evaluating (4.26)

Equation (F.5) derived here provides a simple expression to evaluate equation (4.26) efficiently. Let us denote $P_D^{(i)}(m_1) = p\{D^{(i)}(m_1+1, m_1+1, \ldots\ldots, m_1+1)\}$. Hence, the unconditional average number of transmissions R_{av} is upper-bounded by,

$$R_{av} \leq 1 + \sum_{i=1}^{\infty} \left[\sum_{m_1=0}^{\infty} \sum_{m_2=0}^{\infty} \ldots \sum_{m_i=0}^{\infty} f_G(m_1) f_G(m_2) \ldots f_G(m_i) \cdot P_D^{(i)}(m_1) \right] \qquad \text{(F.1)}$$

For mathematical simplification but without any loss in generality, let us assume that m_1 will take the maximum value for the number of simultaneous users during transmission of each the combined packets, i.e., $m_1 = max(m_1, m_2, \ldots\ldots, m_i)$. Subsequently, (F.1) can be restated as,

$$R_{av} \leq 1 + \sum_{i=1}^{\infty} \left[\sum_{m_1=0}^{\infty} f_G(m_1) \left\{ \sum_{m_2=0}^{\infty} f_G(m_2) \ldots \sum_{m_i=0}^{\infty} f_G(m_i) \right\} P_D^{(i)}(m_1) \right] \qquad \text{(F.2)}$$

The right-hand side of (F.2) can be re-written in the form of a binomial series,

$$RHS = 1 + \sum_{i=1}^{\infty} \left[{}^{i}C_1 \sum_{m_1=0}^{\infty} f_G^1(m_1) \left(\left\{ \sum_{t=0}^{m_1-1} \frac{G^t}{t!} \right\} e^{-G} \right)^{i-1} P_D^{(i)}(m_1) + \ldots\ldots \right.$$

$$\left. + {}^{i}C_{i-1} \sum_{m_1=0}^{\infty} f_G^{i-1}(m_1) \left(\left\{ \sum_{t=0}^{m_1-1} \frac{G^t}{t!} \right\} e^{-G} \right)^{1} P_D^{(i)}(m_1) + \sum_{m_1=0}^{\infty} f_G^{i}(m_1) \; P_D^{(i)}(m_1) \right] \qquad \text{(F.3)}$$

Therefore, equation (F.3) can simplified as,

$$RHS = 1 + \sum_{i=1}^{\infty} \sum_{m_1=0}^{\infty} P_D^{(i)}(m_1) \left[\sum_{k=1}^{i} {}^{i}C_k \, f_G^k(m_1) \left(\left\{ \sum_{t=0}^{m_1-1} \frac{G^t}{t!} \right\} e^{-G} \right)^{i-k} \right] \tag{F.4}$$

which reduces to,

$$RHS = 1 + \sum_{i=1}^{\infty} \sum_{m_1=0}^{\infty} \left[(f_G(m_1) + g_G(m_1))^i - (g_G(m_1))^i \right] P_D^{(i)}(m_1) \tag{F.5}$$

where $f_G(m)$ and $g_G(m)$ are given by (4.21) and (4.28), respectively. ${}^{a}C_b$ denotes the binomial coefficient defined as,

$${}^{a}C_b = \frac{a!}{(a-b)!\,b!} \tag{F.6}$$

VITA

Surname: Annamalai Given Names: Annamalai Jr.

Place of Birth: Kuala Kangsar, Malaysia Date of Birth: January 17, 1969

Educational Institutions Attended:

University of Victoria, Canada 1995 to 1997

Universiti Sains Malaysia, Malaysia 1989 to 1993

Degrees Awarded:

Bachelor of Engineering (Hons.) Universiti Sains Malaysia, 1993

Honours and Awards:

M. A. Sc. Studies

University of Victoria Graduate Research Assistantship (1995-1997)

University of Victoria Graduate Teaching Fellowship (1996)

B. Eng. Studies

Federal Scholarship (1989-1993)

Best Electronics Project Award of the Intel Technology-USM Electronics Design Competition for the project entitled, "Design and Development of Computer-Aided ECG" (1993)

Publications:

Journal

A. Annamalai, V. K. Bhargava, "Adaptive Retransmission Diversity with Packet Combining for Slotted DS-CDMA Packet Radio Networks," submitted to *Wireless Personal Communications*.

A. Annamalai, "Micro-Diversity Reception of Spread-Spectrum Signals on Nakagami Fading Channels," submitted to *IEEE Trans. on Communications*.

A. Annamalai, V. K. Bhargava, "Evaluation of Direct-Sequence CDMA Communications with Multiple Chip Rates in an Integrated Network," (in preparation).

P. A. Venkatachalam, Annamalai Jr., "Implementation of a Computerized Patient Monitoring System," *Journal of Engineering Science & Technology*, Universiti Sains Malaysia, pp. 87-97, Third Quarter 1993 (in Malay).

VITA, Continued

Publications, Continued:

Conference

A. Annamalai, V. K. Bhargava, "Some Results on FDM/DS-CDMA Signalling Scheme for Wireless Communication Networks," *Proc. IEEE International Conference on Personal Wireless Communications*, pp. 116-122, New Delhi, 19-21 February 1996.

A. Annamalai, "On Optimum Signalling Scheme for Third-Generation Wireless Systems with Integrated Traffic," *British Columbia Advanced System Institute Graduate Presentation Day*, Vancouver, March 1996.

A. Annamalai, V. K. Bhargava, "Performance of Selection Combining Time-Diversity ARQ in Slotted DS/CDMA Wireless Packet Radio Networks," *Proc. International Symposium on Information Theory and Its Applications*, pp. 460-463, Victoria, 17-20 September 1996.

A. Annamalai, "Selection Diversity Reception of Spread-Spectrum Signals with Unequal Mean Strengths," to appear in *Proc. 47th IEEE Vehicular Technology Conference,* Phoenix, 5-7 May 1997.

A. Annamalai, V. K. Bhargava, "Evaluation of a Low-Complexity Rake Receiver for Indoor Wireless Communications," to appear in *International Wireless and Telecommunications Symposium,* Shah Alam, 14-16 May 1997.

A. Annamalai, V. K. Bhargava, "Analysis of an Adaptive ARQ Protocol over Slowly Varying Wireless Communication Channels," to appear in *International Wireless and Telecommunications Symposium,* Shah Alam, 14-16 May 1997.

Partial Copyright License

I hereby grant the right to lend my thesis (or dissertation) to users of the University of Victoria Library, and to make single copies only for such users or in response to a request from the Library of any other university, or similar institution, on its behalf or for one of its users. I further agree that permission for extensive copying of this thesis for scholarly purposes may be granted by me or a member of the University designated by me. It is understood that copying or publication of this thesis for financial gain shall not be allowed without my written permission.

Title of Thesis/Dissertation: **Issues in DS-CDMA Integrated Wireless Access Networks**

Author 

(Signature)

ANNAMALAI (JR) ANNAMALAI

29 JANUARY, 1997

(Date)